Heinrich Pette Institute

Leibniz Institute for Experimental Virology

The role of the murine cytomegalovirus protein m139 in viral tropism

Dissertation

submitted to the

Department of Chemistry

Faculty of Mathematics, Informatics and Natural Sciences

University of Hamburg

In fulfillment of the requirements for the degree of

Doctor of Natural Sciences (Dr. rer. nat.)

by

Olha Puhach

born in Zaporizhzhya, Ukraine

Hamburg 2019

Approval for publication: 13.08.2020

Prof. Dr. Wolfram Brune (first reviewer)

Prof. Dr. Adam Grundhoff (second reviewer)

Day of oral defense: 05.05.2020

This study was conducted between December 2014 and December 2019 at the Heinrich Pette Institute Leibniz Institute for Experimental Virology under the supervision of Prof. Dr. Wolfram Brune and Prof. Dr. Melanie Brinkmann.

Моїм батькам

Oral and poster presentations

Parts of this thesis were presented at the following conferences:

HPI Joint Scientific Retreat	October 2016, Hamburg, Germany Poster
27th Annual Meeting of the Society for Virology	March 2017, Marburg, Germany Poster
43rd International Herpesvirus Workshop	July 2018, Vancouver, Canada Oral presentation
HPI Joint Scientific Retreat	October 2018, Hamburg, Germany Oral presentation
29th Annual Meeting of the Society for Virology	March 2019, Duesselforf, Germany Poster
HPI Joint Scientific Retreat	September 2019, Hamburg, Germany Oral presentation
14th Mini-Herpesvirus Workshop	September2019, Braunschweig, Germany Oral presentation

Table of Contents

1 Abstract 17

2 Zusammenfassung 19

3 Introduction 21

3.1 Cytomegalovirus and its importance as a human pathogen 21

3.2 Cytomegalovirus nomenclature and structure 22

3.3 Cytomegalovirus replication cycle 23

3.4 Cytomegalovirus species specificity 25

3.5 Cytomegalovirus cell tropism 27

3.5.1 Role of endothelial cells in cytomegalovirus pathogenesis 28

3.5.2 Role of macrophages in cytomegalovirus pathogenesis 29

3.6 Cellular antiviral defenses 31

3.7 Modulation of innate immune signaling by cytomegaloviruses 34

3.7.1 Interferon-inducible protein 204 36

3.8 Host factors crucial for viral replication 37

3.8.1 RNA helicase DDX3 38

3.8.2 E3 ubiquitin protein ligase UBR 5 41

4 Aims of the study 45

5 Results 47

5.1 Role of the MCMV protein complex m139-m141 in viral replication 47

5.2 Characterization of the m139 protein during MCMV infection 50

5.3 Role of m139 in determining the cell tropism range of murine cytomegalovirus 53

5.4 The interplay between m139 and interferon-inducible protein p204 during MCMV infection 54

5.5 Interaction partners of m139 in endothelial cells 58

5.6 Characterization of the m139 interacting host proteins DDX3 and UBR5 60

5.7 Impact of m139 in the DDX3-mediated antiviral signalling 65
5.8 Role of the m139 gene product in MCMV replication in vivo 69
5.9 The m139 protein is a host range factor 71
6 Discussion 75
6.1 Role of the m139 protein in MCMV replication 75
6.2 m139 as a part of a complex with MCMV proteins m140 and m141 75
6.3 m139 as a novel modulator of IFN-β antiviral signalling 76
6.4 Role of the m139 protein in MCMV macrophage tropism 77
6.5 Role of the m139 protein in MCMV endothelial cell tropism 79
6.5.1 Modulation of the RNA helicase DDX3 by m139 80
6.5.2 Modulation of E3 ubiquitin ligase UBR5 by m139 82
6.6 Coordinated regulation of DDX3 and UBR5 by m139 82
6.7 m139 as MCMV host range determinant 83
6.8 Summary 85
7 Materials 87
7.1 Cell lines 87
7.2 Viruses 88
7.3 Virus mutants generated in this work 88
7.4 Bacteria 89
7.5 Plasmids 89
7.6 Plasmids generated for this work 91
7.7 Primers 92
7.8 Antibodies 95
7.8.1 Primary antibodies 95
7.8.2 Secondary antibodies 96
7.8.3 Nuclear dyes 96
7.9 Chemicals and reagents 96

7.9.1 Antibiotics ... 96

7.9.2 Enzymes ... 97

7.9.3 Molecular mass standards ... 97

7.9.4 SILAC reagents ... 97

7.9.5 Other reagents and chemicals ... 97

7.10 Kits ... 98

7.11 Media and buffers ... 98

7.11.1 Cell culture media and buffers ... 98

7.11.2 Cell culture media ... 99

7.11.3 Bacteria medium ... 99

7.11.4 Agarose gel electrophoresis ... 99

7.11.5 SDS polyacrylamide gel electrophoresis (SDS-PAGE) ... 100

7.11.6 Buffers for immunoprecipitation ... 101

7.11.7 DNA preparation from bacteria ("Mini prep") ... 102

8 Methods ... 103

8.1 Molecular biology methods ... 103

8.1.1 Preparation of *E.coli* DH10B electrocompetent bacteria ... 103

8.1.2 Preparation of *E.coli* GS1783 electrocompetent bacteria ... 103

8.1.3 Transformation of bacteria ... 104

8.1.4 Storage of bacteria ... 104

8.1.5 Preparation of BAC and plasmid DNA at the large scale ("midi prep") ... 104

8.1.6 Preparation of BAC and plasmid DNA at the smaller scale ("mini prep"). 104

8.1.7 Polymerase chain reaction ... 105

8.1.8 DNA restriction ... 105

8.1.9 Agarose gel electrophoresis ... 106

8.1.10 DNA purification ... 106

8.1.11 DNA ligation ... 106

8.1.12 Extraction of total RNA 106

8.1.13 Complementary DNA (cDNA) synthesis 107

8.1.14 Quantitative polymerase chain reaction (qPCR) 107

8.1.15 DNA sequencing 107

8.1.16 *En passant* BAC muthagenesis 107

8.1.17 Gibson assembly cloning 108

8.2 Cell biology and virology methods 109

8.2.1 Cell culture 109

8.2.2 Stable isotope labeling by amino acids in cell culture (SILAC) 109

8.2.3 Transfection of plasmid DNA 109

8.2.4 Transfection of BAC DNA 110

8.2.5 Production of retrovirus and lentivirus 110

8.2.6 Transduction of cells 111

8.2.7 Generation of knockouts using CRISPR/Cas9 method 111

8.2.8 Infection of cells with MCMV 111

8.2.9 Preparation of MCMV stocks 112

8.2.10 Titration of MCMV stocks 112

8.3 Protein biochemistry methods 113

8.3.1 Cell lysis for immuboblotting 113

8.3.2 Protein concentration measurement 113

8.3.3 SDS polyacrylamide gel electrophoresis (SDS-PAGE) and western blot ... 113

8.3.4 Immunoprecipitation 114

8.3.5 Immunoprecipitation for mass spectrometry analysis 115

8.3.6 Immunofluorescence 116

8.3.7 Luciferase reporter assay 116

8.3.8 Dual luciferase assay 116

8.3.9 Cell fractionation assay 117

8.3.10 Coomassie Staining 117

8.4 Liquid chromatography–mass spectrometry (LC-MS/MS) 117

8.4.1 LC-MS/MS data analysis and processing 118

8.5 In vivo experiments 119

9 References 121

10 Appendix 131

10.1 Curriculum vitae 131

10.2 List of abbreviations 132

10.3 List of the hazardous substances 135

10.4 Acknowledgments 137

10.5 Declaration upon oath 139

1 Abstract

Cytomegaloviruses (CMVs) have a highly restricted host range but exhibit a remarkably broad cell tropism in their natural host. The molecular basis of this broad tropism lies in the large viral genome, which contains a large number of genes encoding factors capable of overcoming cellular barriers and conferring the ability to replicate even in the face of specific cellular defense mechanisms. Macrophages and endothelial cells play important roles in the pathogenesis of CMV infection, as they promote viral dissemination and persistence in the host. Additionally, macrophages are important for the regulation of innate and inflammatory immune responses, thus linking the anti-viral immune defense to the immune-mediated pathogenesis. The protein m139 encoded by murine cytomegalovirus (MCMV) was previously identified as an important determinant of viral replication in murine macrophages, but the underlying mechanism has remained unknown. The aim of my doctoral research study was to characterize the function of m139 on the molecular level and to understand its role as a host range factor. I could show that m139 is an early protein, which localizes to the cytoplasm, and is also recruited to viral replication compartments within the host cell nucleus. By combining stable isotope labelling by amino acids (SILAC) with affinity purification and mass spectrometry, I identified two host proteins, the DEAD box RNA helicase DDX3 and the E3 ubiquitin ligase UBR5, as interaction partners of m139. Both factors were found to be recruited to viral replication compartments. Inactivation of m139 in the MCMV genome resulted in a replication defect in macrophages and endothelial cells. The latter was rescued in DDX3 and UBR5 knockouts cells, suggesting that m139 modulates the DDX3 and UBR5 dependent pathways to facilitate efficient MCMV replication in these cells. In macrophages, m139 was also found to be important for viral replication and a negative regulator of DDX3-dependent type I interferon induction. The biological importance of m139 in MCMV replication and dissemination in mice was confirmed in vivo. I could further show that inactivation of m139 facilitates MCMV replication in human epithelial cells. Thus, m139 has opposite functions: while it enhances MCMV replication in murine macrophages and endothelial cells, it is detrimental for viral replication in human cells.

2 Zusammenfassung

Zytomegalieviren (CMVs) sind in ihrem Wirtspektrum sehr eingeschränkt, besitzen aber einen bemerkenswert breiten Zelltropismus und können viele verschiedene Zelltypen ihres natürlichen Wirts infizieren. Die molekularen Ursachen dieses breiten Tropismus liegen im großen viralen Genom begründet. Eine große Anzahl von Genen kodiert für Faktoren, welche in der Lage sind, Zellabwehrmechanismen zu überwinden und so dem Virus eine effiziente Replikation zu ermöglichen. Makrophagen und Endothelzellen spielen eine wichtige Rolle in der Pathogenese der CMV-Infektion, da sie die virale Verbreitung und Persistenz im Wirt begünstigen. Darüber hinaus sind Makrophagen für die Regulation angeborener und entzündlicher Immunantworten von großer Bedeutung und verbinden so die antivirale Immunabwehr mit der immunvermittelten Pathogenese. Das murinen Cytomegalievirus (MCMV). Protein m139 wurde zuvor als wichtiger Faktor für die Virusreplikation in murinen Makrophagen identifiziert, jedoch sind die zugrunde liegende molekularen Mechanismen bisher unbekannt. Ziel meiner Doktorarbeit war es, die Funktion und die molekularen Mechanismen von m139 zu charakterisieren und zu untersuchen welchen Einfluss m139 auf das Wirtspektrum ausübt. Ich konnte zeigen, dass m139 als *Early* Protein klassifiziert ist, das im Zytoplasma lokalisiert und zu den Virusreplikationskompartimente im Wirtszellkerns rekrutiert wird. Mittels *stable isotope labelling by amino acids in cell culture* (SILAC) in Kombination mit einer Affinitätsreinigung und anschließender Massenspektrometrie konnte ich zwei Wirtsproteine, die DEAD Box RNA-Helikase DDX3 und die E3 Ubiquitin-Ligase UBR5, als Interaktionspartner von m139 identifizieren. Beide Proteine werden während einer Infektion zu den Virusreplikationkompartimenten rekrutiert. Die Inaktivierung von m139 im MCMV-Genom führte zu einem Replikationsdefekt in Makrophagen und Endothelzellen. Letzteres konnte in DDX3- und UBR5-Knockout-Zellen gerettet werden. Die Ergebnisse deuten darauf hin, dass m139 Einfluss auf DDX3- und UBR5 abhängige Signalwege nimmt und so eine effiziente MCMV-Replikation in diesen Zellen ermöglicht. Darüber hinaus wurde m139 auch als wichtiger Faktor für die MCMV-Replikation und als negativer Regulator der DDX3-abhängigen Typ-I-Interferoninduktion in Makrophagen identifiziert. In Maus in vivo Experimenten wurde die biologische Bedeutung von m139 für die Replikation und Verbreitung bestätigt. Desweiteren konnte ich zeigen, dass die Inaktivierung von m139 die MCMV-Replikation in humanen Epithelzellen bewirkt. So hat m139 konträre Funktionen: Während m139 die MCMV-Replikation in murinen

Makrophagen und Endothelzellen verbessert, ist es für die Virus Replikation in humanen Zellen nachteilig.

3 Introduction

3.1 Cytomegalovirus and its importance as a human pathogen

Cytomegalovirus (CMV) infection was first described at the end of the 19th century when the typical cytopathic effects, such as intracellular inclusions and cellular enlargement, were observed in histological samples from infected patients. Thanks to the advancement of cell culture techniques, the virus was firstly isolated in the 1950s [1]. CMV is highly seroprevalent among the human population worldwide; in developed countries, CMV seropositivity rates vary from 33 to 77%, whereas in developing countries, particularly in sub-Saharan Africa, it reaches almost 100% (Figure 1) [2].

Human cytomegalovirus (HCMV) can be transmitted by contact with bodily fluids like saliva, tears, urine, stool, breast milk, and semen, as well as via solid-organ transplantation and hematopoietic stem cell transfusion [2, 3]. Poor socio-economic conditions, such as bad nutrition, crowded living conditions, as well as additional herpes virus coinfections, are among the risk factors for HCMV transmission [4].

Primary HCMV infection tends to induce a strong immune response and therefore does not cause serious disease. However, due to its ability to establish latency, HCMV does not get cleared from the host. During latency, HCMV genomes are maintained in the host cell while active replication is absent [5]. In contrast to an asymptomatic course of infection among immunocompetent individuals, in immunocompromised patients, such as AIDS patients and transplant recipients, HCMV infection causes retinitis, pneumonitis, enterocolitis, esophagitis, and hepatitis. Historically, HCMV infection was documented as an opportunistic infection in human immunodeficiency virus (HIV) patients [2]. Moreover, HCMV is the leading cause of congenital infection and birth defects, yet the awareness worldwide is low. Infection of the fetus can lead to motor and cognitive disorders, hearing loss, visual impairment, and premature death. Infection of seronegative mothers during the first trimester carries a higher risk of severe HCMV infection of the fetus. Moreover, the possibility of symptomatic congenital infection as a result of the HCMV reactivation during pregnancy is highly discussed [3, 6].

Various antiviral drugs are available for treatment of CMV infections, such as ganciclovir, foscarnet, and cidofovir. Nucleoside analogues ganciclovir and cidofovir inhibit the viral polymerase activity and act as chain terminators, whereas pyrophosphate analogue foscarnet inhibits the viral DNA polymerase by blocking the pyrophosphate binding site. However, all listed drugs often cause a high cytotoxicity and antiviral resistance to these drugs is often reported [7]. A newly approved drug, letermovir, inhibits the viral terminase complex. Even though this drug shows lower cytotoxicity, viral resistance is still documented [8]. So far, no HCMV vaccine has been developed. One of the complications in the development of a vaccine against HCMV is the absence of an animal model due to its strict species-specificity.

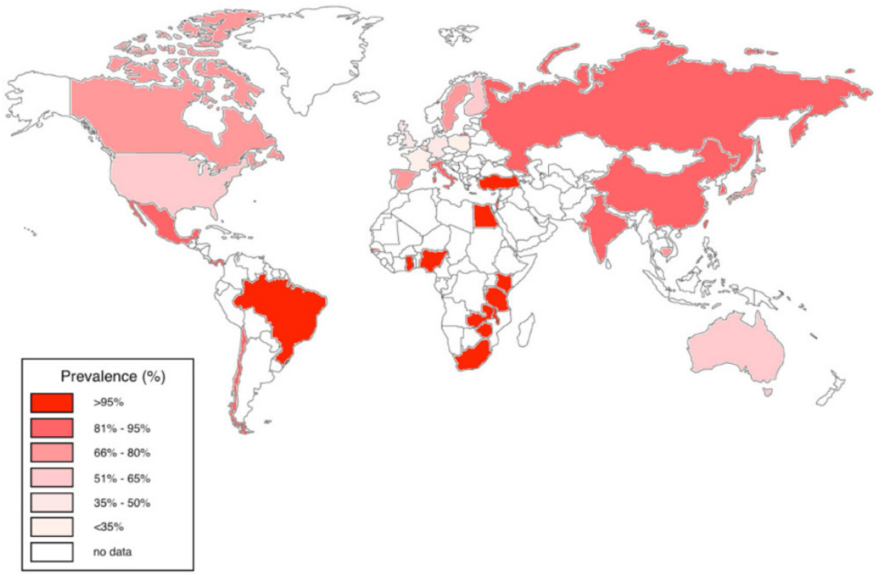

Figure 1. Cytomegalovirus seropositive rates worldwide. Picture acquired from [2].

3.2 Cytomegalovirus nomenclature and structure

The herpesvirus family comprises a group of large enveloped viruses with double-stranded DNA genomes. Due to their biological properties and viral genome structure, they are subdivided into three subfamilies: α-, β-, and γ-herpesviruses. Cytomegalovirus belongs to the subfamily *Betaherpesvirinae* of the *Herpesviridae* family. Primate viruses, such as HCMV, are classified to the genus *Cytomegalovirus*, whereas rodent viruses, such as, murine cytomegalovirus (MCMV) are of the genus *Muromegalovirus* [9]. DNA genomes from both HCMV and MCMV have large coding capacities. It was originally estimated that MCMV encoded 170 proteins, whereas HCMV comprises 192 ORFs with the potential to encode proteins [10, 11]. Mature CMV viral particles are enveloped and 150-200 nm in diameter (Figure 2). The viral DNA is encapsulated within a T=16 capsid. The capsid is surrounded by an amorphous tegument harboring most of the proteins within the virion, most of which are phosphoproteins. The tegument is surrounded by a lipid envelope, which is decorated with virus-encoded glycoproteins. Host proteins and mRNAs were also found to associate with CMV virions [12-14].

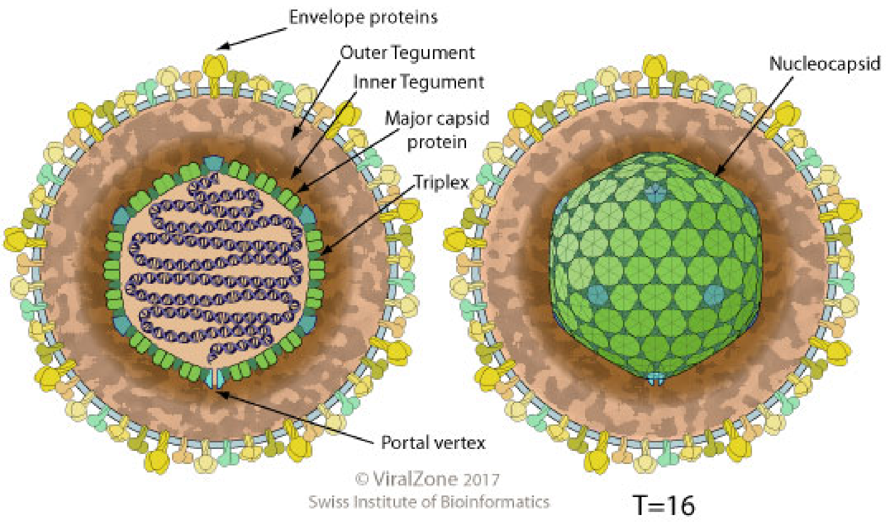

Figure 2. Schematic representation of the CMV virion structure. Image acquired from https://viralzone.expasy.org.

3.3 Cytomegalovirus replication cycle

The viral replication cycle starts with entry into the host cell by fusion of the viral envelope with the plasma membrane or endosomes (Figure 3A) [15]. The HCMV glycoprotein 'trimer' complex gH/gL/gO binds to the platelet-derived growth factor receptor alpha (PDGFRα) [16]; this interaction is essential for viral entry into fibroblasts. In contrast, the so called "pentamer" complex gH/gL/pUL128/pUL130/pUL131 interacts with Neuropilin-2, promoting entry into endothelial, epithelial, and myeloid cells [17]. Glycoprotein B (gB) functions as a homotrimer and mediates membrane fusion during viral entry [18]. Following entry, genome-containing capsids together with tegument proteins are delivered to the nucleus. The cellular microtubule network, which serves as an intracellular transport machinery, it is hijacked for the transport of CMV capsids to the nucleus. In HCMV-infected cells, this transport is guided by tegument proteins UL47 and UL48 [19]. When the capsids reach the nucleus, viral DNA enters it through the nuclear pores (Figure 3B). Some other HCMV tegument proteins, such as pp65 and pp71, are delivered to the nucleus independently of the capsid. Following entry into the nucleus, the viral genomes are found to associate with nuclear dot-like structures formed around the promyelocytic leukemia (PML) protein, known as PML nuclear bodies. PML bodies comprise more than 160 different proteins, which serve as a host restriction factors and mediate intrinsic innate immunity. Immediate-early protein IE1 of both HCMV and MCMV disrupts PML bodies and promotes initiation of viral immediate-early (IE) gene expression [19-22]. The expression of viral genes occurs in a transcription cascade and is divided into temporal classes, namely immediate-early (IE), early (E), and late (L) (Figure 3C). IE genes are first to be transcribed after infection and appear to be essential for viral replication and gene expression. *De novo* synthesis of IE proteins is required for the transcription of viral early genes. Many of them are necessary for productive DNA replication [23]. Late genes encode proteins required for the morphogenesis of cytomegalovirus virions. They have been subdivided into two categories: leaky-late and "true late" genes. Both are expressed only at late times post infection, but true late genes are dependent on viral DNA replication. Activation of the major immediate early promoter (MIEP) drives transcription of the major IE genes. MIEP contains several cis-acting sites for host transcription factors, which differentially regulate its activity [24]. Differential regulation of MIEP chromatin structure takes place in HCMV latency and reactivation in myeloid cells [25]. The expression of IE genes is followed by early gene expression and DNA replication in the nucleus. Initiation of viral DNA replication takes place in the cis-acting origin of replication and comprises circularization and concatemer formation. CMV encodes six core proteins that have been shown to be necessary for DNA replication: DNA polymerase (MCMV protein M55 and HCMV protein UL54), polymerase accessory protein (M44, UL44), primase (M70, UL70), helicase (M105, UL105), primase-associated factor (M102, UL102), and single-stranded DNA-binding protein (M57, UL57) [26]. Capsid assembly takes place in the nucleus, starting from the formation of an immature capsid shell and subsequent DNA packaging into the immature capsids [27]. Immature capsids then partially acquire tegument. However, this process is not completely understood. Partially tegumented capsids reach the cytoplasm following the process of nuclear egress. During egress, CMV-encoded kinases phosphorylate nuclear lamina which leads to its distortion (Figure 3D) [28]. Final tegumentation and envelopment of CMV particles takes place at the assembly complex in the cytoplasm [29]. To generate a cytoplasmic viral assembly complex (vAC), CMV remodels the Golgi apparatus, endoplasmic reticulum (ER), and the endosomal machinery. In the vAC, the immature virions acquire the tegument and the envelope (Figure 3F). The envelope is derived from cellular membranes and modified by the embedding of viral glycoproteins. Mature virions associated with secretory vesicles reach the plasma membrane and get released into the extracellular space (Figure 3G) [30, 31].

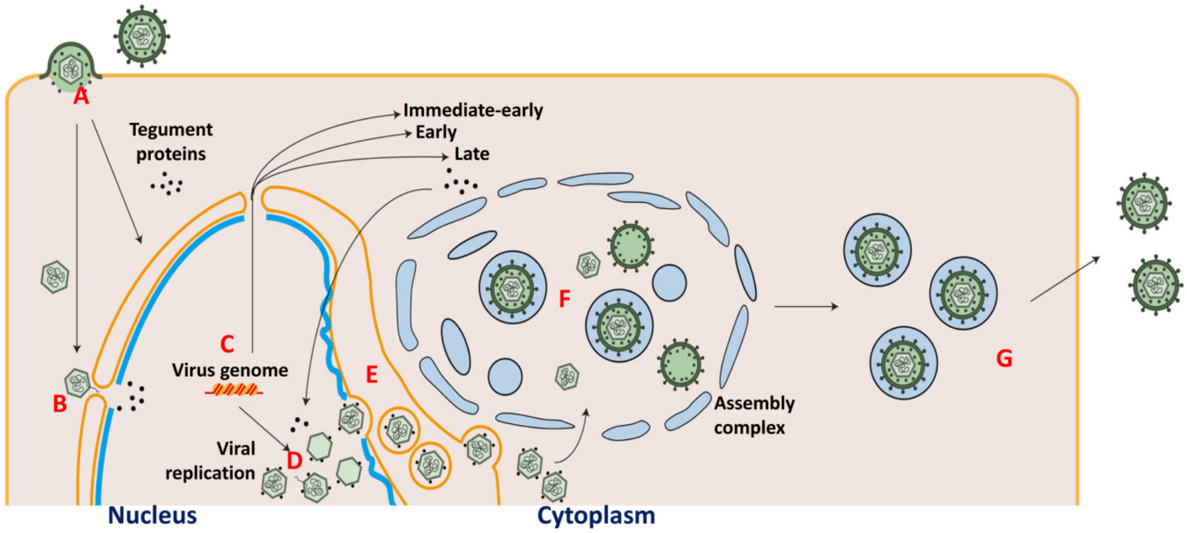

Figure 3. Schematic representation of the CMV replication cycle. (A) Virions enter into the cell. Upon entry, capsid and tegument proteins are released into the cytoplasm. (B) Tegument proteins and capsids travel to the nucleus, delivering viral DNA. (C) Viral DNA in the nucleus gets circularized and viral replication takes place, leading to the expression of viral genes in a cascade manner. (D) Following the expression of early genes, viral replication takes place in the nucleus. (E) Capsid assembly starts in the nucleus, followed by nuclear egress to the cytoplasm. (F) Capsids associated with tegument proteins reach the viral assembly complex (vAC), where capsids acquire the tegument and envelope. (G) Mature particles are released from the cells. Figure is modified from [32].

3.4 Cytomegalovirus species specificity

Species-specific differences in mammalian genomes create unique environments for the viruses. Host factors evolve under positive selection to control viral replication, while viruses also adapt to compensate for changes in the host. This continuous co-evolution arms race can result in a narrow host range [33]. Cytomegaloviruses are strictly species-specific and able to replicate only in the cells of their own or a closely related species. HCMV can replicate in chimpanzee skin fibroblasts, and MCMV can replicate in rat cells. Nevertheless, both viruses fail to replicate in cells of more distant species [34, 35]. Even though numerous details of interaction between CMVs and their hosts were revealed over the last decades, the molecular mechanisms of their species specificity have not been identified yet.

During infection of non-permissive cells, CMV will undergo entry, the viral DNA will be injected into the nucleus and express IE genes, but viral replication will be blocked at a later step in the viral replication cycle [36]. Infection of human cells by wildtype MCMV leads to the activation of caspase-9-dependent apoptosis in these cells. Overexpression of cellular Bcl-2 family apoptosis inhibitors or their viral homologs, such as HCMV-encoded mitochondria-localized inhibitor of apoptosis (vMIA), promotes viral replication in human cells. Moreover, the same strategy allows replication of rat CMV in human cells, demonstrating that species specificity is related to apoptosis [37].

For a number of viruses, productive infection in a new species requires novel mutations to adapt to the host [38]. This pattern was observed in case of adaptation of MCMV to human cells [39]. An adapted stain of MCMV, named as MCMV/h, spontaneously acquired the ability to replicate in human retinal pigment epithelial (RPE-1) cells two weeks post infection. MCMV/h forms larger replication compartments, causes less apoptosis, and is able to more efficiently disrupt PML nuclear bodies in comparison to WT MCMV. Next generation sequencing of this mutant has revealed a number of alterations in comparison to the parental strain. The reintroduction of the mutations in the M112/113 region into WT MCMV was sufficient to facilitate replication in human cells. However, this mutant did not replicate as efficiently as MCMV/h [40]. Two other spontaneously arisen MCMV mutants, MCMV/h2 and MCMV/h3, were isolated and sequenced. The MCMV gene M117 was identified as another host range determinant; the mutations in this gene were detected in all MCMV human-adapted strains. Mutations in M117 did not impair viral replication in murine cells in vitro, but was crucial for viral dissemination in vivo. In MCMV-infected murine cells, M117 is found in the viral replication compartments and appears to modulate the cellular DNA synthesis and cell cycle progression. M117 interacts with E2F transcription factors, which leads to the expression of E2F target genes. MCMV with a deletion or mutation in M117 does not activate E2F-dependent transcription and therefore promotes MCMV replication in human cells [41]. However, M117 MCMV mutants, like M112/113 mutants, do not replicate as well as MCMV/h, MCMV/h2, or MCMV/h3. This implies that mutations in other viral genes contribute to more efficient MCMV replication in human cells.

3.5 Cytomegalovirus cell tropism

Broad cell tropism in vivo is one of the hallmarks of cytomegaloviruses. A high variety of organ tissues are infected in the course of CMV infection. Endothelial and epithelial cells as well as fibroblasts are the most prominent targets for CMV. Leukocytes, neurons, and smooth muscle cells are also susceptible for CMV infection [42]. HCMV infection starts from infection of epithelial cells (Figure 4). Further replication leads to the spread to the peripheral blood through endothelial cells, where HCMV infects monocytes. HCMV infection activates monocytes and promotes their replication and dissemination in tissues, where they differentiate into permissive macrophages. HCMV-induced macrophages can migrate into the bone marrow, where they infect myeloid progenitor cells and establish latency in these cells (Figure 4) [43]. Latent viral genomes are maintained in an episomal form in $CD33^+$ and $CD34^+$ cells in the bone marrow and $CD14^+$ peripheral blood mononuclear cells, retaining a potential for reactivation [6]. Epithelial cells are the source of infectivity in saliva, stools, and urine and are considered an important player in the transmission to infants from seropositive mothers through breast milk [44].

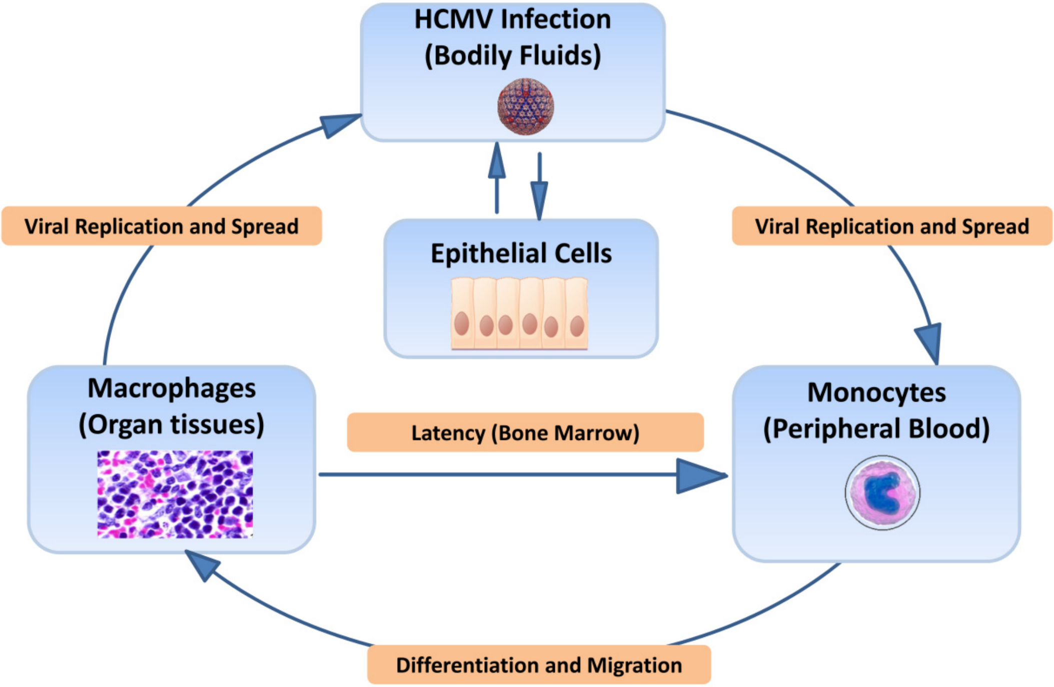
HCMV Infection
(Bodily Fluids)
Viral Replication and Spread
Epithelial Cells
Viral Replication and Spread
Macrophages
(Organ tissues)
Latency (Bone Marrow)
Monocytes
(Peripheral Blood)
Differentiation and Migration

Figure 4. Dissemination of HCMV in its host. The primary targets of HCMV, *i.e.* epithelial cells, are infected by HCMV-containing bodily fluids. The virus replicates and spreads to monocytes in the peripheral blood. Following differentiation into permissive macrophages, they migrate to organ tissues. HCMV–induced macrophages are then able

to migrate to the bone marrow, where they establish latency in myeloid progenitor cells. Modified from [45].

3.5.1 Role of endothelial cells in cytomegalovirus pathogenesis

Endothelial cells form the endothelium, the interior cell layer of blood and lymphatic vessels. Endothelial cells are highly metabolically active and important for both innate and acute immune responses. During the early steps of development, endothelial progenitor cells, known as angioblasts, arise from hemangioblasts. Angioblasts then give rise to endothelial cells of arteries, veins, and capillaries [46]. In the blood vessels, endothelial cells form a continuous layer connected by tight junctions. Continuous endothelium forms the blood-brain barrier, serving as a safeguard against microbes and toxins. Thicker endothelium is found in the heart, skeletal tissue, testes, and ovaries. Discontinuous endothelial cells, which are interrupted by gaps, are found in the endocrine and kidney [47].

Endothelial cells play a pivotal role in the trafficking of blood cells between blood and underlying tissues, the control of vasomotor tone, angiogenesis, and maintenance of blood fluidity [48]. Endothelial tissues are used as a gateway for transport of different molecules and leukocytes. Transfer of material across the cells is mediated by caveolae and vesiculo–vacuolar organelles [49]. Trafficking of leukocytes between blood and underlying tissues is mediated either through or between endothelial cells. This transport is associated with the synthesis of cell adhesion molecules by endothelial cells. Together with leukocytes, endothelial cells are the main players in inflammatory reactions. They produce cytokines and growth factors, serving for the recruitment of leucocytes to the sites of inflammation [48]. Stimulation of endothelial cells with lipopolysaccharides (LPS), tumor necrosis factor-a (TNF-a), or IL-1 results in further production of cytokines and growth factors, as well as upregulation of proadhesive and procoagulant genes [48, 50].

Proliferation of endothelial cells is an essential part of the formation of new blood vessels. Blood vessel formation, known as vasculogenesis and angiogenesis, happens during embryogenesis, while in adults proliferation of endothelium occurs only during wound healing and reproduction. However, during solid tumor growth and metastasis, the proliferation of endothelium is highly stimulated, this leads to the generation of new vascular network, known as neoangiogenesis [48].

Endothelial cells have been recognized as important targets of HCMV infection. They promote hematogenous dissemination of HCMV. As a result, HCMV-infected microvascular endothelial cells are found in the gastrointestinal tract, liver, kidney, and brain. Those cells are permissive for productive lytic infection [44]. The possibility of the liver endothelium to harbor latent HCMV is highly discussed. Notably, liver sinusoidal endothelial cells were detected as sites of latency for MCMV [51].

HCMV infection promotes a number of changes in endothelium secretion potential and morphology. Cell adhesion factors ICAM-1, VCAM-1, and E-selectin are upregulated in HCMV-infected endothelial cells. Additionally, the permeability of the endothelium is increasing during HCMV infection due to the changes in tight and adherent junctions due to viral protein expression. These changes in endothelium lead to the enhanced monocyte migration [52]. CMV was shown to promote transplant arteriosclerosis in heart transplant patients, while ganciclovir prophylaxis following heart transplantation diminishes the risk of arteriosclerosis [53]. Infection of endothelial cells by HCMV increases the adherence of blood platelets to endothelial cells by increasing the secretion of the von Willebrand factor, which is a known factor in hemostasis and induction of arterial thrombosis. This effect of HCMV can be overcome by application of HCMV antivirals [54]. Ultimately, HCMV binding to β1 and β3 integrins and the epidermal growth factor receptor (EGFR) leads to the activation of phosphatidylinositol 3-kinase (PI3K) and the mitogen-activated protein kinase (MAPK). Activation of these signaling pathways promotes proliferation and motility of endothelial cells associated with neoangiogenesis [55].

3.5.2 Role of macrophages in cytomegalovirus pathogenesis

Macrophages are multifunctional cells, which are best known for their role in immunity. Phagocytic activity of macrophages is used for the host defense against pathogens as well as for “housekeeping” purposes, such as removal of apoptotic cells [56]. The mononuclear phagocyte system, which is also known as reticuloendothelial system, is a subgroup of leukocytes represented by a population of bone-marrow derived myeloid cells; these cells circulate in the blood as monocytes and settle in tissues as macrophages [57]. Monocytes originate from macrophage and dendritic cell precursors (MDPs) in the bone marrow. The migration of monocytes to inflamed tissues, where they can differentiate into inflammatory dendritic cells (DCs) or inflammatory macrophages, is CC-chemokine receptor 2 (CCR2)-dependent [58]. The functional phenotype of macrophages is determined by their microenvironment; according to the type of activation, macrophages are divided in two groups: classically activated M1 and alternatively activated M2 macrophages. The agonists of Toll-like receptors promote diverse patterns of gene and protein expression. As a result of this activation, M1 macrophages show a proinflammatory and anti-microbial phenotype, while M2 macrophages reduce inflammation and promote fibrosis and tissue healing. This classification remains in use even though M2 type macrophages consist of cells with different biochemical and physiological profiles. Interferon-γ (IFNγ) produced by T helper 1 (Th1) cells, CD8+ T cells, or by natural killer (NK) cells as well as and tumour-necrosis factor (TNF) produced by antigen-presenting cells (APCs) give rise to classically activated macrophages. Granulocytes and Th2 cells produce interleukin-4 (IL-4), which promotes activation of wound-healing by alternatively activated macrophages [59].

Both monocytes and differentiated macrophages are important targets of CMV infection. Moreover, HCMV appears to orchestrate the polarization and differentiation of infected macrophages/monocytes to a phenotype sharing features of both M1 and M2 macrophages in order to maintain the balance between pro-inflammatory and anti-inflammatory signals produced by macrophages [60]. The findings about HCMV infection of monocyte and macrophages were validated in a mouse model. MCMV-infected blood monocytes are recruited to the sites of MCMV infection by chemokine homolog MCK2 and further disseminate virus by migration to other organs [61]. Moreover, during acute spleen infection, MCMV has been found in the marginal zone of macrophages [62]. In addition to being targets of MCMV infection, macrophages are important players in antiviral innate and inflammatory responses. At the sites of MCMV infection, activated macrophages produce interferon alpha and beta (IFN-α/β), tumor necrosis factor alpha (TNF-α), interleukin (IL)-1 alpha, IL-6, and IL-12. These cytokines are important for the suppression of MCMV replication and MCMV clearance from target organs [63, 64].

3.5.2.1 Role of the US22 family protein m139 in MCMV macrophage tropism

Gene duplication events during the evolution β-herpesviruses have resulted in the formation of ORF families. MCMV and HCMV share four gene families. One of these conserved gene families is US22 [10]. The US22 gene family is the largest gene family among the cytomegaloviruses, comprising 12 MCMV, 13 HCMV, and 11 Rat CMV (RCMV) genes [65]. The US22 gene products have stretches of hydrophobic and charged residues and up to four conserved sequence motifs. Most of the US22 genes are not essential for viral replication in cell culture but play a role in viral pathogenesis and cell survival. Some of the US22 proteins were shown to be important for viral tropism. HCMV-encoded UL23 is important for replication in fibroblasts, whereas UL24 is a tropism factor for endothelial cells [23, 66]. In MCMV, there was a set of genes identified to be important for the replication in differentiated macrophages but not fibroblasts. Those genes are M36, M43, m139, m140 and m141. The MCMV genes m139, m140, and 141 are homologues to HCMV genes US22, US23 and US24 [66]. Deletion of the m139-m141 region leads to impaired MCMV replication in differentiated macrophages, and this MCMV mutant is highly attenuated in vivo [63]. Products of the genes m139, m140, and m141 can form a complex upon infection and colocalize in the perinuclear region [67].

3.6 Cellular antiviral defenses

Viruses are highly diverse and expeditiously evolving pathogens; therefore they represent an ongoing challenge for the development of defense mechanisms by their host. Considering that viruses are obligatory parasites and highly dependent of the cellular machinery, during the long co-evolution with their hosts they have generated strategies to both avoid and take advantage of the host immune defense mechanisms. Innate immune responses represent the first line of defense against viral infections. Upon viral infection, pathogen recognition receptors (PRRs) detect the pathogen-associated molecular patterns (PAMPs) of viruses. This leads to the initiation of complex signaling pathways culminating in the activation of interferon and proinflammatory responses [68]. Activation of macrophages, natural killer (NK) cells, and cytotoxic T lymphocytes occurs during proinflammatory responses. Cytokines, such as interleukin-1 (IL-1), IL-6, IL-8 and tumor necrosis factor (TNF-α), are key modulators of inflammation [69]. IFN also plays a crucial role in the control of viral infection [70]. Secretion of interferons is crucial for the amplification of the response and spread to neighboring cells in order to augment IFN signaling. All the IFNs are capable of enacting an antiviral state but vary with respect to their structure and tissue specificity. Despite the numerous types of IFNs, there are only three types of IFN receptors on the cell surface: type I IFN receptor (IFNAR), type II IFN receptor (IFNGR), and type III IFN receptor (IFNLR). IFN-α and IFN-β, which in the context of CMV are the most studied, are type I IFNs [71].

Toll-like receptors (TLRs), retinoic acid-inducible gene I (RIG-I) like receptors (RLRs), Nod-like receptors (NLRs), and C-type lectins were identified as PRRs. Viral nucleic acids are the main PAMP recognized by PRRs upon viral infection. Endosome-located TLR3 and TLR7 recognize viral RNA, while TLR9 recognizes viral DNA. This leads to the recruitment of adaptor myeloid differentiation primary response 88 (MYD88) and TNF receptor associated factor (TRAF6) [72]. TRAF6 further activates the IKK complex. The IKK complex is formed by the IκB kinases (IKK) IKKα and IKKβ together with the regulatory subunit IKKγ. Activation of this complex facilitates release of NF-κb from its inhibitor Iκb, leading to the translocation of this transcription factor to the nucleus, where it activates the IFN-β promoter [73]. RIG-I contains carboxyterminal domains that bind to viral RNA, which induce a conformational change. The interaction with viral RNA leads to the interaction with the signaling adaptor mitochondrial antiviral-signaling protein (MAVS). Aggregation of MAVS on mitochondrial membranes results in the activation of a second IKK complex, which comprises IKKε and TBK1. Upon stimulation by PRR-mediated signalling, they phosphorylate and activate interferon regulatory factor 3 (IRF3) and 7 (IRF7). Upon activation, these transcription factors form homo- and heterdimers and translocate to the nucleus where together with NF-κB, IRF3 and IRF7 form an active complex on the IFN-β promoter [68, 71, 74]. DDX3 is a newly identified sensor of viral RNA, which is also involved in the activation of IRF3-dependent IFN signaling [75, 76] (Figure 5). The role of this factor in the innate immunity is characterized in the chapter 3.8.13.8.1

Additionally, there is an extensive number of DNA-sensing PRRs. Among these, the most prominent examples are DNA-dependent activator of IFN (DAI), RNA polymerase III, DExD/H-box helicases, the cytosolic DNA sensor cyclic GMP–AMP synthase (cGAS), and stimulator of interferon genes (STING). Upon interaction with DNA, cGAS is activated and converts GTP and ATP into cyclic GMP–AMP (cGAMP). cGAMP binds to the ER-localized adaptor STING, leading to its oligomerization. STING oligomers translocate to the Golgi, where they interact with the TBK1 and IKK complexes; they activate IFN-β expression through IRF3. Alongside with IRF3, STING activates NF-κB for IFN-β activation, as well as TNF and proinflammatory cytokines, such as IL-6 [77]. Gamma-interferon-inducible protein 16 (IFI16) has two DNA binding motifs and at the steady-state localizes to the nucleus. Upon infection, IFI16 translocates to the cytoplasm, where it potentiates STING and cGAS as well as IRF3 signaling [78] (Figure 5). Recently identified orthologue of IFI16, murine protein p204, have also been shown to be implicated in IFN signaling. The physiological role of this protein is described in the chapter 3.7.1. One of the major DNA sensors is the IFN-inducible protein absent in melanoma 2 (AIM2). AIM2 detects cytosolic DNA and interacts with apoptosis-associated speck-like protein containing a caspase activation and recruitment domain (ASC). In association with other cytosolic factors, they form AIM2 inflammasomes and trigger NF-κB and caspase-1 activation [79].

Following the release from the cells, IFNs bind to their receptors on the cell surface in an autocrine and paracrine fashion. IFN-induced oligomerization of IFNAR results in the activation of Janus kinase-signal transducer and activator of transcription (JAK-STAT) pathway [80]. Activation of this pathway promotes phosphorylation of STAT1 and STAT2. Phosphorylated STATs form a heterodimer and together with the IFN regulatory factor 9 (IRF9) form the ISG factor 3 (ISGF3) complex. Translocation of the ISGF3 complex to the nucleus leads to the transcriptional activation of IFN-stimulated genes (ISGs). Many of ISG-encoded proteins directly target pathways required during the virus life cycle and are therefore called restriction factors [80, 81].

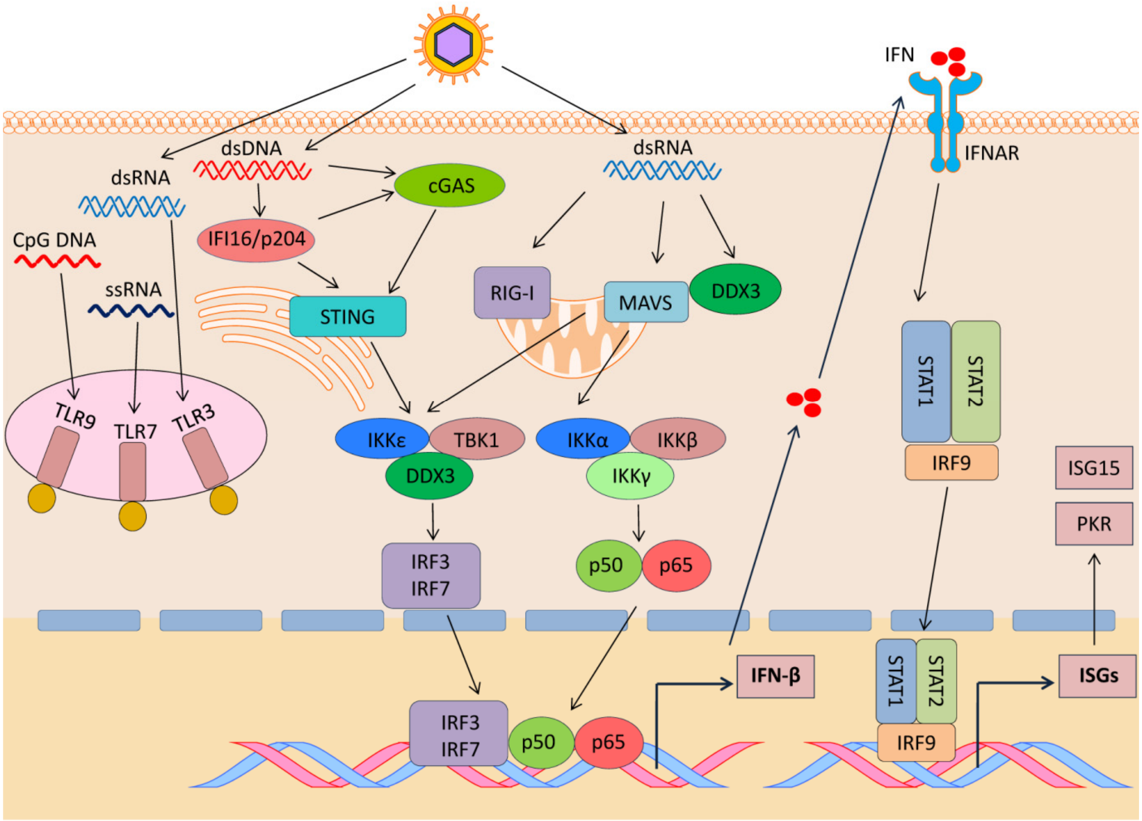
IFN
IFNAR
dsDNA
dsRNA
dsRNA
cGAS
CpG DNA
IFI16/p204
ssRNA
STING
RIG-I
MAVS
DDX3
TLR9
TLR7
TLR3
STAT1
STAT2
IKKε
TBK1
IKKα
IKKβ
DDX3
IKKγ
IRF9
ISG15
PKR
IRF3
IRF7
p50
p65
IFN-β
STAT1
STAT2
ISGs
IRF3
IRF7
p50
p65
IRF9

Figure 5. Innate immune responses during viral infection. Upon viral entry, a number of pathogen-associated molecular patterns (PAMPs) are sensed by host pathogen recognition receptors (PRRs). Among these are retinoic acid-inducible gene I (RIG-I),

mitochondrial antiviral-signaling protein (MAVS), stimulator of interferon genes (STING), Toll-like receptors (TLRs), etc. Activation of PRRs leads to the further activation of transcription factors of IFN, such as interferon-regulatory factor 3 and 7 (IRF3/7) and nuclear factor kappa-light-chain-enhancer of activated B cells (NF-κB). NF-κB is comprised of two subunits: p50 and p65. Produced IFN subsequently activates the JAK-STAT signaling pathway, which augments the antiviral response through production of interferon-stimulated genes (ISGs).

3.7 Modulation of innate immune signaling by cytomegaloviruses

Even though upon infection host cells are able to induce IFN secretion and the production of cytokines in order to limit viral propagation, CMV has evolved sophisticated strategies to counteract IFN and inflammatory restrictions. The evolutionary success of CMVs is dependent on their ability to curtail innate immunity defense mechanisms. The interferon response to CMV infection is very complex. The detection of CMV at early times post infection leads to an initial peak in IFN production. Virion-associated factors are recognized by the cell and activate IRF3 and NF-κB [82, 83]. Lymphotoxin β receptor (LTβR) signaling is required for induction of IFN, which limits viral replication and the severity of the disease. The second peak of IFN induction is TLR-dependent and starts about 36 hours after infection of mice [84].

CMVs modulate IFN signaling pathways at different stages. HCMV dampens signaling downstream of MAVS by fragmentation of mitochondria by viral protein vMIA. Additionally, vMIA targets antiviral signaling by interacting with peroxisomal MAVS [85] (Figure 6). Multiple CMV proteins were discovered to curtail STING-mediated IFN signaling. HCMV-encoded IE86 protein prompts the degradation of STING in a proteasome-dependent way. STING translocation to the perinuclear microsomes and further recruitment of TBK1 and IRF3 are blocked by the UL82 protein [86]. The deubiquitinase (DUBs) UL48 impedes STING ubiquitination, which abrogates recruitment of TBK1 crucial for IFN activation [87]. pp71, encoded by HCMV gene UL31, reduces cGAMP accumulation upon HCMV infection and consequently inhibits cGAS [79]. During MCMV infection, the m152 protein binds STING and delays its trafficking to the Golgi compartment, resulting in inhibition of STING-mediated IRF but not NF-κB signaling [88]. Another DNA sensor, IFI16, is targeted by HCMV tegument protein pp65 (ppUL83). It binds to the pyrin domain of IFI16 and therefore abolishes DNA sensing by IFI16 [87, 89]. Additionally, the viral kinase UL97 interacts with IFI16 and phosphorylates it; as a result of this phosphorylation IFI16 is relocalized to the cytoplasm, where it is prevented from inducing an IFN response [90]. pp65 was shown to inhibit AIM2 inflammasomes by direct interaction with AIM2 [87]. In the case of NF-κB, CMVs promote both its activation and downregulation. MCMV protein M45 activates NF-κB at early times post infection and later in infection M45 downregulates NF-κB [83, 84]. In HCMV-infected cells, NF-κB inhibition is mediated by phosphorylation and activation of IKKβ by UL26 [91].

As well as IFN production, CMV also efficiently controls IFN signaling. JAK1 was shown to be reduced in HCMV-infected cells [92]; however, the exact viral factor responsible for this process is not known to date. During MCMV infection, the M27 protein facilitates STAT2 downregulation, blocking both IFN-α/β and IFN-γ responses [84, 93] (Figure 6). ISGs are also a subject of CMV modulation. One of the well-described examples of ISGs targeted by CMVs is ISG15 and the dsRNA-dependent protein kinase R (PKR). ISG15 is known to promote protein ISGylation stimulating disruption of viral life cycle progression and boosting antiviral immunity. UL26 together with IE1 suppress expression of ISG15 upon HCMV infection [94]. dsRNA-dependent protein kinase R (PKR) recognizes dsRNA and upregulates mechanisms leading to inhibition of viral and cellular protein synthesis. US22 family proteins IRS1 and TRS1 are a dsRNA-binding proteins, which inhibit PKR-induced shutoff of protein synthesis. On the one hand, they can bind directly to dsRNA preventing it from binding by other dsRNA sensors [90, 95]. m142 and m143, the MCMV homologues of IRS1 and TRS1, are known to counteract PKR activation during MCMV infection [84, 96] (Figure 6). Even though numerous viral antagonists targeting innate signaling have been discovered to date, there is still activation of the innate immune signaling upon infection, confirming continuous coevolution between cytomegaloviruses and their host.

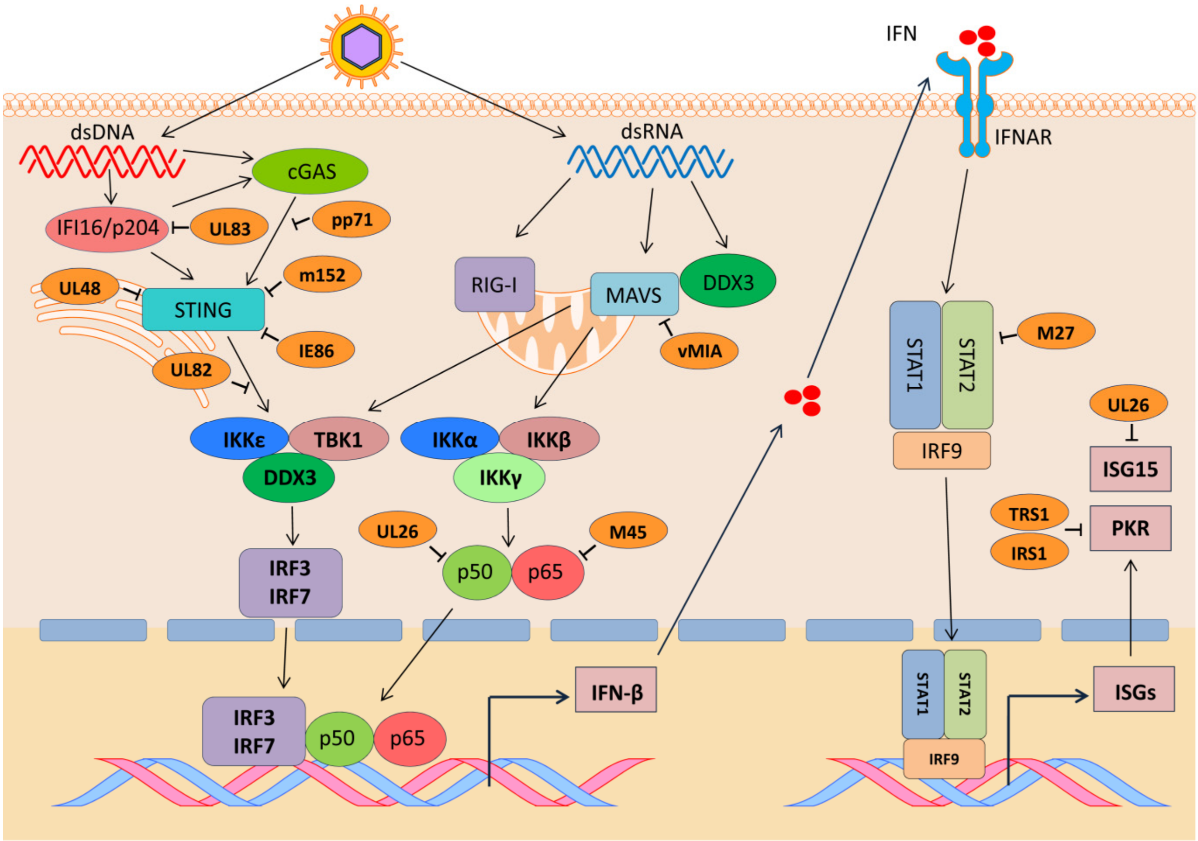
IFN
dsDNA
cGAS
dsRNA
IFNAR
IFI16/p204
UL83
pp71
UL48
m152
STING
IE86
UL82
RIG-I
MAVS
DDX3
vMIA
STAT1
STAT2
M27
IRF9
UL26
ISG15
IKKε
TBK1
DDX3
IKKα
IKKβ
IKKγ
UL26
M45
p50
p65
IRF3
IRF7
TRS1
IRS1
PKR
IFN-β
IRF3
IRF7
p50
p65
STAT1
STAT2
IRF9
ISGs

Figure 6. Modulation of the interferon-β response by human and murine cytomegalovirus. HCMV- and MCMV-encoded proteins (depicted in orange) downregulate different PRRs as well as downstream signalling molecules involved in the transcriptional activation of IFN-β and IFN-stimulated genes (ISGs).

3.7.1 Interferon-inducible protein 204

One of the key signaling molecules involved in DNA sensing upon viral infection and further IFN induction are PYHIN-domain proteins, also known as p200 proteins. This family includes four human (IFI16, AIM2, MNDA, and IFIX) and six mouse (p202a, p202b, p203, p204, MNDAL, and AIM2) PYHIN-domain proteins [97]. Most of the p200 proteins have been characterized by their ability to sense foreign DNA. Human IFI16 and mouse interferon-inducible phosphoprotein 204 (p204) are often described as orthologues, even though the sequencing homology between those proteins is rather low. They are both characterized by the presence of a pyrin (PYD) domain at the N-terminus. PYD domain is a death domain (DD) protein fold, which is essential for interactions with other PYD-containing proteins. In addition to PYD domains, PYHIN-domain proteins contain a conserved DNA-binding HIN-200 domain, and in the case of p204 and IFI16 there are two of these domains (Figure 7) [98].

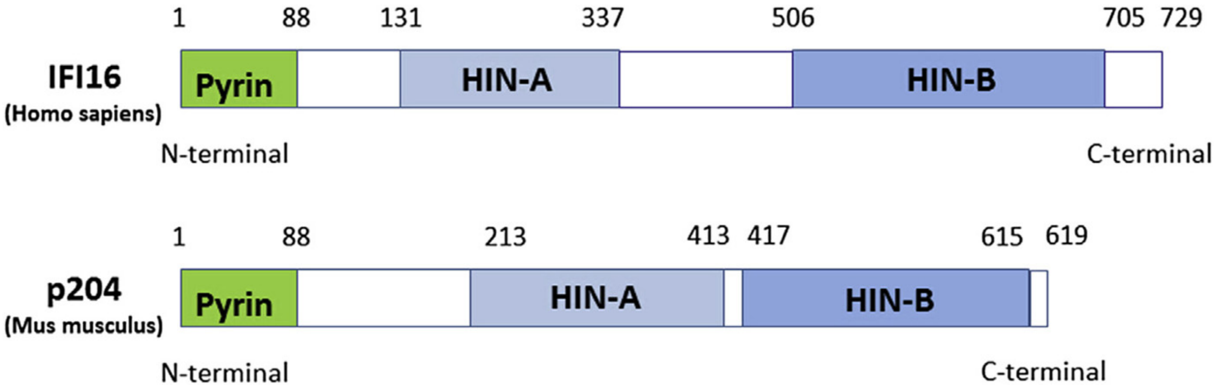

Figure 7. Molecular structure of mouse interferon-inducible protein p204 and its human orthologue IFI16. Picture acquired from [98].

At first, p204 was studied due to its role in cell proliferation and differentiation. The basal expression level of p204 varies depending on the tissue type and increases upon cell differentiation or IFN treatment. Under normal physiological conditions, p204 is localized in the nucleus, but it can also be found in the cytosol in the course of cell differentiation. p204 can also relocate to the cytoplasm upon phosphorylation [97, 99-101]. Cell proliferation is regulated by p204. The overexpression of p204 in mouse embryo fibroblasts (MEFs) promotes G1/S arrest of the cell cycle, as a result of p204 binding with retinoblastoma protein (pRb) [102].

More recent studies uncovered its role in antiviral signaling. p204 acts as a DNA sensor and activates IFN-β expression upon recognition of foreign DNA (Figure 6) [103]. Previously, p204 was found to recognize DNA and further activate IFN signaling via STING in herpes simplex virus (HSV)-1 infection. Furthermore, knockdown of p204 led to the impairment of NF-κB and IRF3-mediated IFN induction and compromised production of pro-inflammatory cytokines [104]. During MCMV infection, p204 was shown to be upregulated in fibroblasts (MEFs) at both the mRNA and protein level. Expression of p204 was found to be essential for MCMV replication and its ability to prompt cell cycle arrest at the G1/S border [105, 106].

3.8 Host factors crucial for viral replication

Viral replication is tightly connected to cellular metabolism. Like other viruses, CMV hijacks key factors of cellular genome expression in order to complete viral genome replication and produce progeny. This is possibly due to sophisticated exploitation of cellular factors required for gene expression. The importance of RNA helicase DDX3 and E3 ubiquitin ligase UBR5 in herpesvirus replication was recently identified [107, 108].

3.8.1 RNA helicase DDX3

RNA helicases have been shown to be crucial factors in RNA biogenesis due to their capacity to reorganize RNA secondary structures and ribonucleoprotein (RNP) complexes, and recent studies suggest that they are also involved in pathogen sensing and inflammasome activation [109, 110]. In particular, DEAD (Asp-Glu-Ala-Asp) box (DDX) helicase 3 (DDX3) is a multifunctional protein that is involved in different steps of RNA metabolism, cell cycle regulation, apoptosis, cancer, and viral infection [111, 112]. The DDX3X gene is located on the X chromosome and has a homologue DDX3Y, which is found in the non-recombining region of the Y-chromosome. They are considered to be functionally redundant. While DDX3X (further referred to as DDX3) is ubiquitously expressed, DDX3Y expression is limited to male germline cells. More recent studies revealed the expression of DDX3Y in certain immune cells, such as T-cells, B- and NK-cells [109, 113].

DDX3 belongs to the family of DDX RNA helicases, which are important players in RNA metabolism. DDX-helicases have two RecA domains, which harbor the motifs for RNA and ATP binding. Once helicases bind to RNA and ATP, they unwind RNA base pairs, and this process results in ATP hydrolysis (Figure 8).

DDX3 is essential for the early steps of embryonic development, such as placental development, and regulation of cell cycle and viability during embryogenesis [114]. Moreover, DDX3 appears to be dispensable for the expression of the genes involved in the vital cellular pathways. Chromatin immunoprecipitation studies showed its direct association with promoters of IFN-β and E-cadherin. Binding of the transcription factor Sp1 to the p21 promoter is enhanced by DDX3 [112].

DDX3 is also an essential component in RNA translation. Taking advantage of CRM1-dependent nuclear export pathways, DDX3 can shuttle between the nucleus and cytoplasm. This way it facilitates the nuclear export of cellular and viral mRNAs. DDX3 was shown to be crucial for the initiation of translation due to its association with translational factors, such as eIF4a, eIF3, eIF4G, eIF2a, and poly(A)-binding protein (PABP). More specifically, it positively regulates translation of some mRNAs that harbor long structured 5′ UTRs, for instance cyclin E1 mRNA, which is detrimental for cell cycle progression [111].

During stress conditions, such as viral infection, cells establish alternative mechanism of RNA processing. More specifically, cellular RNA granules, such as stress granules (SG) and processing bodies (P-bodies), are used as transport granules for mRNAs associated with RNA-binding proteins [115]. As a part of RNA helicase complex, DDX3 is implicated in the formation of different mRNA decay particles, including SGs and P-bodies, in an ATP-dependent manner [111, 116]. Likewise, activation of the inflammasome depends on the interaction between DDX3 and NLRP3. However, the sequestration of DDX3 to the stress granules appears to be crucial for the inhibition of NLRP3 inflammasome activation and decrease in production of inflammasome-dependent cytokines [110].

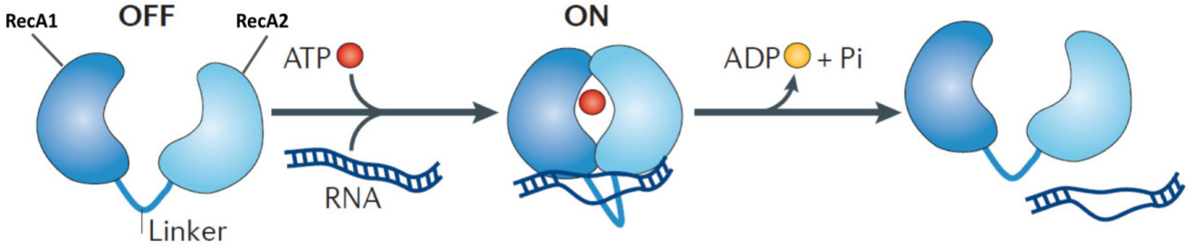

Figure 8. Schematic illustration of the mechanism of DEAD-box helicases. DDX3 helicases have short RecA domains connected by a linker in an open conformation (OFF). Upon binding to ATP and RNA, it changes conformation (ON). This readjustment is essential for ATP hydrolysis. This process triggers the release of the dissociated RNA strands and unwinds RNA base pairs. Modified from [111].

Numerous studies have identified DDX3 as part of the IFN-β signaling pathway. DDX3 was proposed to act as an RNA sensor and activate MAVS, as it was shown in HIV-1 infected dendritic cells [75]. Upon activation, it associates with the IKKε/TBK1 complex and leads to the autophosphorylation of IKKε and downstream activation of IRF3. TBK1 can phosphorylate DDX3, which subsequently leads to its binding and activation of the IFN-β promoter (Figure 9). DDX3 directly interacts with TRAF3 and facilities K63-linked autoubiquitination of TNF receptor-associated factor 3 (TRAF3), which was shown to be necessary for its association with IRF3 and MAVS and the subsequent enhancement of type I IFN signalling upon stimulation of the RIG-I pathway (Figure 9) [117]. Viruses have evolved a number of evasion mechanisms to counteract DDX3-mediated IFN-β activation.

Virus-encoded antagonists of DDX3 were identified for Vaccinia virus (VACV), Hepatitis C virus (HCV), and influenza virus [118-120].

Depending on the virus, DDX3 can either stimulate or repress viral replication. For Arenaviruses, DDX3 acts in a proviral fashion by promoting viral transcription and replication [121]. For HIV-1, DDX3 stimulates HIV-1 translation promoting viral mRNA nuclear export due to its ability to interact with the export protein CRM1 [122, 123]. In contrast, during influenza virus infection DDX3 exerts an antiviral effect by controlling virus-induced stress granule formation [124]. During Hepatitis B virus (HBV) replication, DDX3 dampens viral DNA synthesis by inhibition of viral reverse transcription [125].

The role of DDX3 in herpesvirus infections was so far poorly investigated. DDX3 was shown to be incorporated into the herpes simplex virus 1 (HSV-1) virions, and its presence in the mature virions affects their infectivity. Moreover, DDX3 protein levels influence HSV-1 gene expression and viral spread [107]. Upon HCMV infection, DDX3 acts as inducer of IRF3-dependent transcription leading to the activation of the IFN-β promoter [126]. DDX3 is packaged into HCMV virions, and its incorporation is dependent on the tegument protein pp65. Furthermore, the expression levels of DDX3 are augmented in HCMV-infected cells, therefore it is suggested to have a positive effect on HCMV replication [127].

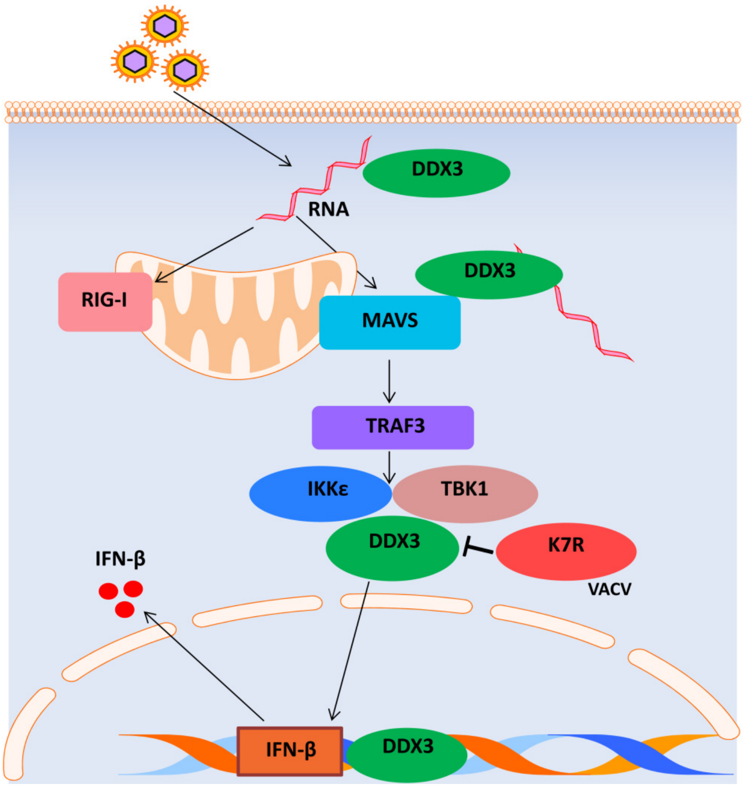

Figure 9. Role of DDX3 in the innate immune response signaling pathway against viruses. DDX3 is thought to act at different points in the IFN-β signaling pathway. (I)

DDX3 is a sensor of foreign RNA. RNA sensing triggers association of DDX3 with MAVS. (II) DDX3 associates with the IKK complex for downstream activation of IFN-β. (III) The promotor of IFN-β is activated upon binding of DDX3. Vaccinia virus (VACV) protein K7 specifically interacts with DDX3 for downregulate IFN-β transcription. Figure was modified from [128].

3.8.2 E3 ubiquitin protein ligase UBR 5

The Ubiquitin-Proteasome System (UPS) regulates a variety of fundamental cellular functions by degradation and functional modification of cellular proteins. Viruses have evolved to take advantage of ubiquitin machinery in order to escape from host immune responses and establish productive infection [129]. Ubiquitin protein ligase E3 component n-recognin 5 (UBR5) is primarily known for its role in cancer and development, but it is also implicated in the regulation of cell proliferation, mitosis, the DNA damage response, and transcription. Recent studies also indicate a role of UBR5 in viral replication. UBR5, also known as EDD (E3 identified by Differential Display), is a member of HECT (homologous to E6-AP C-terminus) E3 ubiquitin ligases. HECT ligases promote the post translation modification of proteins by forming a linkage between small protein ubiquitin (Ub) and the substrate proteins. Like other members of the HECT E3 Ub ligase family, UBR5 also has a HECT domain but does not use it for ubiquitination. Instead, the ubiquitin activation (UBA) domain is required for the reaction with Ub, and the zinc finger Ubiquitin Recognin Box (UBR) domain is essential for substrate recognition (Figure 10). However, UBR5 is a rather intriguing member of the HECT ligase family as among its numerous interaction partners, not all of the proteins are targeted for ubiquitination [130]. UBR5 is expressed in a wide range of cell types and found to be overexpressed or mutated in numerous cancers [131]. UBR5 is an essential protein for the growth of embryonic stem cells and the development of mouse embryos. Moreover, UBR5 is a crucial factor in the developmental processes as it transcriptionally activates Wnt/β-catenin signaling [132]. Knockout of UBR5 in mice leads to a failure of yolk sac development and chorioallantoic fusion, which is lethal [130, 133].

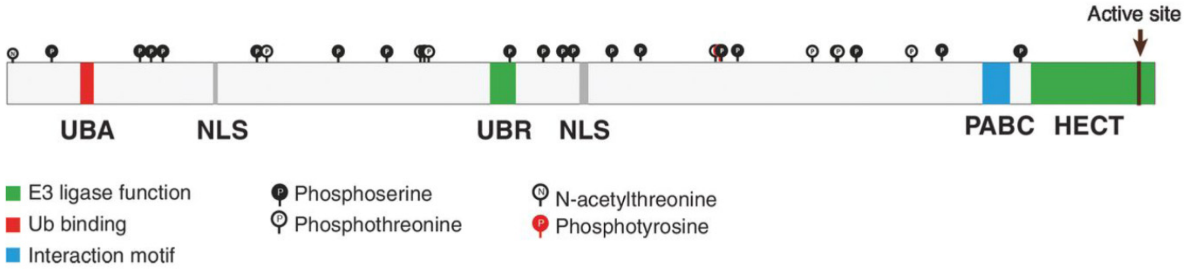

Figure 10. Schematic representation of the functional domains and posttranslational modification of UBR5. Ubiquitin activation (UBA), nuclear localization sequence (NLS), the Ubiquitin Recognin Box (UBR), Poly-Adenylation Binding Protein (PABC/MLLE) domain. Modified from [130].

The modulation of transcription is one of the key aspects of UBR5 function. Primarily, it was identified as a transcriptional modulator of progesterone and estrogen [130]. Recently, it was demonstrated that in T-helper (T_H17) lymphocytes, UBR5 decreases expression of pro-inflammatory cytokine IL17 by proteasomal degradation of its transcription factor RORγt [134]. A number of emerging roles of UBR5 in the DNA damage response was also reported. Upon DNA damage, UBR5 promotes phosphorylation of the serine/threonine-protein checkpoint kinase 2 kinase (CHK2), which is required for cell survival as it enables cell cycle arrest and DNA repair [135]**.** The ubiquitylation of histones after DNA breakage appears to be controlled by UBR5 [136]. Activation of another DNA damage regulator Ataxia-telangiectasia-mutated (ATM) at the DNA damage sites also requires UBR5 [137]. Moreover, it was recently shown that UBR5 controls the chromatin state during DNA replication, and therefore it is a critical factor for cell cycle progression [138].

Modulation of UBR5 was also observed upon viral infection. In cells infected with human papilloma virus (HPV), viral oncoprotein E6 and cellular ubiquitin ligase E6AP form a complex, which is used to degrade several host factors, specifically p53. UBR5 affects the proteolytic activity of the E6/E6AP complex. Consequently, the knockdown of UBR5 in HPV-infected cells reduces p53 levels and enhances cell survival and promotes cell cycle progression [139]. In HCMV-infected cells, UBR5 is an important factor for mRNA translation. Translation initiation factor poly(A)-binding protein 1 (PABP1) is curtailed in recruitment of the ribosome at the 5′ end of mRNA. This process can be inhibited by PABP-interacting protein 2 (Paip2), which appears to be a target for degradation by UBR5 [140].

During HCMV infection, activation of PABP1 by HCMV-encoded protein UL38 stimulates the translation of viral mRNAs. UBR5 together with its target Paip2 are also upregulated upon HCMV infection. Simultaneous increase of these factors is crucial for viral replication [108].

4 Aims of the study

The ability of cytomegaloviruses to replicate in a broad cell range within the host highly influences their pathogenesis. Some of the CMV US22 family proteins were described as determinants of cell tropism. Among them, the MCMV gene m139 was identified as important for viral replication in differentiated macrophages [66]. During MCMV infection, the m139 protein forms a complex with MCMV proteins m140 and m141 [67]. Together, these proteins are necessary for efficient viral replication in differentiated macrophages *in vitro* and in vivo [63]. However, the functions and mechanisms of action of the m139 – m141 proteins have remained unknown. Additionally, a mutation in m139 was identified in one of the human cell-adapted MCMV mutants previously isolated in our laboratory [39], suggesting that m139 might have a role as host range factor. To gain further insights into the mechanisms of CMV cell tropism and host species restriction, this study aimed at identifying the physiological role of the m139 gene product.

Previous studies have shown that deletion of the m139 gene from MCMV caused a replication defect in macrophages but no impact on replication in fibroblasts, suggesting that m139 might regulate viral replication in a cell type-dependent fashion. Therefore, the first aim of this study was to evaluate the role of m139 in determining the cell tropism of MCMV *in vitro* and its importance of m139 on viral replication in vivo. In addition, the impact of m139 on MCMV adaptation to replication in human cells was examined.

The second aim of this study was to find out which host factors and molecular pathways are modified by m139 upon MCMV infection. To this end, proteins interacting with m139 were identified by affinity purification and mass spectrometry. The identified interactions were verified and functionally analyzed with viral mutagenesis and CRISPR/Cas9 gene editing.

5 Results

5.1 Role of the MCMV protein complex m139-m141 in viral replication

In one of the first attempts to characterize the full MCMV coding potential, the viral genome was cleaved by the restriction enzyme HindIII into 16 fragments (HindIII A to HindIII P) [141]. The genetic locus containing the genes encoding for m139 as well as the two proximal m140 and m141 were firstly identified as a part of the HindIII-J region. In the following study, messenger RNAs originating from the m139-m141 locus were found to be transcribed from right to left (*i.e.* from the complementary strand), with early kinetics, and were classified as belonging to the US22 gene family, as they contain four US22-like motifs. Additionally, m139-141 have stretches of hydrophobic and charged residues, which are shared by US22 proteins [142]. While m139 encodes two proteins of 72 and 61 kDa, m140 and m141 each encode single proteins of 56 and 52 kDa, respectively. It was shown that the gene products of m139, m140, and m141 can interact with each other and form a complex in infected cells [67].

In order to gain insight into the biological roles of this complex, a triple mutant MCMV expressing tagged versions of m139, m140, and m141 was generated on the backbone of the MCMV Smith strain by *en passant* mutagenesis. This mutant, named MCMV V5139-FLAG140-141HA, carries a V5 epitope tag on the N-terminus of the m139 protein, a FLAG tag on the N-terminus of the m140 protein, and an HA tag on the C-terminus of the m141 protein. When murine NIH/3T3 fibroblasts were infected with MCMV V5139-FLAG140-141HA, the tagged versions of m139, m140, and m141 proteins were detected by western blot. As shown in Figure 1, tagged versions of m139, m140, and m141 exhibited previously described molecular weights. Notably, only the larger isoform of m139 is tagged because the smaller isoform starts at methionine 28, which is after the epitope tag [143]. All three proteins were detected after 2 hours post infection, suggesting that the gene products of m139-141 ORFs are early proteins (Figure 11).

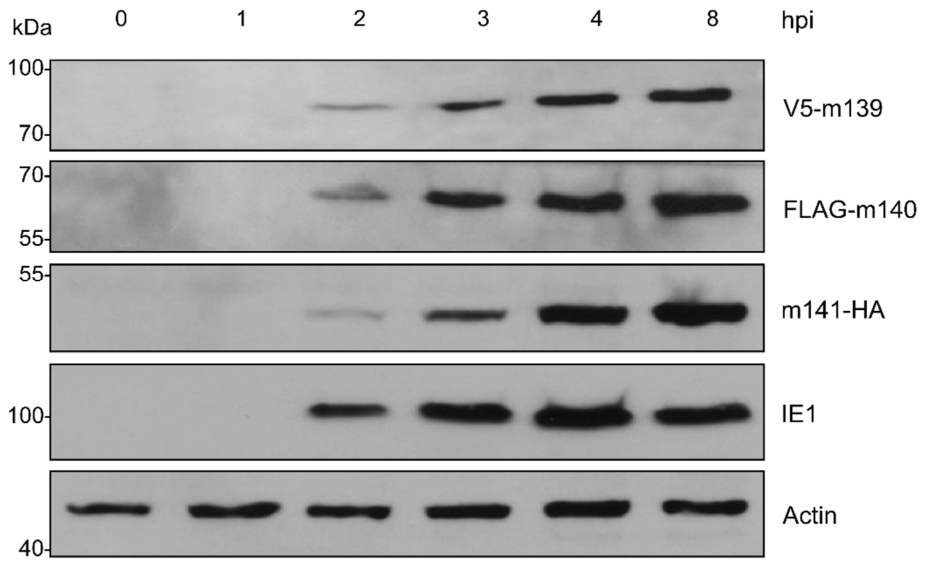

Figure 11. Expression kinetics of viral proteins V5-m139, FLAG-m140, and m141-HA. NIH/3T3 cells were infected with MCMV V5139-FLAG140-141HA at a multiplicity of infection (MOI) of 2 $TCID_{50}$/cell. Protein lysates were prepared at the indicated time points and analyzed by Western blot. Cell lysates were subjected to immunoblotting with antibodies specific for V5, FLAG, HA, MCMV immediate-early protein 1 (IE1), and actin.

In order to characterize the subcellular localization of the m139-m141 gene products, 10.1 fibroblasts were infected with MCMV V5139-FLAG140-141HA and analyzed by immunofluorescence. As shown in Figure 12, while m140 and m141 were detected predominantly in the cytoplasm, m139 was detected in the cytoplasm with a dispersed distribution and in the nucleus with a dot-like distribution.

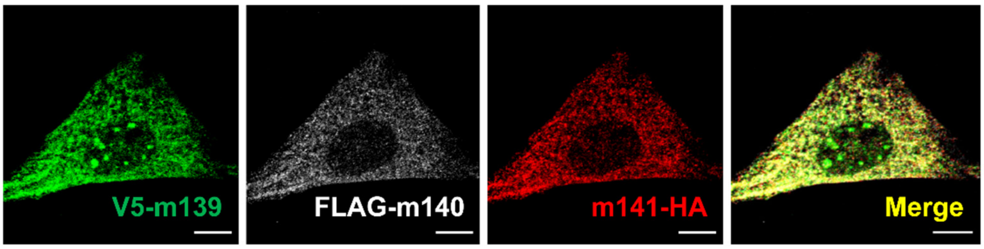

Figure 12. Intracellular localization of viral proteins V5-m139, Flag-m140, and m141-HA in MCMV infection. 10.1 cells, seeded on coverslips, were infected with MCMV V5139-Flag140-141HA at MOI of 1 $TCID_{50}$/cell. 8 hours post infection (hpi) cells were fixed for immunostaining. Antibodies specific for V5, FLAG, and HA were applied. Subcellular localization of the tagged proteins was imaged by confocal microscopy. Scale bar, 10 µm.

Previous studies have shown that MCMV transposon-insertion mutants lacking m139, m140, or m141 fail to replicate efficiently in macrophages. However, these mutants do not show a replication defect in fibroblasts [63, 66]. Therefore, the impact of this region on MCMV replication was further analyzed. In order to achieve a precise removal of these three genes with minimal effects on neighboring genetic regions, the m139-141 gene region was deleted from the MCMV Smith strain by *en passant* mutagenesis.

The MCMV Δm139-141 virus lacks the three genes of interest and was used to infect murine fibroblasts. The immediate-early proteins 1 and 3 (IE1 and IE3) and early proteins M45, M57, and M142 were expressed with similar kinetics as wild type (Figure 13A). On the contrary, in murine J774A.1 macrophages the mutant MCMV Δm139-141 virus exhibited a different viral protein expression profile than the MCMV WT (Figure 13B). While the immediate-early protein IE1 and IE3 as well as the early proteins M45 and M57 were expressed at similar levels in macrophages, the early proteins E1 and m142 were expressed at much lower levels in Δm139-141 infected macrophages as compared to MCMV WT infected cells. This data confirms the previous observations and suggest that the m139-141 genes are important in macrophages.

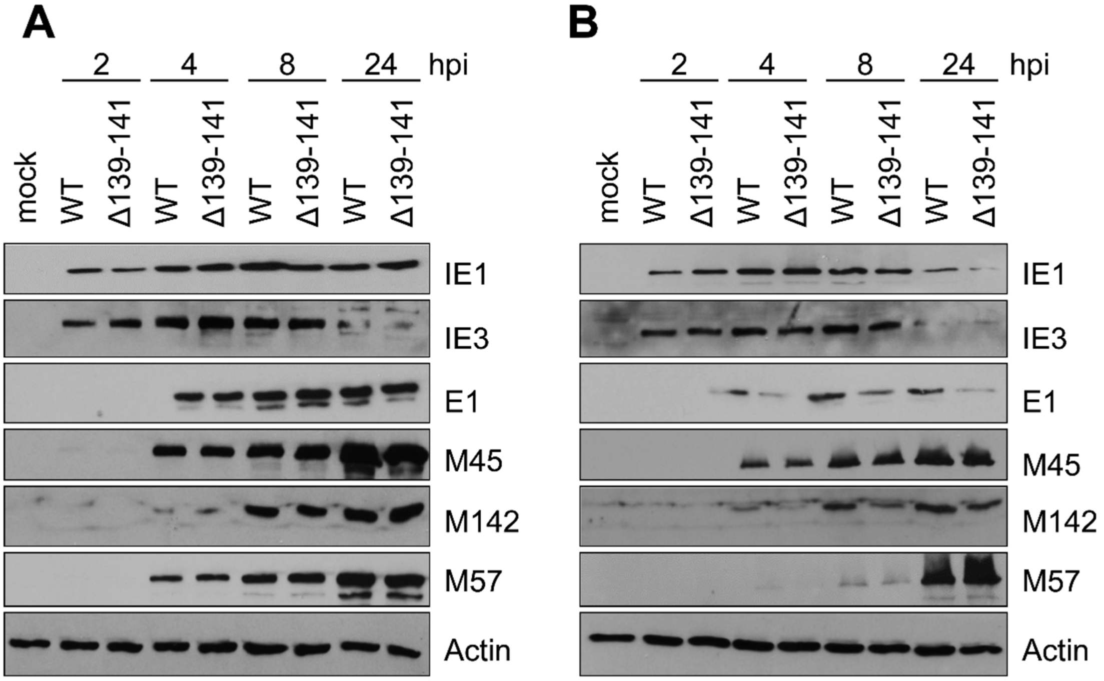
A
2
4
8
24
hpi
mock
WT
Δ139-141
WT
Δ139-141
WT
Δ139-141
WT
Δ139-141
IE1
IE3
E1
M45
M142
M57
Actin
B
2
4
8
24
hpi
mock
WT
Δ139-141
WT
Δ139-141
WT
Δ139-141
WT
Δ139-141
IE1
IE3
E1
M45
M142
M57
Actin

Figure 13. Expression kinetics of MCMV proteins in Δm139-141- and WT-infected fibroblasts (A) and macrophages (B). 10.1 fibroblasts and J774A.1 macrophages were infected at MOI of 5 $TCID_{50}$/cell. At indicated time points cells were lysed. Cell lysates were subjected to immunoblotting with antibodies specific for MCMV immediate early proteins 1 and 3 (IE1 and IE3) and early proteins 1 (E1), M45, M142, and M57. Actin is used as a loading control.

5.2 Characterization of the m139 protein during MCMV infection

Due to the peculiar distribution pattern of m139 protein in both the cytoplasm and the nucleus of infected cells, the physiological role of m139 during MCMV replication was further analyzed. By *en passant* mutagenesis, an MCMV m139-HA mutant was generated after insertion of an HA tag on the C-terminus of m139 in order to tag both of the m139 isoforms. Unlike MCMV V5139-Flag140-141HA, cells infected with MCMV m139-HA expressed detectable levels of both m139 isoforms, namely the 72 and 61 kDa proteins (Figure 14).

In order to verify the classification of m139 as an early gene, the expression m139-HA was investigated by cycloheximide (CHX) release assay (Figure 14). In this assay, cells were either left untreated or treated with CHX, a known inhibitor of the translation elongation. 4 hours post infection, cells were washed and incubated in normal medium, in order to relieve the inhibition, or in medium containing Actinomycin D (ActD), an inhibitor of DNA-dependent transcription. As shown in Figure 14, while untreated and CHX only treated 10.1 cells expressed both IE1 and the early protein M112-113 (E1), cells treated with CHX and ActD expressed only the IE1 protein but not the early protein M112-113 (E1) or m139-HA protein, thus confirming that m139 is a true early gene.

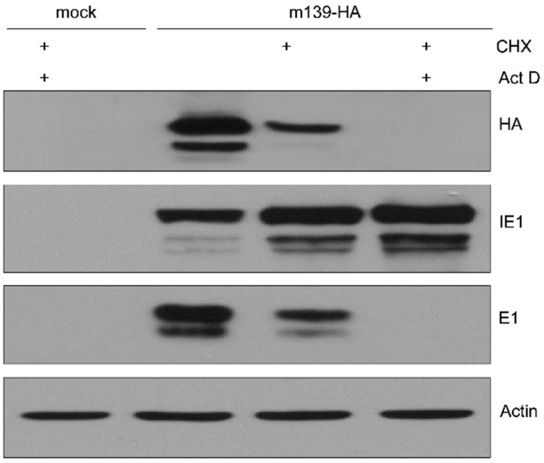

Figure 14. Expression kinetics of m139 gene product. Murine 10.1 fibroblasts were treated with cycloheximide (CHX 5μg/ml) for 30 minutes prior to infection with MCMV m139-HA at MOI 3 $TCID_{50}$/cell. At 4 hpi, cells were washed and either left untreated of treated with Actinomycin D (ActD 50μg/ml) for an additional 4 hours. Cell lysates were prepared at 8 hpi and analyzed by immunoblot.

Earlier studies report conflicting localization profiles for m139 during MCMV infection. At late times post-infection in both fibroblasts and macrophages, m139 has been detected in both nuclear and cytoplasmic fractions [143]. However, m139 has also been found in the cis-Golgi compartment, in proximity of its interaction partners m140 and m141 [67]. In order to clarify the subcellular localization during infection, cell fractionation analyzes were conducted in 10.1 fibroblast cells infected with MCMV m139-HA. As shown in Figure 15A, at early and late times post infection, m139 was present in both cytoplasmic and nuclear fractions in comparable amounts. To get more details about the localization of m139, immunofluorescence assays were also conducted in the same cells (Figure 15B). As shown in Figure 15B and C, at early and late times post infection, m139 was detected in the nucleus with a punctate distribution. While m139 localized in a dispersed fashion in the cytoplasm early in infection, it was found in dot-like structures in proximity to the nucleus at later times post infection.

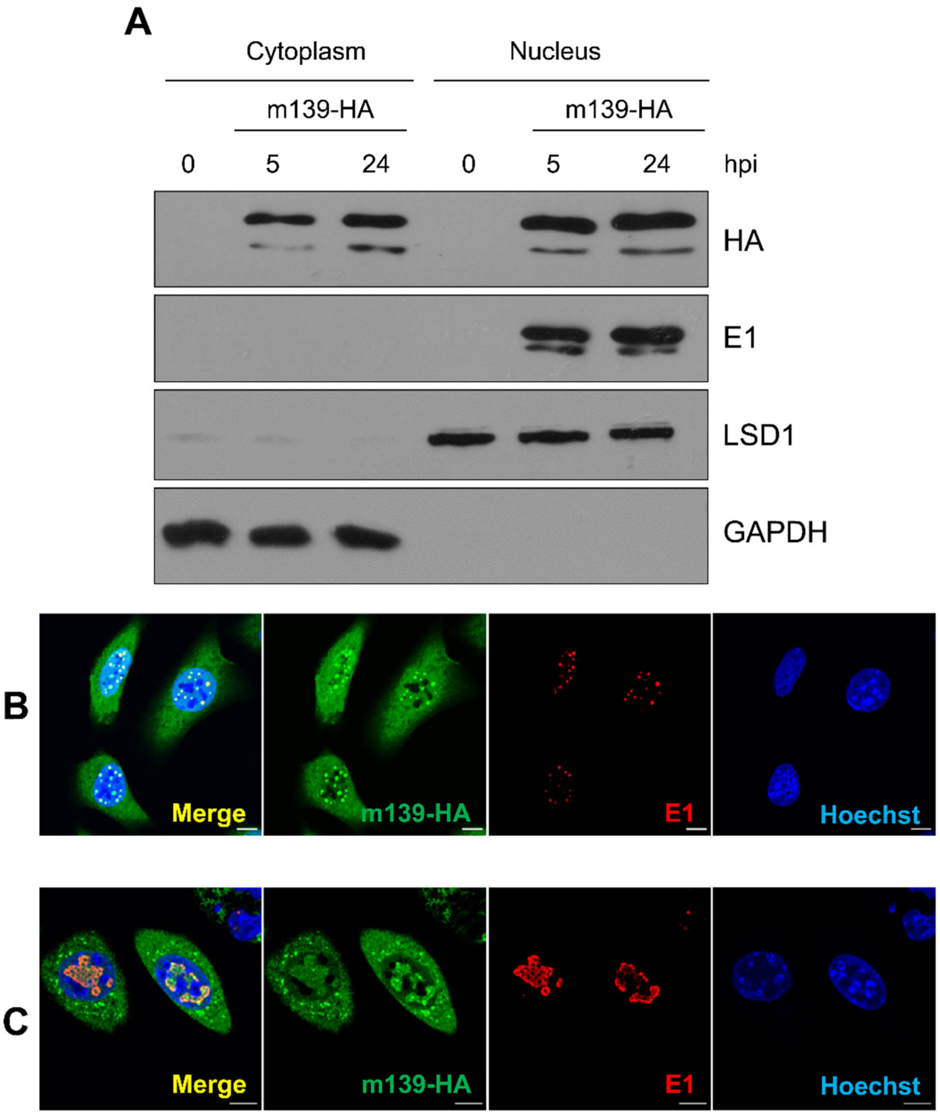

Figure 15. Subcellular localization of the m139 gene product. A. 10.1 fibroblasts were infected by MCMV m139-HA at MOI 5 $TCID_{50}$/cell. At 5 and 24 hours post infection, nuclear (N) and cytoplasmic (C) fractions were separated and further analyzed by Western blotting. B, C. 10.1 fibroblast were infected at MOI 1 $TCID_{50}$/cell prior to fixation at 5 (B) and 24 hpi (C). Immunofluorescence staining was performed with anti-HA and anti-E1 antibodies and DRAQ5 for nuclear staining. Images are representative of 3 experiments imaged by confocal microscopy. Scale bar, 10 µm.

The peculiar distribution of m139 in the nucleus resembled the architecture of the viral replication compartments, structures formed by E1 proteins at sites where viral and cellular proteins assemble to efficiently replicate the viral genomes [144]. Indeed, staining for E1 in MCMV-infected cells revealed that m139 and E1 co-localize in the viral replication compartment during the course of MCMV infection.

Taking into account that m139 is found in both the nucleus and the cytoplasm of infected cells, its amino acid sequence was analyzed for a nuclear localization signal and a nuclear export signal (NES). Using computational tools, the potential NES peptide ESDGLYYAARNIDQL was mapped to the C-terminal residues 283-297 of m139 protein. Consistent with this finding, exogenous expression of HA-m139 from an expression vector exhibited an exclusively cytoplasmic localization (Figure 16A). Considering that upon infection m139 is found in the replication compartment, I hypothesized that E1 could be involved in the nuclear relocalization of m139. As shown in Figure 16B, co-expression of m139 and E1 lead to the recruitment of m139 to E1 nuclear dots, suggesting that formation of E1 dots in the nucleus is crucial for recruitment of m139 to the replication compartment (Figure 16B).

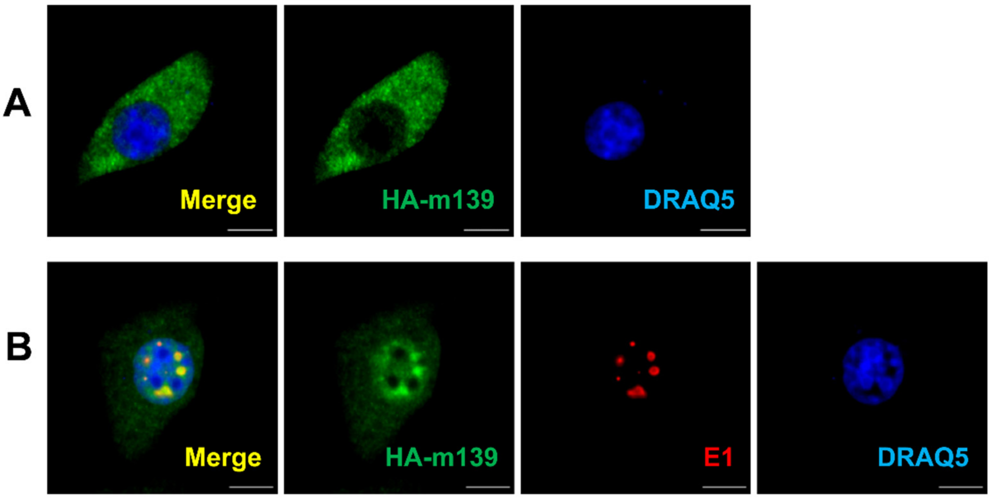

Figure 16. m139 is recruited to E1 nuclear dots by E1 proteins. NIH/3T3 fibroblasts were transfected with HA-m139 alone (A) or HA-m139-HA and E1 (B). 24 hours later, cells were fixed and investigated by immunofluorescence. Antibodies specific for HA-tag

and E1 proteins were applied. Nuclei were stained using DRAQ5. Images are representative of 4 experiments and were taken with a confocal microscope. Scale bar, 10 µm.

5.3 Role of m139 in determining the cell tropism range of murine cytomegalovirus

Even though the findings obtained with the mutant MCMV Δm139-141 virus suggest that the m139-141 genes are important for replication in macrophages, it was crucial to identify the effect of m139 on viral replication in different cell lines. In order to investigate this aspect, an MCMV m139-STOP mutant was generated. This mutant was created by the insertion of an HA tag and single nucleotide mutation at the N-terminus of m139, which resulted in the generation of a STOP codon. The insertion of a STOP codon abolished the expression of both isoforms of m139 but left both m140 and m141 unaffected.

As shown in Figure 17, the replication properties of the MCMV m139-STOP mutant were compared to the wildtype MCMV m139-HA by multistep replication kinetics in different murine cell types. Epithelial TCMK-1 cells, 10.1 fibroblasts, SVEC4-10 endothelial cells and immortalized bone marrow derived macrophages (iBMDM) were used. In 10.1 fibroblasts and epithelial TCMK-1 cells, MCMV m139-STOP mutant replicated to the same levels as MCMV m139-HA (Figure 17A and B). By contrast, the inactivation of m139 led to significantly reduced replication in endothelial SVEC4-10 cells (Figure 17C). Comparison of MCMV m139-HA to MCMV WT demonstrates that the HA epitope tag inserted at the C-terminal end of the m139 ORF has no effect in this assay. Similarly, the deletion of m139 also led to a noticeable growth deficit in iBMDM (Figure 17D). These results confirmed that m139 is required for efficient MCMV replication in specific cell lines, such as macrophages and endothelial cells, but is dispensable in fibroblasts and epithelial cells.

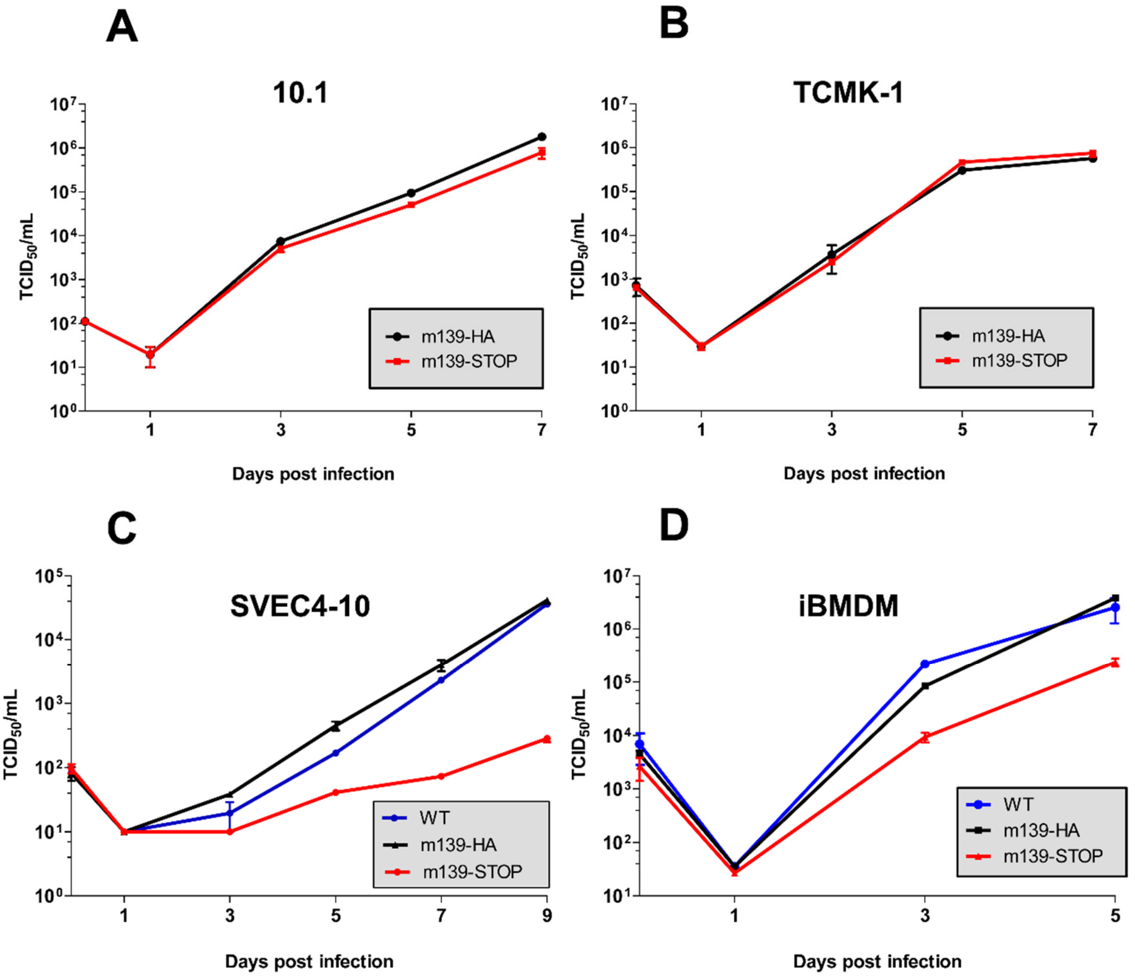

Figure 17. Replication kinetics of m139 mutants in different murine cell lines. Monolayers of 10.1 fibroblasts (A) or epithelial TCMK-1 cells (B) were infected with m139-HA and m139-STOP MCMV at MOI 0.01 $TCID_{50}$/cell. C. Endothelial SVEC4-10 cells were infected with MCMV WT, m139-HA, and m139-STOP at MOI 0.01 $TCID_{50}$/cell. Supernatants from all infected cell types were collected for titration at the indicated time points. D. Immortalized bone marrow derived macrophages (iBMDM) were infected with MCMV WT, m139-HA, and m139-STOP at MOI 0.025 $TCID_{50}$/cell. Supernatants from infected cells were collected for titration at the indicated time points. Viral titers are shown as mean ±SEM.

5.4 The interplay between m139 and interferon-inducible protein p204 during MCMV infection

Myeloid cells are important innate immune effectors and major inducers of IFNs upon CMV infection [64]. In a recent screen for MCMV-encoded inhibitors of the cGAS-STING signaling pathway, m139 was identified as one of several possible inhibitors of the IFN-β promoter [88]. The effect of m139 on IFN-β induction was investigated in bone marrow-derived macrophages containing luciferase under the control of the IFN-β promoter

[145]. Upon MCMV m139-HA infection, an increase in luciferase expression was detected, indicating that IFN-β was activated. Infection with MCMV m139-STOP resulted in significantly higher induction of IFNβ, suggesting that m139 is involved in curtailing IFN-β induction (Figure 18).

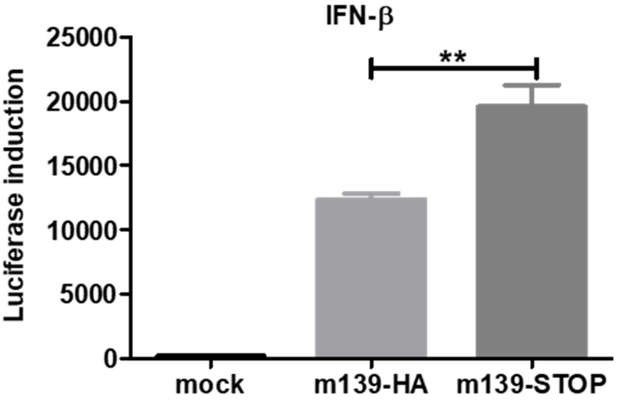

Figure 18. Impact of m139 on IFN-β activation in macrophages. Reporter bone marrow derived macrophages expressing luciferase under the control of the IFN-β promoter were infected with MCMV m139-HA or m139-STOP. At 8 hpi, cells were lysed and luminescence was measured. Mean ±SEM of 3 independent replicates are shown. **, p<0.01.

Given the inhibitory effect of m139 on IFN-β production, m139 may influence the signalling molecules involved in the activation of IFN-β signalling. Considering the localization of m139 to the virus replication compartments in the nucleus, I hypothesized that m139 might affect nuclear DNA senor p204.

Since previous studies have reported that p204 expression levels vary between cell types [100], the endogenous levels of p204 in various murine cell lines were compared. While the macrophage cell lines RAW264.7 and J774A.1 did not express detectable levels of p204, murine SVEC4-10 endothelial cells exhibited the highest p204 expression levels (Figure 19). Remarkably, MCMV m139-STOP also showed a replication defect in SVEC4-10 cells (Figure 17D).

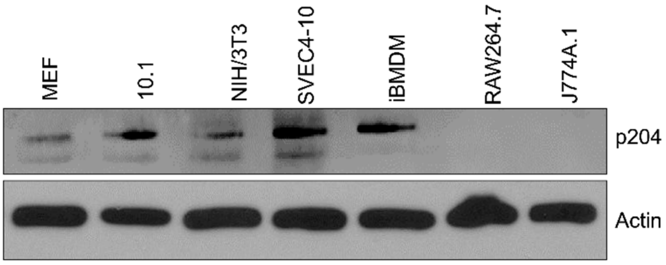

Figure 19. Expression of p204 in different murine cell lines. WT immortalized MEFs, 10.1, NIH/3T3, SVEC4-10, IBMDM, RAW264.7, and J774A.1 cells were lysed using NP-40

buffer. 30 μg of each lysate was used for immunoblotting with antibodies for p204 and actin.

Since it has been previously shown that the interferon-inducible protein p204 is primarily found in the nucleus but is recruited to the cytoplasm upon phosphorylation [100], SVEC4-10 cells stably expressing p204-Myc were generated in order to investigate the localization of p204 during the course of MCMV infection. While in uninfected cells p204 was localized in the nucleus in a dispersed fashion (Figure 20A), upon MCMV m139-HA infection p204 localized to the viral replication compartments at early times post infection and became almost undetectable at later times post infection (Figure 20B). Surprisingly, in cells infected by MCMV m139-STOP, p204 remained associated with the nuclear replication compartments (Figure 20C).

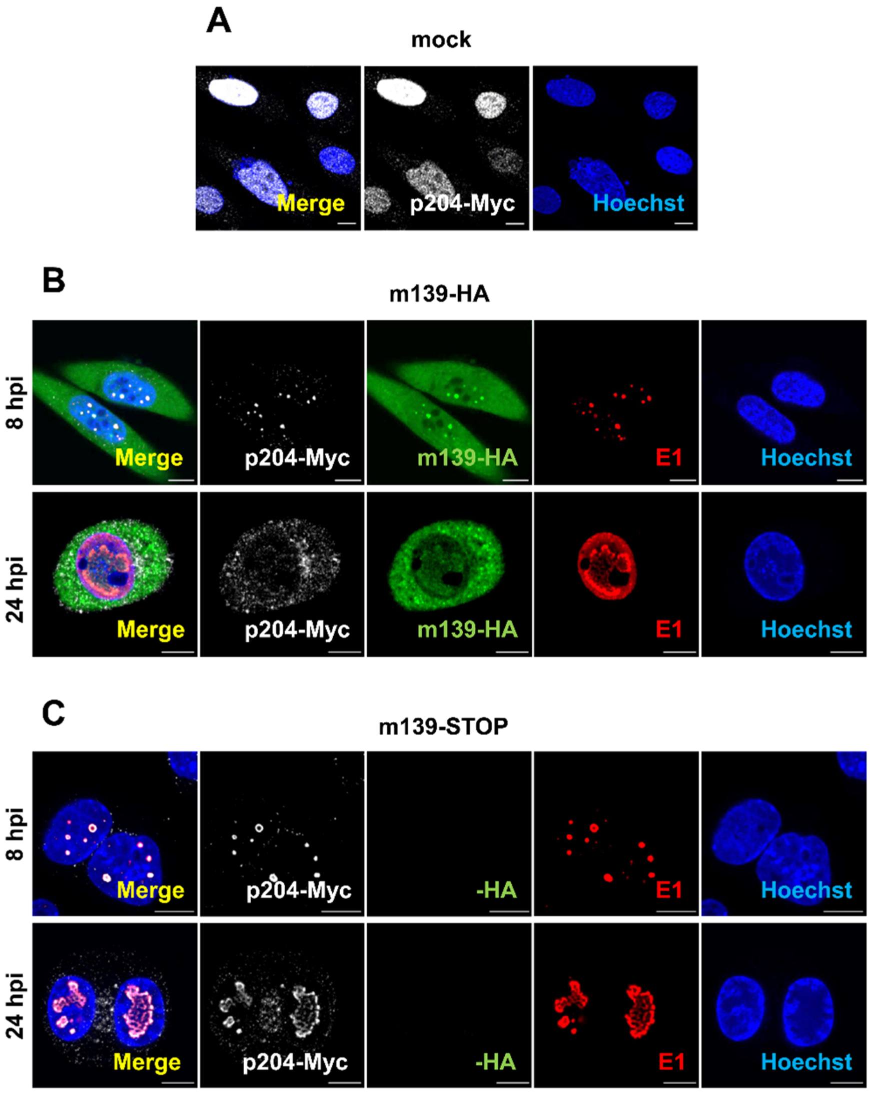
A
mock
Merge
p204-Myc
Hoechst
B
m139-HA
8 hpi
24 hpi
Merge
p204-Myc
m139-HA
E1
Hoechst
C
m139-STOP
8 hpi
24 hpi
Merge
p204-Myc
-HA
E1
Hoechst

Figure 20. Effect of m139 on the localization of p204 upon MCMV infection. A. Uninfected SVEC4-10 cells stably expressing p204-Myc were fixed and stained for

immunofluorescence, and p204-Myc transduced SVEC4-10 cells were infected either by MCMV m139-HA (B) or MCMV m139-STOP (C) using an MOI 1 $TCID_{50}$/cell and fixed at 8 and 24 hpi. Subcellular localization of p204-Myc, m139-HA, and E1 was analyzed by immunofluorescence using Myc, HA, and E1 specific antibodies. Images representative of 2 independent experiments were taken with a confocal microscope. Scale corresponds to 10 µm.

Next, the effect of m139 on the expression levels of endogenous p204 during MCMV infection was examined. SVEC4-10 were infected either with MCMV WT or MCMV Δm139 mutant, in which the complete m139 ORF was deleted by BAC mutagenesis. As it shown in Figure 21, p204 expression levels decreased upon infection with MCMV WT. Protein levels of p204 were slightly higher in MCMV Δm139-infected compared to MCMV WT-infected cells at late times postinfection (Figure 21). Taken together, these results suggested that m139 might be involved in the downregulation of p204 during infection.

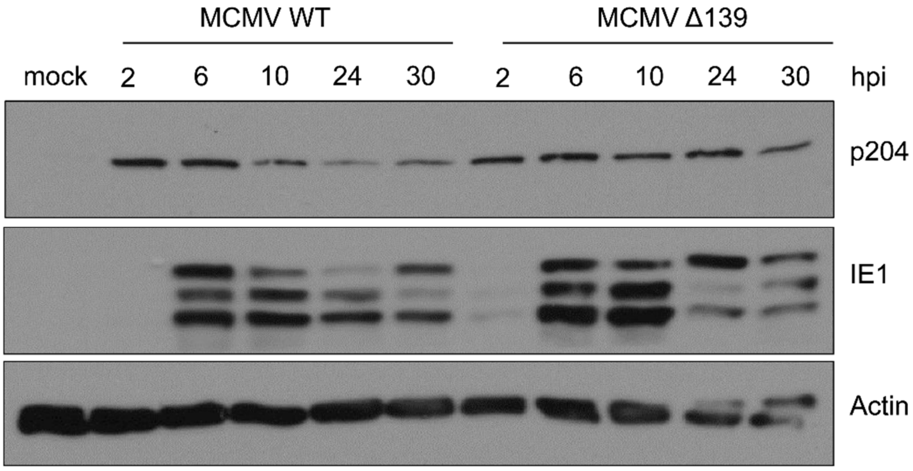

Figure 21. p204 expression during infection MCMV infection is reduced by the m139 protein. SVEC4-10 cells were infected with MCMV WT or MCMV Δm139 at MOI 5 $TCID_{50}$/cell. Protein lysates were prepared at the indicated time points and analyzed by Western blot. Cell lysates were subjected to immunoblotting with antibodies specific for p204, IE1, and actin.

Given the observed modulation of p204 expression and localization by m139 upon infection, the role of p204 in MCMV replication in SVEC4-10 cells was assessed. p204 knockout ($p204^{-/-}$) SVEC4-10 cells were generated using CRISPR/Cas9 gene editing (Figure 22A). In order to perform multistep replication analyzes using MCMV WT and MCMV Δm139 mutant. Similar to MCMV m139-STOP, the MCMV Δm139 mutant had a replication deficient in SVEC4-10 cells (Figure 22B). The knockout of p204 did not affect the replication of wild type MCMV. However, in $p204^{-/-}$ SVEC4-10 cells the replication impairment exhibited by the MCMV Δm139 mirrored the replication defect exhibited by MCMV Δm139 in normal SVEC4-10 cells (Figure 22B), thus suggesting that p204 did not account for the replication defects in these cells. Even though m139 has an effect on p204 expression and intracellular localization during MCMV infection of endothelial cells, p204 does not influence replication properties of MCMV Δm139.

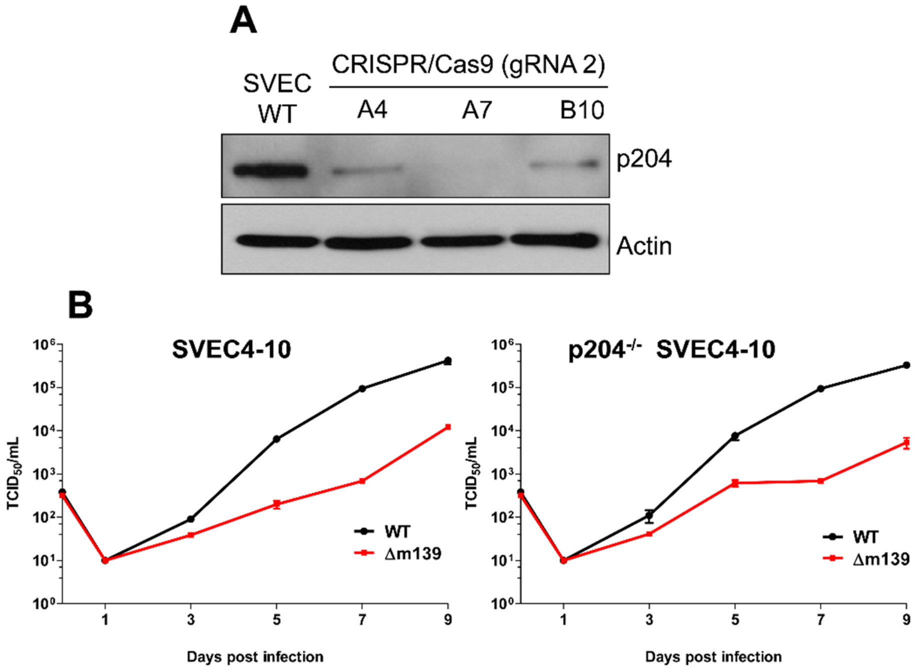

Figure 22. Impact of p204 expression on the Δm139 replication in murine endothelial cells. A. Cell lysates were obtained from different single-cell clones of p204 knock-out (p204-/-) SVEC4-10 cells and tested by immunoblotting using antibodies specific to p204 and actin. Cell lysate from WT SVEC4-10 cells was used as a control. B. Monolayers of p204-/- (clone A7) and WT SVEC4-10 cells were infected with m139-HA and m139-STOP MCMV at MOI 0.01 $TCID_{50}$/cell. At the indicated time points post infection, supernatants were collected for titration. Viral titers are shown as mean ±SEM.

5.5 Interaction partners of m139 in endothelial cells

In order to gain further insight into the role of m139 in MCMV replication, it was important to identify m139-intecting proteins upon MCMV infection. Using stable isotope labelling amino acids in cell culture (SILAC) coupled to affinity purification-mass spectrometry (AP-MS), interaction partners of m139 among both host and viral proteins were identified. Immunoprecipitation products from MCMV m139-HA -infected SVEC4-10 cells compared to MCMV WT were analyzed. The candidates with an enrichment $\log_2$ ratio <2 or less than 2 unique peptides detected were excluded from the analysis. This approach identified 11 putative interaction partners of m139 (Table 1). Already known interaction partners of m139, the US22 proteins m140 and m141, were found in the screen [67]. Another MCMV US22 protein, m142, was identified as a possible interaction partner. Among host proteins, Myosin phosphatase Rho-interacting protein (Mprip), E3 ubiquitin-protein ligase UBR5, Ankycorbin, GEM-interacting protein (Gmip), Interferon-induced protein with tetratricopeptide repeats 1 (IFIT1), Codanin-1 (Cdan1), ATP-dependent RNA helicase DDX3, and Unconventional myosin-Ic (Myo1c) were detected in the SILAC screen. These proteins are identified as parts of numerous cellular pathways. DDX3X, UBR5, and IFIT1 were previously described to affect HCMV replication and therefore were prioritized [108, 126, 146].

Table 1. m139 interaction partners identified by affinity purification-mass spectrometry (AP-MS)

Protein name	Number of peptides in 1st replicate	Ratio L/H	Number of peptides in 2nd replicate	Ratio H/L
Myosin phosphatase Rho-interacting protein (Mprip)	14	56.3380	11	53.1283
MCMV protein m141	31	46.729	27	58.7299
MCMV protein m140	26	39.5257	19	35.92
E3 ubiquitin-protein ligase UBR5	12	14.8038	8	31.2637
Ankycorbin	20	18.9036	12	22.4951
GEM-interacting protein (Gmip)	8	16.3666	5	20.3356
Interferon-induced protein with tetratricopeptide repeats 1 (IFIT1)	13	7.0522	12	14.70475
ATP-dependent RNA helicase DDX3	2	7.93344	2	5.92995
Codanin-1 (Cdan1)	3	3.6711	3	7.8102
MCMV protein m142	9	3.0516	12	2.5817
Unconventional myosin-Ic (Myo1c)	2	2.0429	2	2.33615

In order to confirm the interaction of m139 with the proteins identified in the AP-MS screen, HA-pull down assays were performed with lysates obtained from SVEC4-10 cells infected with MCMV m139-HA or MCMV M45-HA, a virus carrying the HA tag on the unrelated protein M45, which served as a negative control. Even though the interaction with IFIT1 was not confirmed, specific antibodies against DDX3 and UBR5 reproduced the SILAC screen results and revealed a physical interaction of DDX3 and UBR5 with m139 (Figure 23).

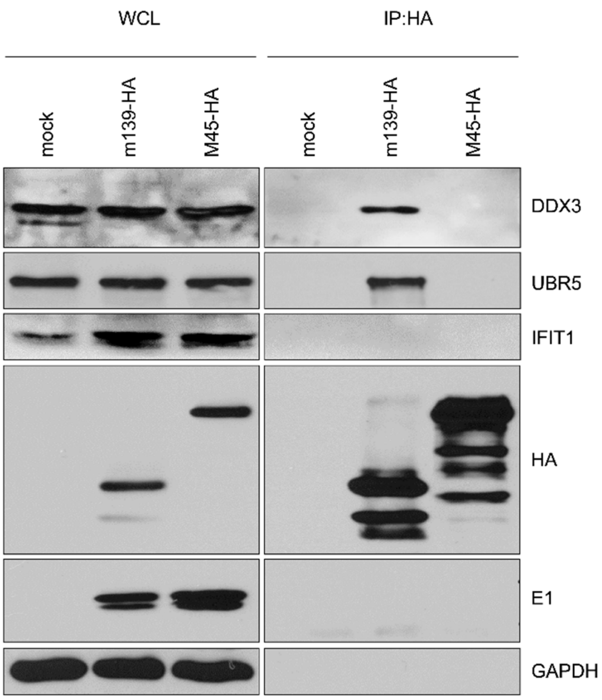

Figure 23. Interaction partners of the m139 gene product. SVEC4-10 cells were infected at MOI 5 $TCID_{50}$/cell, lysed, and subjected to immunoprecipitation (IP) using an anti-HA affinity matrix. Immunoprecipitates were detected using immunoblotting. Antibodies specific for DDX3, UBR5, HA, E1, and GAPDH were used.

5.6 Characterization of the m139 interacting host proteins DDX3 and UBR5

DDX3 is a multifunctional protein that is well known for its role in the numerous steps of RNA biogenesis as well as in IFN signalling [76, 109, 111]. Considering the cytoplasmic and nuclear distribution of m139, it was important to dissect in which intracellular compartment m139 and DDX3 could interact. To analyze this aspect, immunofluorescence assays were performed in MCMV-infected SVEC4-10 cells. In uninfected cells, DDX3 appeared to be homogeneously distributed in the cytoplasm and a small fraction accumulated in nuclear dots, which supposedly correspond to nuclear speckles, where DDX3 interacts with pre-mRNAs [147] (Figure 24). In MCMV infected cells, DDX3 preserved its dual localization as it was found in both the cytoplasm and nucleus. In the nucleus of MCMV infected cells, DDX3 was already recruited to the viral replication compartments at early times post infection as shown by its co-localization with the viral protein E1. Interestingly, upon infection with MCMV m139-STOP, the recruitment of DDX3 to the replication compartments is very faint, thus suggesting that during MCMV infection, DDX3 might be recruited to the replication compartments by m139.

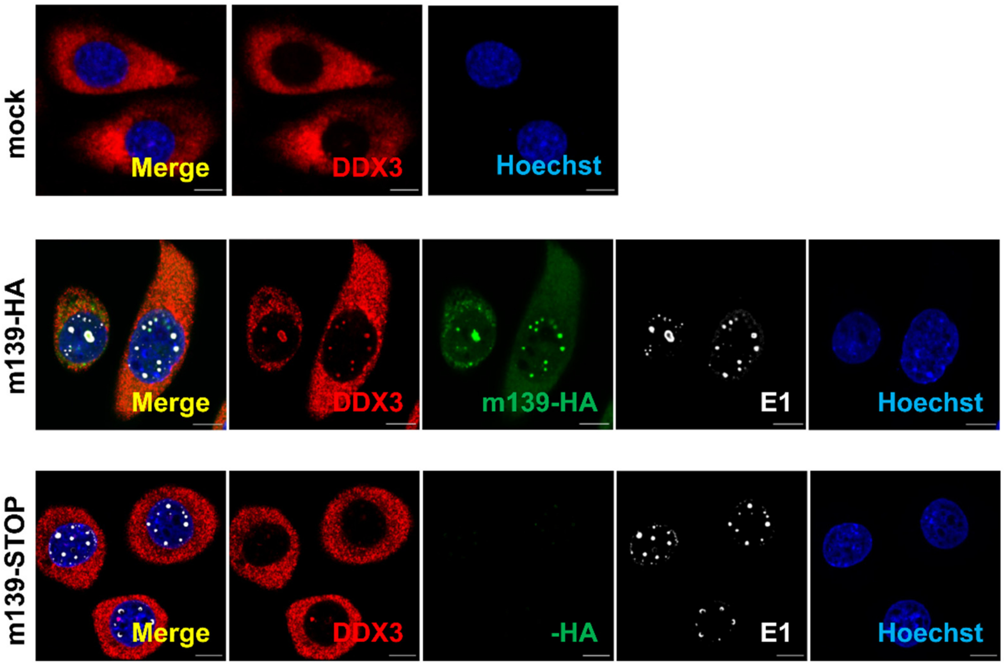

Figure 24. DDX3 is recruited to the viral replication compartments by m139. SVEC4-10 cells infected with MCMV m139-HA or MCMV m139-STOP at MOI 1 $TCID_{50}$/cell and fixed at 8 hpi. Subcellular localization of DDX3, m139-HA, and E1 was analyzed by immunofluorescence using anti-DDX3 and anti-HA antibodies. Hoechst was used for the nuclear staining. Images representative of 3 independent experiments were imaged by confocal microscopy. Scale bar, 10 µm.

In infected cells, DDX3 could act in two possible fashions: DDX3 could be a factor required for virus replication or it could act as a restriction factor. In the case of MCMV, the role of DDX3 had not been elucidated. Considering the replication defect of MCMV m139-STOP in endothelial cells, it was worthwhile to test whether DDX3 played any role. Taking advantage of CRISPR/Cas9 technology, DDX3 knockout SVEC4-10 cells ($DDX3^{-/-}$ SVEC4-10) were generated (Figure 25A). A complete knockout of DDX3 is SVEC4-10 cells was not achieved, as low expression levels of DDX3 were detected in only one cell clone and were progressively increasing upon passaging of the cells. Considering the importance of DDX3 for cellular proliferation, there is probably a positive selection for cells with intact DDX3 [148]. Next, multistep replication kinetics were performed in $DDX3^{-/-}$ as well as wildtype SVEC4-10 cells using MCMV m139-HA and m139-STOP viruses. As it was previously observed, m139-STOP MCMV had a replication defect in WT SVEC4-10 cells (Figure 25B). In contrast, in $DDX3^{-/-}$ SVEC4-10 cells the MCMV m139-STOP virus replicated to the same extent as MCMV m139-HA, demonstrating that the replication defect caused by the absence of m139 was complemented by DDX3.

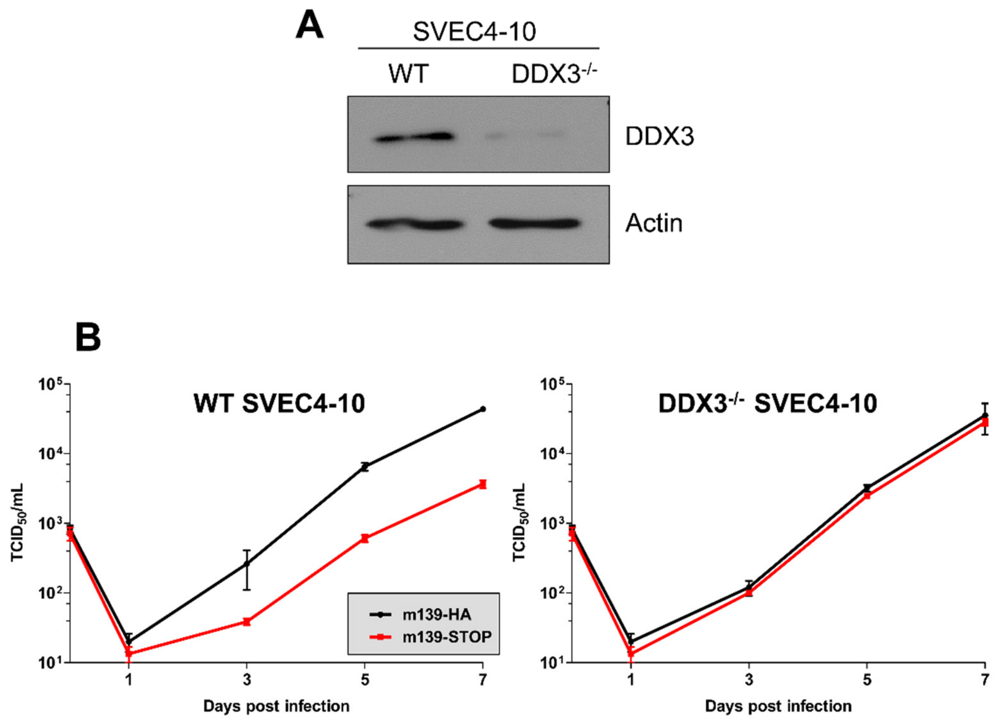

Figure 25. Replication defect of m139-STOP MCMV in SVEC4-10 cells is DDX3-dependent A. Cell lysates from DDX3 incomplete knockout (DDX3$^{-/-}$) and WT SVEC4-10 cells analyzed by western blot for expression of DDX3 protein. Antibodies specific for DDX3 and actin were used. B. Monolayers of WT (B) and DDX3$^{-/-}$ SVEC4-10 (C) cells were infected by m139-HA and m139-STOP MCMV at MOI 0.01 TCID$_{50}$/cell. At the indicated time points post infection, supernatants were collected for titration. Viral titers are shown as mean ±SEM.

The second interaction partner of m139 identified by SILAC analysis, the host protein UBR5, is predominantly known for its role in DNA damage response, transcription, and cell cycle progression. The described functions of UBR5 are restricted to its nuclear localization [136, 149, 150], and immunofluorescence analyzes revealed that in uninfected cells, UBR5 was diffusely distributed in the nucleus (Figure 26). Upon MCMV infection UBR5 appeared to be enriched in the viral replication compartment starting at 8 hours post infection. However, recruitment of UBR5 is not dependent on m139 expression, as cells infected with either MCMV m139-HA or MCMV m139-STOP both showed UBR5 enriched in the replication compartments.

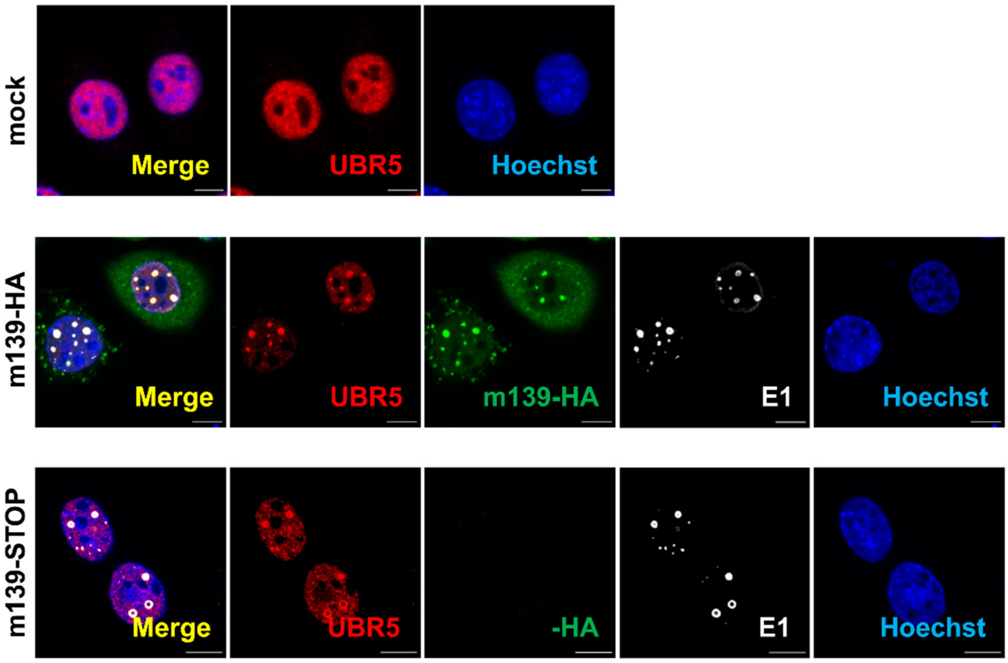

Figure 26. UBR5 is enriched at the sites of viral replication upon MCMV infection. SVEC4-10 cells were infected with m139-HA or m139-STOP MCMV at MOI 1 $TCID_{50}$/cell and fixed at 8 hpi. Subcellular localizations of UBR5, m139-HA, and E1 were analyzed by immunofluorescence using anti-DDX3 and anti-HA antibodies. Hoechst was applied for nuclear staining. Images representative of 3 independent experiments were imaged by confocal microscopy. Scale bar, 10 µm.

Similarly to DDX3, the replication defect of MCMV m139-STOP could also be UBR5-dependent. UBR5 knockout ($UBR5^{-/-}$) SVEC4-10 cells were generated using CRISPR/Cas9 gene editing, and the replication properties of MCMV m139-HA and m139-STOP was assessed (Figure 27A). The replication defect exhibited by the MCMV m139-STOP virus in wild type SVEC4-10 disappeared in $UBR5^{-/-}$ cells (Figure 27B). These results suggest that the replication defect of the m139-STOP virus is both UBR5 and DDX3-dependent.

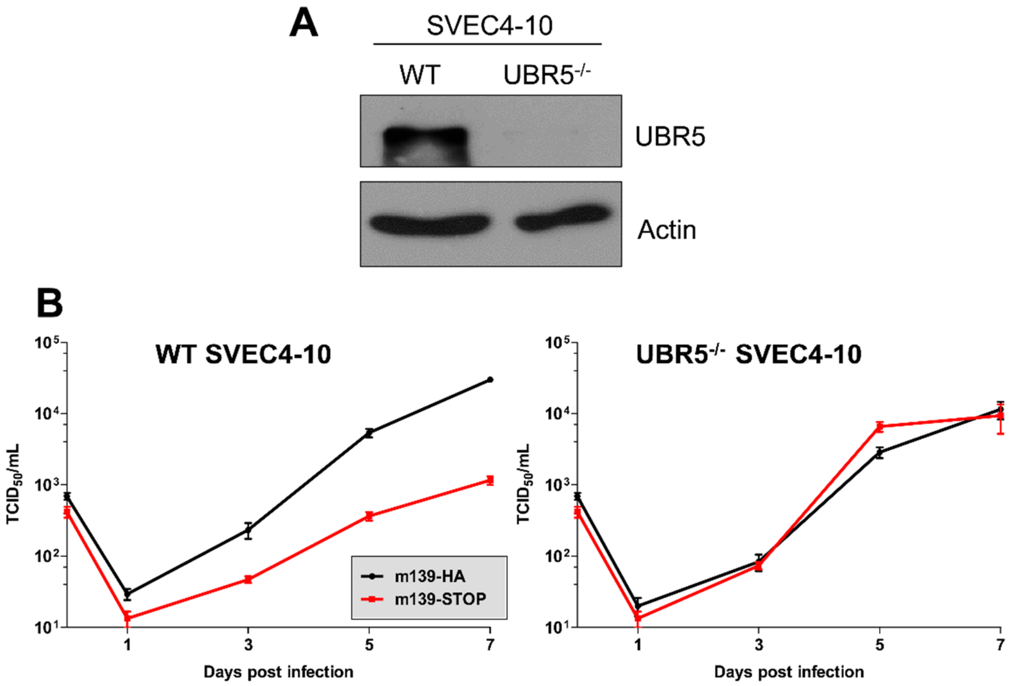

Figure 27. Replication defect of m139-STOP MCMV in SVEC4-10 cells is UBR5-dependent. A. UBR5 knock-out (UBR5$^{-/-}$) and WT SVEC4-10 cells were lysed. The expression of UBR5 was detected by Western blotting. B. Monolayers of wild type (WT) and UBR5$^{-/-}$ SVEC4-10 cells were infected with MCMV 139-HA or MCMV m139-STOP viruses with a MOI 0.01 TCID$_{50}$/cell. Supernatants were harvested at the indicated time points post infection and titrated. Viral titers are shown as mean ±SEM.

The findings that during MCMV infection both UBR5 and DDX3 are recruited to the nuclear replication compartment and, moreover, that both of them play a role in the modulation of MCMV replication in endothelial cells suggests a possible interplay between these host factors. I hypothesized that the interaction of m139 with DDX3 might be dependent on UBR5 and *vice versa*. To evaluate this hypothesis, m139-pull down assays were performed in the UBR5$^{-/-}$ and DDX3$^{-/-}$ SVEC4-10 cells. As shown in Figure 28A, in the presence of reduced amounts of DDX3 as in the DDX3$^{-/-}$ cells the interaction between m139 and UBR5 was significantly reduced. Likewise, in the absence of UBR5, as in the UBR5$^{-/-}$ cells, the interaction between m139 and DDX3 was also significantly reduced (Figure 28B). All together these findings imply that UBR5 and DDX3 interact with m139 and can regulate MCMV replication in endothelial cells in an interdependent fashion.

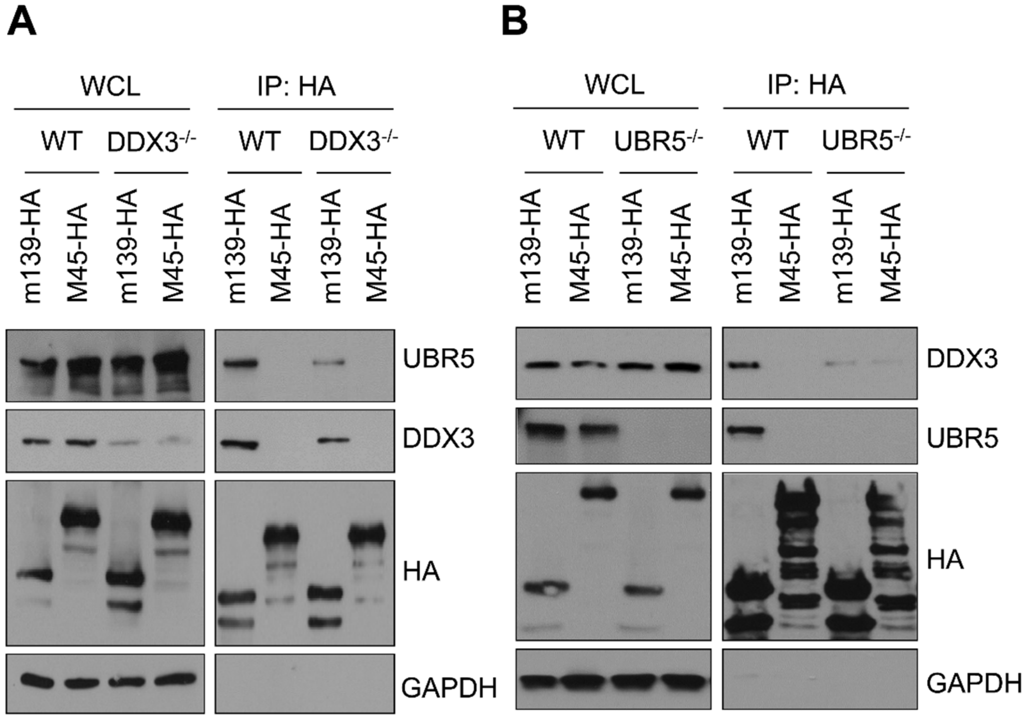

Figure 28. Interaction of m139 with DDX3 depends on UBR5 and *vice versa*. WT (A) and DDX3$^{-/-}$ SVEC4-10 cells (B) were infected with m139-HA MCMV or M45-HA MCMV as a control at MOI 5 TCID$_{50}$/cell. Cell lysates subjected to immunoprecipitation (IP) using anti-HA affinity matrix. Immunoprecipitants were analyzed by western blot using specific antibodies for UBR5, DDX3, HA, and GAPDH. B. WT and UBR5$^{-/-}$ SVEC4-10 cells were infected with m139-HA or M45-HA MCMV at MOI 5 TCID$_{50}$/cell. Cell lysates were immunoprecipitated and analyzed as described in A.

5.7 Impact of m139 in the DDX3-mediated antiviral signalling

Multiple studies have recently revealed a role of DDX3 as mediator of the IFN-β antiviral response. Vaccinia virus (VACV) protein K7 is a known antagonist of DDX3-mediated antiviral signalling. K7 inhibits association of DDX3 with the IKKε/TBK1 complex, preventing activation of IRF3 and IRF7 and thus diminishing IFN-β induction [118]. To address whether m139 has a similar effect on IFN-β signalling, a luciferase-based reporter assay in HEK-293A cells was performed. IFN-β induction was monitored using a reporter plasmid containing the firefly luciferase gene under the control of the murine IFN-β promoter (IFNβ-Luc). IFN-β induction was induced by overexpression of DDX3 and IKKε. In this reporter assay, the expression of m139 significantly inhibited IFN-β promoter activity in comparison to empty vector. Expression of VACV protein K7 resulted in a similar downregulation of IFN-β, while MCMV protein m140, which was used as a negative control, did not alter IFN-β induction (Figure 29A). HCMV US22 proteins IRS1 and US22, which are homologous to m139, were also tested using the same reporter assay.

However, none of the tested HCMV proteins exhibited a similar effect on DDX3-mediated IFN-β induction (Figure 29B).

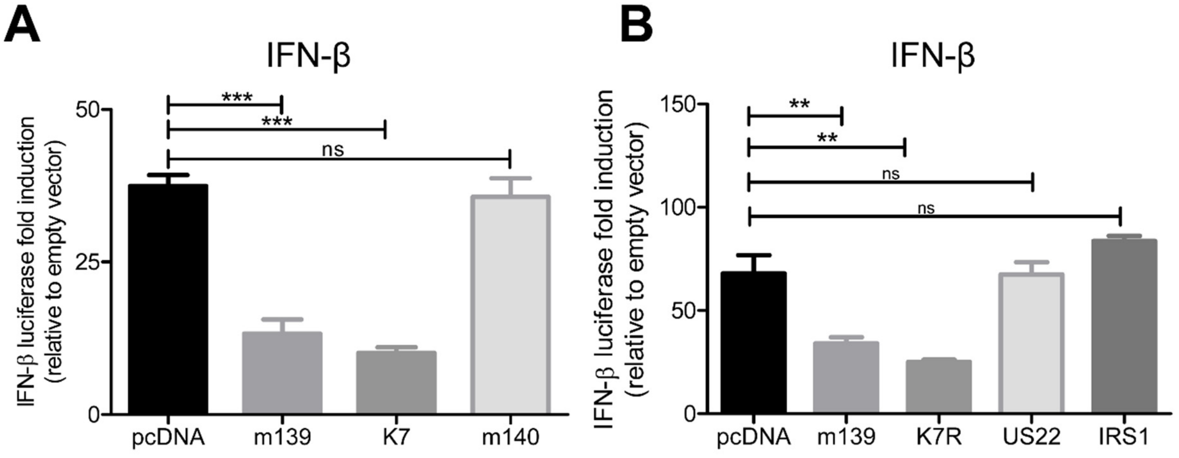

Figure 29. Like VACV protein K7, m139 inhibits DDX3-mediated IFN-β induction. A. HEK-293A cells co-transfected with expression plasmids for DDX3 and IKKε, a reporter plasmid containing firefly luciferase under the control of the murine IFN-β promoter (IFNβ-luc), Renilla luciferase, as well as the indicated plasmids expressing m139, m140, K7 or empty vector (pcDNA). Luciferase fold induction was calculated based on firefly luciferase values normalized to Renilla luciferase values from the same samples. Means ±SEM of 3 independent replicates are shown. ns, not significant; *, $p<0.05$; **, $p<0.01$; ***, $p<0.001$. B. Same assay as in A was performed with plasmids expressing IRS1, US22, K7, m139 or empty vector (pcDNA).

Since m139 seems to downregulate DDX3-mediated IFN-β induction in a similar fashion as VACV protein K7, two chimeric mutant viruses were generated in order to elucidate the mechanism of action. Firstly, MCMV K7[Δ m139], which has the majority of m139 replaced with VACV gene K7 with an HA epitope tag (HA-K7). Secondly, MCMV K7[m139-STOPΔm02-06] in which ORFs m02-m06 were replaced by HA-K7 under a strong promoter. MCMV K7[m139-STOPΔm02-06] was generated in the backbone of m139-STOP MCMV (Figure 30A). 10.1 fibroblasts were infected with the chimeric viruses and expression of HA-K7 was confirmed by immunoblotting (Figure 30B). As expected, the expression of HA-K7 was higher in 10.1 infected with K7[m139-STOPΔm02-06] due to the stronger promoter.

Next, the replication properties of these two recombinant viruses were assessed in immortalized macrophages. In multistep replication kinetics, replication of these chimeric mutants was compared to MCMV m139-STOP and MCMV m139-HA. Both K7[Δm139] and K7[m139-STOPΔm02-06] MCMVs replicated to levels similar to MCMV m139-HA thus suggesting that the K7 protein of VACV might functionally substitute for m139 (Figure 30B). The replication properties of the K7 recombinant mutants were tested in SVEC4-10 cells. In this cell line, K7[Δm139] replicated like m139-STOP MCMV whereas K7[m139-STOPΔm02-06] had slightly higher replication levels. However, the replication properties of this mutant were different from m139-HA MCMV (Figure 30C). Taken together, the replacement of m139 by VACV protein K7 led to a rescue of the replication phenotype in differentiated macrophages but not in endothelial cells. This suggests that the observed MCMV replication defect in macrophages is dependent on modulation of DDX3-mediated IFN-β expression by m139 while the m139 replication defect in endothelial cells has a different mechanism.

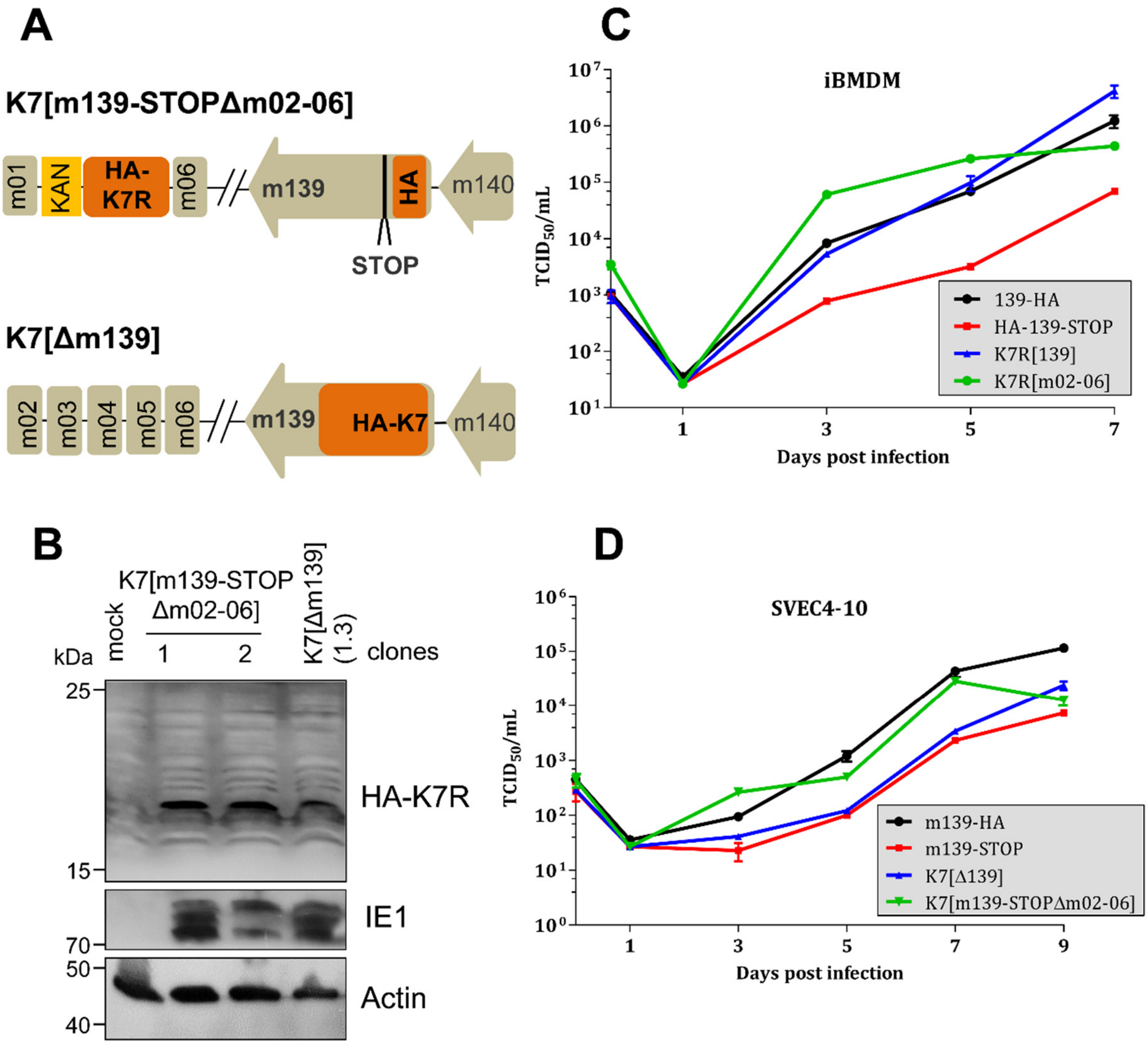

Figure 30. Replication properties of K7 recombinant viruses in macrophages and endothelial cells. A. Schematic representation of K7[Δ m139] and K7[m139-STOPΔm02-06] MCMV mutants. B. 10.1 cells were infected with K7[m02-06] (clones 1 and 2) and K7[Δ m139] (clone1.3) at MOI 10 TCID50/cell. Cells were lysed 24 hpi and subjected to

western blot. Specific anti-HA, anti-IE1, and anti-Actin antibodies were applied. iBMDM (C) and SVEC4-10 (C) were infected with m139-HA, m139-STOP, K7[Δ m139] (clone1.3), and K7[m139-STOPΔm02-06] (clone1) at MOI 0.025 (D) and 0.01 (C) $TCID_{50}$/cell. At the indicated time points post infection, supernatants were collected for titration. Viral titers are shown as mean ±SEM.

It was previously demonstrated that upon HCMV infection, DDX3 contributes to the DNA sensor DAI/ZBP1-dependent IFN response. Like DDX3, DAI is involved in the IRF3-dependent IFN-β induction [126]. Considering that both DDX3 and DAI are involved in the same pathway, I decided to study viral multistep replication kinetics in DAI/ZBP1 knockout ($ZBP1^{-/-}$) SVEC4-10 cells [151]. Similar to what was already shown in WT SVEC4-10 cells, the MCMV m139-STOP virus presented a growth defect in $ZBP1^{-/-}$ SVEC4-10 cells (Figure 31). Remarkably, the replication defect of the m139 knockout virus in $ZBP1^{-/-}$ SVEC4-10 cells was even more prominent than the one observed in WT SVEC4-10 cells (Figure 17D).

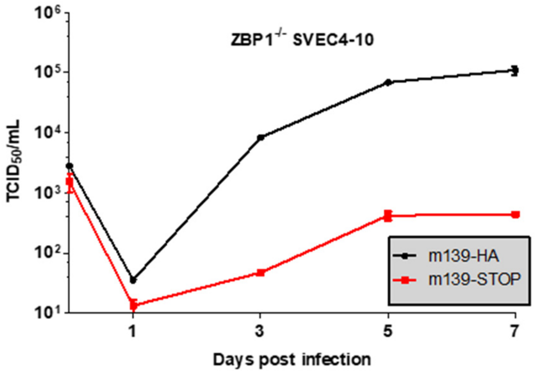

Figure 31. Multistep replication kinetics in $DAI^{-/-}$ SVEC4-10 cells. $ZBP1^{-/-}$ SVEC4-10 cells were infected by m139-HA and m139-STOP at MOI 0.04 $TCID_{50}$/cell. At the indicated time points post infection, supernatants were collected for titration. The experiment was done in triplicate. Mean ±SEM are shown.

As the effect of m139 on IRF3-dependent induction was not observed in endothelial cells, IFN-β transcription upon MCMV infection was evaluated in endothelial cells versus macrophages. The IFN-β induction in SVEC4-10 cells was not investigated so far. IFN-β transcription was assessed in the presence or absence of m139. Vesicular stomatitis virus (VSV), a known IFN-β inducer, was used as a control in this assay (Figure 32). As expected, infection with VSV resulted in massive IFN-β transcription in iBMDMs. Upon infection with m139-HA MCMV, IFN-β transcription was also detected, but at a lower level.

Infection with m139-STOP MCMV resulted in significantly higher IFN-β transcription in comparison to m139-HA MCMV. This result fits with the previously observed effect of m139 on IFN-β signaling in macrophages (Figure 32A). IFN-β transcription upon VSV infection in SVEC4-10 cells was evidently limited in comparison to VSV-induced IFN-β transcription in macrophages, indicating lower potential of SVEC4-10 cells to induce IFN-β. Both m139-HA and m139-STOP MCMVs induced IFN-β transcription, but there was no significant difference detected between these two mutants (Figure 32B).

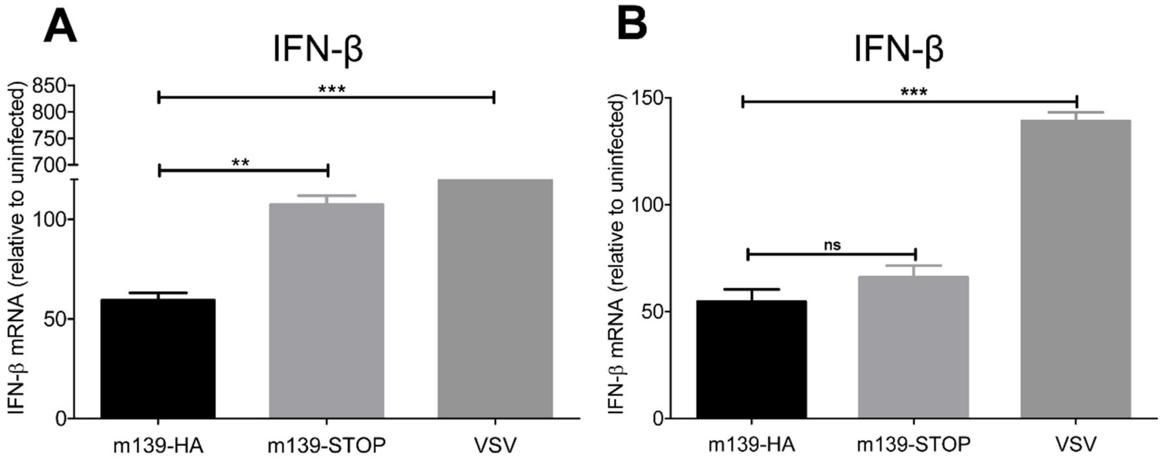

Figure 32. m139 is involved in modulation of IFN-β transcription in macrophages but not endothelial cells. Immortalized BMDM (iBMDM) (A) or SVEC4-10 cells (B) were infected with m139-HA MCMV or m139-STOP MCMV at MOI 0.2 $TCID_{50}$/cell or Vesicular stomatitis virus (VSV) at MOI 1 pfu/ml. 3 hpi cells were washed with PBS and the media was replaced with fresh media. RNA was isolated at 6 hpi for MCMV-infected samples and 4 hpi for VSV-infected samples. Obtained values were normalized to actin. Data is shown as mean ± SD and combined from three independent replicates. ns, not significant; *, p<0.05; **, p<0.01; ***, p<0.001.

Altogether, these results suggest that the observed replication defect of m139-STOP MCMV in differentiated macrophages is due to the involvement of m139 in the DDX3-mediated IFN signalling in macrophages. However, it appears that in SVEC4-10 cells, the m139-STOP MCMV defect is not dependent on IFN-β induction but rather some other function of DDX3.

5.8 Role of the m139 gene product in MCMV replication in vivo

The correlation between the MCMV replication defect in macrophages and impaired replication in vivo was reported [63]. m139 is required for efficient viral replication in macrophages and endothelial cells. To investigate the effect of m139 on viral replication and dissemination in vivo, WT BALB/c mice were infected with MCMV m139-HA, m139-STOP, or K7[Δm139]. Viral titers were determined in salivary gland homogenates on day 14 post infection (dpi). Salivary gland titers from m139-STOP and K7[Δm139] MCMVs were significantly reduced (Figure 33). These results confirm the importance of m139 in viral dissemination in vivo. The substitution of m139 by K7 in the K7[Δm139] recombinant virus did not rescue the viral dissemination defect of the m139-defecient virus.

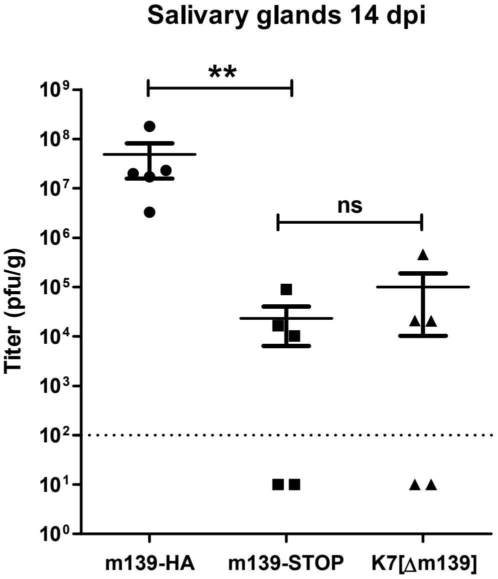

Figure 33. MCMV lacking m139 failed to disseminate to salivary glands following footpad inoculation. BALB/c mice were inoculated in the footpad (FP) with 10^5 pfu with m139-HA, m139-STOP, or K7[Δm139] MCMV. Salivary glands were harvested 14 days post infection, and viral titers were determined by plaque assay. Mean titers ±SEM are shown. Detection limit was 10^2 pfu/g. ns, not significant; *, $p<0.05$. In vivo experiment was performed by Dr. E. Ostermann.

It was shown that MCMV inoculated in the footpad first reaches the popliteal lymph nodes (PLN), where subcapsular sinus macrophages appear to be the most acutely infected cells [152]. Therefore, viral titers were evaluated in lymph node 3 days post infection. As shown in Figure 34, infection with MCMV m139-STOP resulted in significant impairment of viral replication in the PLN. Notably, productive viral replication was detected only in one mouse out of five. Remarkably, infection with K7[Δm139] recombinant virus moderately improved viral replication in lymph node.

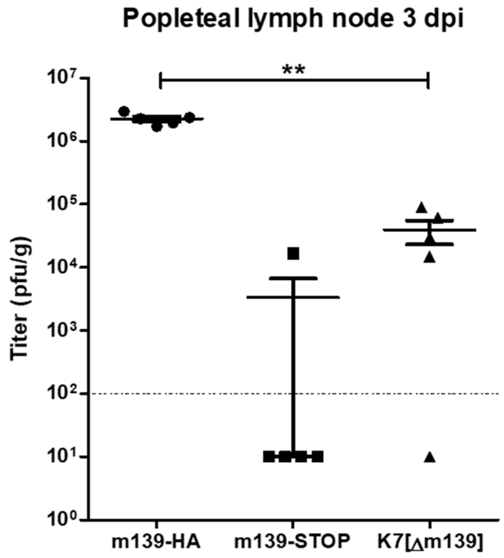

Figure 34. MCMV lacking m139 failed to replicate efficiently in popliteal lymph nodes. BALB/c mice were inoculated in the footpad (FP) with 10^5 pfu with m139-HA, m139-STOP, or K7[Δm139] MCMV. Popliteal lymph nodes (PLN) were harvested 3 days post infection, and viral titers were determined by plaque assay. Mean titers ±SEM are shown. Detection limit was 10^2 pfu/g. **, $p<0.01$. In vivo experiment was performed by Dr. E. Ostermann.

5.9 The m139 protein is a host range factor

Cytomegaloviruses are known for their narrow host range, as they are able to replicate only in cells of their own or closely related species. Some years ago, a spontaneously adapted MCMV mutant, MCMV/h, that is able to replicate in human retinal pigment epithelial (RPE-1) cells was isolated in our laboratory [40]. Afterwards, additional human cell-adapted MCMV mutants named MCMV/h2 and MCMV/h3 were obtained in the same manner. Next generation sequencing of the three viruses revealed that the MCMV gene M117 was mutated in all three of the MCMV mutants. Even though the mutation in M117 was sufficient to allow MCMV replication in RPE-1 cells, mutations in other MCMV genes contributed to adaptation and facilitated MCMV replication in RPE-1 cells [39, 40]. Since m139 was mutated in the MCMV/h3 (Figure 35), I investigated its potential role as a host range factor.

The single nucleotide deletion (cytosine 297) in m139 found in the MCMV/h3 was inserted by BAC mutagenesis into a GFP-expressing wildtype MCMV (WT MCMV) as well as into an MCMV-GFP carrying the mutant M117 from MCMV/h3. The two viruses were further referred to as MCMV m139mut/h3 and MCMV m139mut/h3+M117mut/h3, respectively, and were used to infect human epithelial RPE-1 cells together with WT MCMV, MCMV M117mut/h3, and the human adapted MCMV/h3.

While MCMV M117mut/h3 could replicate in human cells, MCMV m139mut/h3, carrying only the mutation in m139, did not (Figure 35). Interestingly, the combination of mutations in both M117 and m139 (MCMV m139mut/h3+M117mut/h3) substantially enhanced viral replication compared to MCMV M117mut/h3.

A

Gene	mutation
M28	C→A
M83	G→T
M114	C→T
M117	ΔT
m125-126	G→T
m139	ΔC

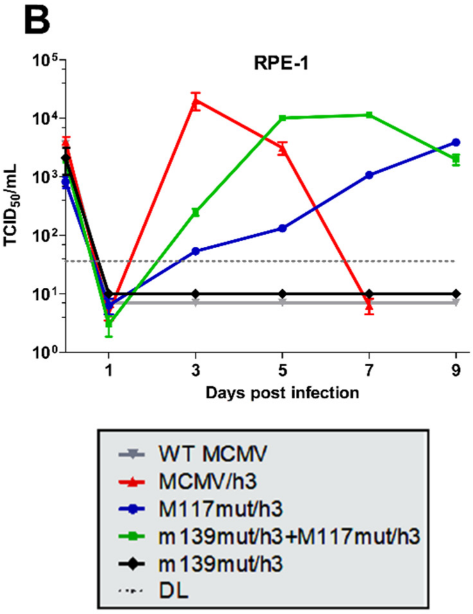

Figure 35. Multistep replication kinetics in human RPE-1 cells. A. List of mutations present in the human cell-adapted MCMV/h3. B. Human RPE-1 cells were infected with MCMV/h3, MCMV M117mut/h3, MCMV m139mut/h3, MCMV m139mut/h3+M117mut/h3, and WT MCMV at an MOI of 0.2 $TCID_{50}$/cell. Supernatants were collected at the indicated time points and MCMV titers were determined (shown as mean ±SEM).

The m139 mutation found in MCMV/h3 is a deletion of cytosine (ΔC) at position 297 in the 5’ end of the m139 ORF. The deletion leads to a frame shift and the formation of a premature STOP-codon, which results in a truncated m139 gene product. The mutated m139 expressed by MCMV/h3, has 166 amino acids, of which only 99 are identical to the wildtype m139 protein (Figure 36A). In order to characterize the expression and distribution of the truncated protein, m139mut was cloned into the same HA-tag expression plasmid used in paragraph 1.2. Upon transfection of NIH/3T3 cells, HA-m139mut was detectable at a molecular size of approximately 25 kDa (Figure 36B). When overexpressed alone, m139mut was exclusively detected homogenously distributed in the nucleus (Figure 36C). Upon co-expression with E1 protein, HA-m139mut did not change its localization pattern. In contrast to wildtype m139-HA (Fig 6.B and C), the truncated HA-m139mut did not localize to the cytoplasm and was not enriched in E1-positive nuclear dots (Figure 36D). Altogether, these findings suggest that the C-terminal part of the m139 protein containing the putative NES is important for the recruitment of m139 to the viral replication compartments in the nucleus.

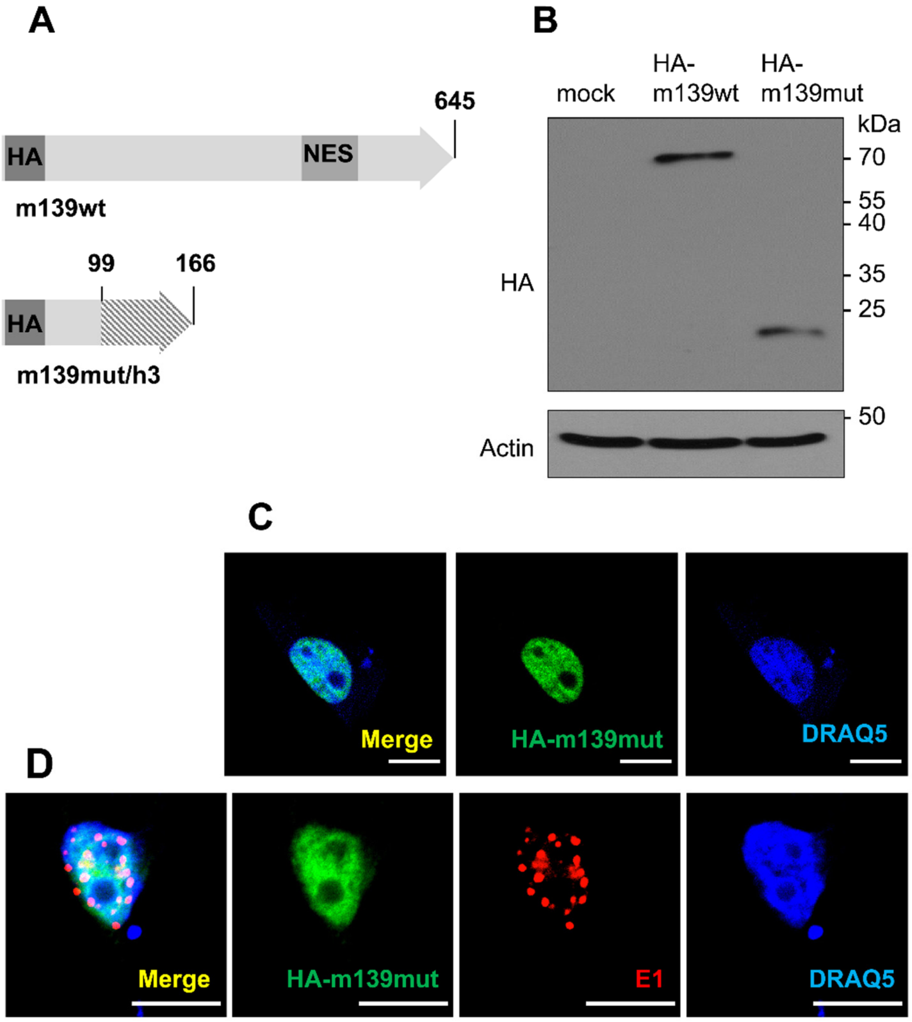

Figure 36. Expression and subcellular localization of the m139/h3 C-terminal mutant. A. Schematic representation of the MCMV wild type and C-terminal truncated m139 protein, m139wt and m139mut/h3, respectively. NES, predicted nuclear export signal. HA, tag. B. Cell lysates obtained from NIH/3T3 cells transfected with HA-m139wt or HA-m139mut expression constructs were analyzed by immunoblotting with antibodies specific for HA and Actin. C. Cells were transfected with HA-m139mut alone or (D) HA-m139mut in combination with E1 protein, fixed, and processed for immunofluorescence. Antibodies specific for HA and E1 were applied. Nuclear staining was done using DRAQ5. Images representative of 3 experiments were imaged by confocal microscopy. Scale bar, 10 µm.

Considering that m139mut is not recruited to the viral replication compartments, it appeared likely that any loss-of-function mutation of m139 would also enhance MCMV replication in RPE-1 cells. To test this hypothesis, MCMV Δm139mut+M117mut/h3 was generated by deletion of the complete m139 ORF by BAC mutagenesis in an MCMV carrying the M117 h3 mutation. As shown in Figure 37, both m139mut/h3+M117mut/h3 and Δm139mut+M117mut/h3 replicate more efficiently in RPE-1 cells in comparison to M117mut/h3, indicating that a lack of m139 can enhance MCMV replication in human cells.

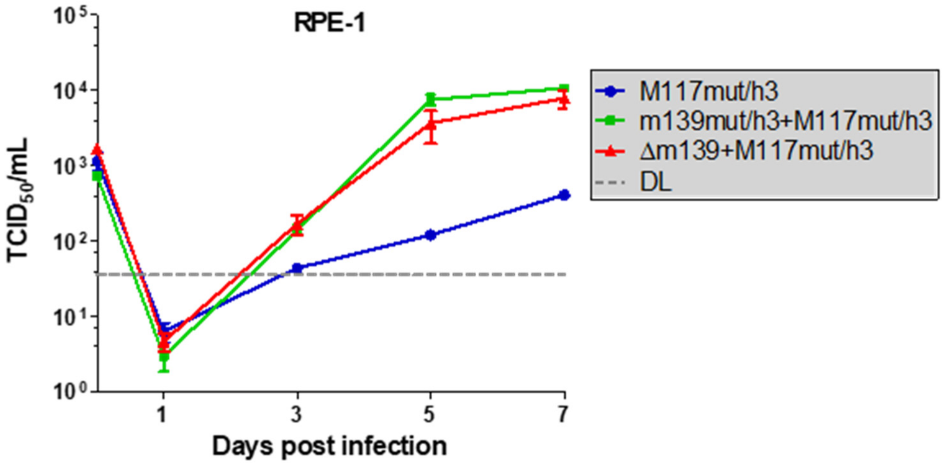

Figure 37. Truncation and complete deletion of m139 enhances virus replication in RPE-1 cells. RPE-1 cells were infected with MCMV M117mut/h3, MCMV m139mut/h3+M117mut/h3, and Δm139mut+M117mut/h3 at MOI of 0.2 $TCID_{50}$/cell. Supernatants were collected at the indicated time points. Viral titers were determined in the supernatants and are shown as mean ±SEM. The experiment was done in triplicate.

6 Discussion

6.1 Role of the m139 protein in MCMV replication

Cytomegaloviruses are well known for their broad cell tropism within their natural host. It has been shown that certain viral proteins determine the efficiency of viral replication in some cell types but are negligible in fibroblasts, the most commonly used cell type in the laboratory. This study aimed at understanding the features and functions of a so far poorly described MCMV protein called m139 that was thought to be important for viral fitness in macrophages [63]. Macrophages and endothelial cells play similar vital roles in CMV pathogenesis as vehicles of CMV spread within the host and as sites of viral persistence [44]. In this study, the role of m139 in viral replication was confirmed in macrophages and further elucidated in endothelial cells, and the pathways used to optimize replication were identified.

In this study, m139 was identified as an early protein (Figure 14) and was found to localize to multiple sites upon MCMV infection (Figure 15). While m139 colocalized with m140 and m141 in the cytoplasm, it was found to be recruited to the viral replication compartments in the nucleus. The replication compartments can be visualized as distinct puncta formed by the viral E1 proteins (Figure 15B, C). Notably, the host proteins UBR5 and DDX3, identified as interaction partners of m139, were also recruited to the virus replication compartments upon MCMV infection, thus leading to the hypothesis that m139, UBR5, and DDX3 might form a functional complex important for viral replication.

So far, it remains unclear how m139 is recruited from the cytoplasm to the nuclear replication compartments. Even though the viral replication compartments recruit large amounts of both cellular and viral proteins [144], a direct interaction between the m139 and E1 proteins was not confirmed, thus suggesting that m139 might be brought to the nucleus by some still unknown viral or host factor/s.

6.2 m139 as a part of a complex with MCMV proteins m140 and m141

The MCMV gene region m139-m141 has originally attracted attention due to its high importance for MCMV replication in macrophages [63]. Even though the molecular mechanisms were not understood, MCMV proteins m139-141 were suggested to regulate MCMV replication in macrophages in a concerted way, as these proteins are shown to interact with each other and form a complex [67]. Indeed, in the current study m140 and m141 were found to be significantly enriched in the SILAC screen for m139 interaction partners (Table 1). Moreover, infection of macrophages, but not fibroblasts, with an MCMV mutant deleted of these three genes resulted in inhibition of viral replication and lower expression levels of representative immediate-early and early viral proteins (Figure 13). Once I confirmed the importance of m139-m141 proteins for MCMV replication in macrophages, I investigated their intracellular localization by using epitope-tagged forms of m139, m140, and m141. I detected their colocalization in the cytoplasm, while m139 was the only one additionally found in the nucleus. In support of a major role of m139 in the regulation of virus-cell host interactions, a recently published reporter screen for the cGAS-STING pathway showed that only m139 exerted a strong inhibitory effect [88] while m140 and m141 did not. These qualities of m139, distinct from its interaction partners, can be supported by the fact that the gene products of m140 and m141 form a complex between themselves independently of the m139 gene product [67]. However, the data obtained in this study are mainly focused on m139 and do not exclude the importance of the m139-m141 complex in MCMV replication. The physiological roles of the m140 and m141 proteins, singularly or in complex with m139, remain to be defined.

6.3 m139 as a novel modulator of IFN-β antiviral signalling

During the long-lasting co-evolution with their hosts, cytomegaloviruses have evolved a large variety of sophisticated mechanisms to counteract innate immune responses. In their large genomes, cytomegaloviruses encode numerous viral immune evasion proteins, which target different parts of the antiviral immune signalling pathway [87]. The IFN-mediated innate immune responses provide a robust first line of defence against viruses [70]. In recent years, a few MCMV proteins have been found to dampen different arms of type I IFN signaling. As an example, the transcription of IFN has been shown to be inhibited by M45 via degradation of the NF-κB essential modulator (NEMO) and subsequent block of NF-κB activation [153]. Another MCMV protein, m152, has been shown to block type I IFN induction by binding to STING and interrupting its trafficking to the Golgi compartment, thus inhibiting STING-mediated IRF signalling [88]. M35 negatively modulates the induction of the IFN-β promoter upon MCMV infection [154], and M27 downregulates STAT2 and inhibits signaling downstream of IFNAR [93]. The importance of type I IFNs in the antiviral response is clearly supported by the multiplicity of viral proteins capable of interfering with either IFN transcription or signalling.

Brinkmann et al. have proposed a role for m139 as a modulator of IFN-β signaling [88], and in the present study, I have elucidated its roles in IFN-β signaling. Infection of macrophages with MCMV lacking m139 resulted in an elevated level of IFN-β induction, implying that m139 is involved in the inhibition of IFN induction in macrophages (Figure 18).

This study revealed the involvement of the RNA helicase DDX3 in the modulation of IFN-β signaling upon MCMV infection. Several studies have investigated the impact of DDX3 on different steps of PRR signaling leading to IFN-β production [128]. The association of DDX3 with the IKK kinases of TBK1 and IKKε leads to the phosphorylation of DDX3 and subsequent IFN-β activation (Figure 38). Moreover, DDX3 was also found to directly bind to the IFN-β promoter [76]. Some DNA viruses were shown to express specific factors to target DDX3-mediated IFN signalling. The HBV polymerase disrupts interactions between DDX3 and IKKε, thereby diminishing IRF-dependent signalling [155]. VACV encodes protein K7, which interacts with DDX3 and blocks its interaction with the TBK1/IKKε complex to prevent activation of the DDX3/TBK1/IKKε complex [68]. Upon HCMV infection, DDX3 activates IRF3-dependent transcription. However, specific antagonists of DDX3 among CMV proteins were previously not detected [126]. Similar to K7, m139 inhibited DDX3 mediated IFN-β expression and IKKε overexpression (Figure 29), suggesting that m139 acts at either the association of DDX3 with the TBK1/IKKε complex or dampens the association of DDX3 with the IFN-β promotor. The replacement of m139 by K7 restored viral replication in macrophages (Figure 30C), suggesting that m139 limits DDX3-mediated IFN-β induction. To find out if this function of m139 is restricted to macrophages, the DDX3-mediated signalling should be investigated in murine fibroblasts, as they show robust IFN-β induction upon MCMV infection [82].

Considering the dual localization of m139 and its ability to recruit DDX3 to viral replication compartments, m139 might interfere with the binding of DDX3 to the IKK complex or directly with its binding to the IFN-β promoter. A more detailed spatio-temporal analysis of the interaction between m139 and DDX3 in macrophages would provide a better understanding of the role of m139 in DDX3-dependent antiviral signalling.

6.4 Role of the m139 protein in MCMV macrophage tropism

Even though earlier studies suggested a role for m139 as a MCMV tropism determinant in macrophages, not all reports reached the same conclusion. While Hanson at al. have shown that m140 and m141, but not m139, are responsible for an MCMV replication defect in macrophages [143], Menard at al. have reported an important role of m139 for efficient replication in macrophages [66]. In order to understand the role of m139 on MCMV tropism in macrophages, we created an MCMV mutant that has m139 deleted by a STOP-codon insertion. As compared to previous studies in which m139-deletion mutants were generated by transposon mutagenesis or deletion mutagenesis [66], the mutant MCMV m139-STOP did not express any of the two m139 isoforms and the transcription of the neighboring genes m140 and m141 was not affected. Since MCMV m139-STOP presented a replication defect in immortalized macrophages, this study supports the interpretation of m139 as an important tropism determinant in macrophages (Figure 17D).

m139 is not the first MCMV protein shown to be important for viral replication in macrophages. Since macrophages are more susceptible to apoptosis, it has been shown that the depletion of cell death inhibitors, such as the anti-apoptotic viral proteins M36 and M45, accounts for impaired MCMV replication in these cells [156]. Given the importance of the innate immune signalling in myeloid cells, it is probable that antagonists of IFN signalling might influence the viral tropism for macrophages. Lack of modulators of IFN signalling, such as M35 or M27, indeed have been shown to restrain MCMV replication in macrophages [93, 154]. The high levels of IFN-β released by macrophages infected with the MCMV m139-STOP and the replication defect in these cells suggests that modulation of IFN-β signaling by m139 is physiologically relevant. Nevertheless, a reduced productive infection was still detected in macrophages infected with MCMV m139-STOP, meaning that m139 is important but not essential for MCMV replication in murine macrophages.

It was previously shown that footpad-inoculated MCMV first reaches the popliteal lymph nodes and then uses subcapsular sinus macrophages for productive infection and release of viral progenies [152]. Intra-footpad inoculation of MCMV m139-STOP had significantly reduced viral replication in the lymph nodes, which confirmed the importance of m139 for viral replication in macrophages in vivo (Figure 34).

Replacement of m139 by the vaccinia virus DDX3 modulator K7 in the MCMV K7[Δm139] recombinant virus partially rescued the replication defect of MCMV m139-STOP *in vitro* (Figure 30C) and led to a slight improvement in viral replication in the lymph nodes (Figure 34). Altogether, these findings indicate that modulation of DDX3-mediated IFN-β induction by m139 is important for viral replication in macrophages. The RNA helicase

DDX3, which fulfils important roles as an RNA sensor and inducer of antiviral immunity including the translational activation of TNF and the proinflammatory chemokine signalling pathways in macrophages [157], was identified as an interaction partner of m139. The targeting of DDX3 by m139 in differentiated macrophages may possibly influence both innate and inflammatory signalling upon MCMV infection in vivo. Thus, the regulation of this arm of antiviral signalling by m139 will require further investigation in the future.

6.5 Role of the m139 protein in MCMV endothelial cell tropism

The ability of CMV to replicate in endothelial cells strongly defines the extent of viral spread through the body and viral dissemination from the circulating blood to the organs [44]. For human cytomegalovirus (HCMV), the viral tropism for endothelial cells greatly varies between different strains and it is dependent by the UL128-131 gene region. UL128, UL130, and UL131 along with gH and gL form the pentameric complex, which is exposed on the viral envelope and is essential for the viral entry into endothelial and epithelial cells. It has been shown that this region is under selective pressure and continuous passaging of HCMV in fibroblasts leads to mutations in this region and loss of endothelial cells tropism [158]. Besides the UL128-131 gene region, HCMV-encoded proteins UL24, UL135, UL136, and US16 have been shown to contribute to viral endothelial tropism [23]. While the HCMV-encoded proteins UL135 and UL136 are required for efficient formation of the viral assembly compartment (VAC) and maturation of virus particles [159], the US16 protein is critical for the entry and post-entry events in both endothelial and epithelial cells [160]. For MCMV, it has been shown that deletion of the tegument protein M45 abrogates viral replication in endothelial SVEC4-10 cells, as M45 expression is needed to prevent necroptosis in these cells [161, 162]. m139-deficient MCMV mutants replicate less efficiently than MCMV WT in endothelial SVEC4-10 cells, indicating that m139 is a novel factor for MCMV endothelial cell tropism.

Knockout of m139 resulted in significantly reduced viral replication in salivary glands 14 days after infection (Figure 33). The same phenotype was also observed for the K7[Δm139] mutant, a virus that replicated like MCMV WT in macrophages but did not rescue MCMV replication in endothelial cells. This observation is noteworthy because it suggests that the role of m139 in MCMV infection of endothelial cells might influence MCMV dissemination in vivo.

Given the importance of m139 in IFN-β modulation, the role of the IFN signalling in endothelial cell infection was investigated. The DNA sensors p204 and ZBP1 were identified as inducers of IRF3-mediated IFN signalling upon infection with DNA viruses [104, 126]. However, knockout of either p204 or ZBP1 in endothelial cells did not improve the replication properties of m139-deficient MCMV mutants, thus ruling out that nucleic acid sensing via p204 or ZBP1 could be functionally connected with m139 promotion of MCMV growth in endothelial cells (Figure 22B, Figure 31). While infection in macrophages with the MCMV m139-STOP mutant triggered higher levels of IFN-β transcription, in endothelial cells the deletion of m139 did not show any impact on IFN-β transcription (Figure 32). Additionally, the replacement of m139 by K7, VACV-encoded antagonist of DDX3-mediated IFN signalling failed to rescue the replication defect in endothelial cells, thus implying that the modulation of DDX3 by m139 was not related to DDX3-mediated IFN-β induction but instead to another function of DDX3. Altogether, the obtained data suggest that m139 does not modulate IFN-β signalling in endothelial cells. The potential roles of the host factors DDX3 and UBR5 in MCMV endothelial tropism are discussed in the following paragraphs.

6.5.1 Modulation of the RNA helicase DDX3 by m139

DDX3 is involved in multiple steps of RNA biogenesis, including transcription, splicing, mRNA export, translation, and RNA decay [112]. Some viruses exploit key DDX3 activities for their viral gene expression. For instance, the HIV Rev protein uses the nuclear-cytoplasmic shuttling of DDX3 for the export and translation of viral transcripts [122]. Lymphocytic choriomeningitis virus (LCMV) takes advantage of the ATPase and helicase activities of DDX3 to promote virus replication [121]. Similarly, upon HSV-1 infection DDX3 modulates viral gene expression in an ATPase-dependent manner [107]. Moreover, DDX3 plays a pro-viral role in HSV-1 and LCMV replication cycles [107, 121]. In the case of HCMV, DDX3 was found to be enriched in virions and upregulated in infected fibroblasts, thus supporting the hypothesis that it may promote viral replication [127]. In this study, I have identified a different role of DDX3 in MCMV replication. In DDX3 knockout (DDX3$^{-/-}$) SVEC4-10 cells, MCMV replicates to similar levels as in WT endothelial cells (Figure 25B), suggesting that in the case of MCMV replication, DDX3 is not a pro-viral factor. However, the fact that in DDX3$^{-/-}$ SVEC4-10 cells the replication defect of the 139-STOP mutant is rescued suggests that DDX3 is manipulated by m139 for efficient viral replication in SVEC4-10 endothelial cells (Figure 25B). DDX3 is stably expressed throughout the MCMV replication cycle, but its subcellular localization changes over time. The change in subcellular localization is highly supported by the previously identified abilities of DDX3 to shuttle between cytoplasm and nucleus [122]. Moreover, the recruitment of DDX3 to the viral replication compartments upon MCMV infection strongly suggests that DDX3 may regulate viral replication. Interestingly, also upon HSV-1 infection, nuclear DDX3 co-localizes with ICP4, which is a marker of viral replication compartments [107, 163].

The HCMV US22 protein is thought to be a possible homologue of m139 [143]. An unbiased proteomics screen for HCMV RNA-associated proteins performed by Moorman at al. has identified US22 as a viral mRNA-binding protein [164]. So far, the role of m139 in RNA processing upon MCMV infection has not been analyzed. However, given the importance of its interaction with DDX3 in endothelial cells, m139 might be involved in the regulation of cellular RNA metabolism during MCMV infection. It remains puzzling why the modulation of DDX3 by m139 is important for replication in specific cells, such as endothelial cells. The work of Soto-Rifo and colleagues showed that DDX3 is required for the translation of some selected transcripts rather than for general translation, and in this scenario, DDX3 could regulate mRNA translation in a cell-specific manner [123], including MCMV-infected endothelial cells (Figure 38).

In addition to RNA biogenesis and IFN signalling, DDX3 has also earned attention due to its role in the generation of cytoplasmic stress granules (SG), where mRNAs together with associated proteins are retained and remain untranslated [165, 166]. SGs are mostly induced by the interferon-stimulated gene PKR [167]. Detection of viral RNA in the cytoplasm by PKR leads to SG assembly (Figure 38). During HCMV infection, the PKR antagonist TRS1 was shown to downregulate this process [168]. Interestingly, another US22 family protein, murine dsRNA binding protein m142, was found in the SILAC screen of m139 interaction partners (Table 1). The MCMV-encoded proteins m142 and m143, as well as their HCMV-encoded homologues, IRS1 and TRS1, block activation of PKR and thereby inhibit the dsRNA-activated antiviral pathways [96, 169]. During Influenza virus infection, the NS1 protein is able to inhibit both PKR and DDX3 in order to suppress virus-induced accumulation of stress granules and to drive viral replication [170]. Therefore, it is possible that m139 interacts with m142 and m143 to regulate the induction and assembly of stress granules. Considering that m139 actively recruits DDX3 to the viral replication compartments (Figure 24), it could be a rerouting strategy of m139 to prevent

DDX3-initiated stress granule formation in order to carry on viral mRNA translation. Strikingly, it was shown that at late times post infection, m139 is found in dot-like structures in the cytoplasm (Figure 15). Even though the formation of stress granules was not observed in m139-STOP infected cells, more extensive analyses of the subcellular localization of DDX3 and m139 at late times post infection would be necessary to clarify the role of m139 in stress granule assembly.

6.5.2 Modulation of E3 ubiquitin ligase UBR5 by m139

In this study, I have identified the E3 ubiquitin ligase UBR5 as a novel factor important for MCMV replication. UBR5 takes part in the cellular ubiquitin-proteasome system (UPS) pathway, and its functions are related cell cycle progression, DNA repair, and transcriptional regulation of gene expression [130]. Even though little is known about the role of UBR5 in viral replication, some RNA and DNA viruses have been recognized as capable of subverting UBR5 during their replication. As an example, upon HIV-1 and HHV-6 infection, UBR5 is hijacked by viral factors for the induction of a cell-cycle arrest at G2/M phase [171, 172]. Moreover, upon HCMV infection, UBR5 upregulation is required for successful viral translation, and UBR5 knock-out impaired viral progeny production [108].

In this study, I showed that in UBR5 knock-out endothelial cells, MCMV replicated less efficiently than in WT cells (Figure 27B), suggesting that UBR5 has a pro-viral function for MCMV. UBR5 is a ubiquitously expressed protein [130], thus it remains puzzling why the replication defect of MCMV m139-STOP specifically in endothelial cells depends on UBR5 expression. So far, only one endothelial cell specific function of UBR5 has been described, namely its contribution to the DNA repair mechanism. Precisely, in murine endothelial cells, peroxisome proliferator activated receptor γ (PPARγ) forms a complex with UBR5, which transcriptionally activates ATM and further induces DNA repair (Figure 38) [173]. ATM-dependent DNA repair was shown to be important for HCMV viral replication [174]. Therefore, it might be possible that upregulation of DNA repair mechanisms by UBR5 stimulates viral replication in endothelial cells.

6.6 Coordinated regulation of DDX3 and UBR5 by m139

In this study, I have detected an interplay between host proteins UBR5 and DDX3 upon MCMV infection. The replication defect of MCMV m139-STOP depends on the expression of both UBR5 and DDX3. Upon MCMV infection, both UBR5 and DDX3 are recruited to the viral replication compartments. While DDX3 is actively recruited by m139, URB5 enrichment in the replication compartments does not depend on m139 (Figure 26). Moreover, the interaction between m139 with DDX3 depends on UBR5 and *vice versa* (Figure 28). One of the possibilities of these co-dependent interactions of DDX3 and UBR5 with m139 is a complex formed by these three proteins in the MCMV replication compartment.

Although the interaction between DDX3 and UBR5 has not been described, there are signalling pathways in which both DDX3 and UBR5 are involved. Specifically, UBR5 and DDX3 are found to regulate cell cycle progression, transcription, and the DNA damage response. UBR5 and DDX3 were identified in the regulation of translation through mRNA-binding protein PABP, which is required for the initiation of translation (Figure 38). UBR5 transcriptionally activates PABP1 expression [140], while DDX3 directly interacts with PABP and specific mRNAs to promote their translation [123]. Remarkably, the transcriptional activation of PABP by UBR5 is modulated by HCMV [108]. Therefore, the investigation of translation upon MCMV infection might bring forward an understanding of the UBR5 and DDX3 interface.

6.7 m139 as MCMV host range determinant

Our laboratory previously identified the murine genes M112/M113 and M117 as host range determinants. Mutations in these genes led to adaptation of murine CMV to human RPE-1 cells and efficient replication. Complete genome sequencing of the MCMV human-cell adapted strains revealed a number of additional mutations in other MCMV genes, among them is one in m139 [40, 41]. Mutation of m139 alone did not allow MCMV replication in human cells. However, the addition of a mutation in m139 to a virus already mutated in M117 significantly increased MCMV replication in human cells (Figure 35). This observation implies that m139 is not sufficient for but rather can enhance MCMV replication in human cells.

Interestingly, the m139 mutation identified in the human-cell adapted MCMV leads to the formation of a small truncated protein, which is not recruited to the viral replication compartments (Figure 36). Moreover, additional loss-of-function mutations of m139 promoted the enhancement of viral replication in human cells, indicating that the lack of m139 can provide an advantage to MCMV replication in human cells. Since RPE-1 cells produce very low level of IFN-β upon MCMV infection [39], it is unlikely that the observed enhancement of viral replication caused by m139 mutations depends on IFN-β signalling. On the contrary, recent work of Ostermann et al. on M117 gene as host range determinant, has revealed the importance of the cell cycle regulation in the adaptation of MCMV to the human cells [41]. Deletions of m139 and M117 from MCMV enhance viral replication, suggesting that they both might be involved in cells cycle regulation. Both interaction partners of m139, DDX3 and UBR5, are involved in the regulation of cell cycle progression. Thus, m139 might regulate cell cycle through its interactions to promote efficient viral replication in murine cells, while in human cells it could be detrimental for the MCMV WT replication.

Upregulation of anti-apoptotic Bcl-2-like proteins was shown to promote MCMV replication in human cells [37]. Recently, the ability of DDX3 to activate anti-apoptotic genes, such as Bcl-xL, cyclin D1, and cyclin E, was detected [175]. If m139 inhibits DDX3-dependent upregulation of anti-apoptotic proteins, its deletion from MCMV might improve MCMV replication. Given that m139 modulates UBR5 and DDX3 in murine cells, the regulation of these host proteins in MCMV-infected human cells needs to be investigated.

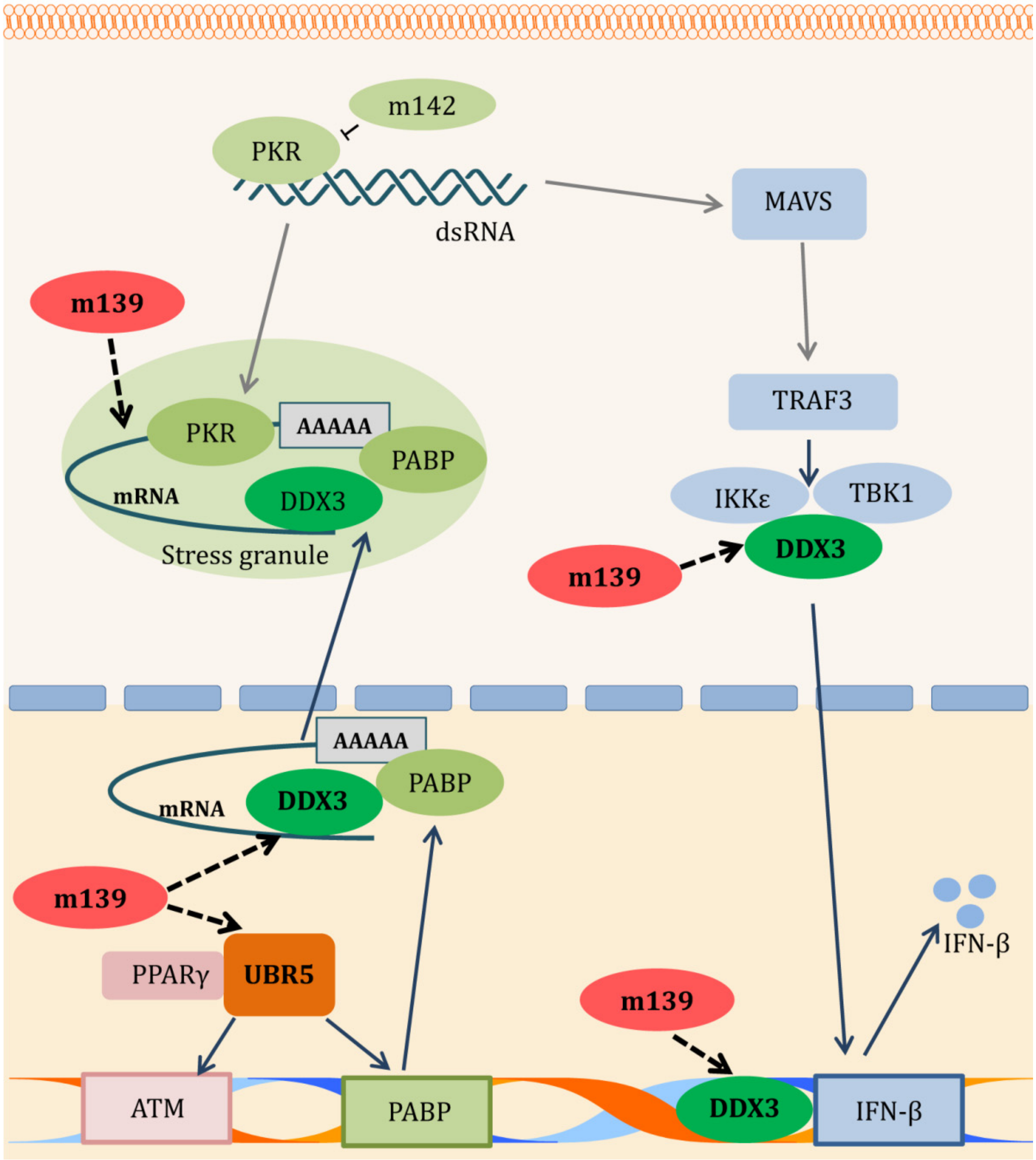
m142
PKR
dsRNA
MAVS
m139
PKR
AAAAA
PABP
mRNA
DDX3
Stress granule
TRAF3
IKKε
TBK1
m139
DDX3
AAAAA
PABP
mRNA
DDX3
m139
PPARγ
UBR5
IFN-β
m139
ATM
PABP
DDX3
IFN-β

Figure 38. Proposed functions of DDX3 and UBR5 and their potential inhibition by m139. IFN-β signaling pathway: DDX3 associates with the TBK1/IKKε complex and directly activates the IFN-β promotor. mRNA translation: DDX3 facilitates export of mRNAs. Stress granule formation: DDX3 and PKR coordinate formation of mRNA-containing stress granules in cytoplasm. ATM activation by UBR5: UBR5 transcriptionally activates ATM, promoting DNA repair mechanisms. Regulation of translation: UBR5 and DDX3 positively regulate translation through mRNA-binding protein PABP.

6.8 Summary

In the present study, the physiological role of the murine cytomegalovirus m139 protein was investigated. m139 was shown to be important for efficient replication in differentiated macrophages and endothelial cells as well as for MCMV dissemination in vivo.

m139 is expressed with early kinetics and was detected in the nucleus and cytoplasm upon MCMV infection. M112/M113 proteins recruit m139 to the viral replication compartments, where it accumulates throughout the course of infection.

RNA helicase DDX3 and the E3 ubiquitin ligase UBR5 were identified as interactors of m139 using affinity purification and mass spectrometry. The interaction of m139 and DDX3 is UBR5-dependent and vice versa, indicating an interplay between these factors. Moreover, m139 recruits DDX3 to viral replication compartments in the nucleus. The replication impairment of the m139-deficient MCMV in endothelial cells was determined by the expression of DDX3 or UBR5. Additionally, this study recognized m139 as a modulator of DDX3-dependent IFN-β induction in MCMV-infected macrophages.

Ultimately, the role of m139 in the cross-species adaptation was dissected. Loss of function mutations of this gene appear to significantly enhance MCMV replication in human cells, but the underlying mechanism remains to be identified.

Taken together the results of this study reveal hitherto unknown functions of the m139 MCMV protein as cell tropism factor and modulator of antiviral immune signaling.

7 Materials

7.1 Cell lines

Name	Description	Source
HEK-293A	Human embryonic kidney epithelial cells, subclone of the 293 Cell	Invitrogen (R705-07)
HEK-293T	Human embryonic kidney epithelial cells transformed with large T antigen	ATCC (CL-11268)
Phoenix	Retroviral packaging HEK-293T cells stably expressing gag, pol, env	[176]
NIH/3T3	Murine embryonal spontaneously immortalized fibroblasts, isolated from NIH/Swiss mice	ATCC (CRL-1658)
SVEC4-10	Murine endothelial cells immortalized by SV40	ATCC (CRL-2181)
10.1	Spontaneously immortalized murine embryonal fibroblasts isolated from BALB/c mice	[177]
J774A.1	Murine macrophages derived from a tumor in a female BALB/c mouse	ATCC (TIB-67)
RPE-1	Human retinal pigment epithelial cells immortalized with human telomerase reverse transcriptase	ATCC (CRL-4000)
RAW264.7	Murine macrophages derived from Abelson murine leukemia virus-induced tumor in a male BALB/C mouse	ATCC (TIB-71)
TCMK-1	Murine kidney epithelial cells immortalized by SV40	ATCC (CCL-139)
M2-10 B4	Murine bone marrow stromal cells	ATCC (CRL-1972)
iBMDM WT	Wild-type immortalized murine bone marrow-derived macrophage	NIAID NIH (NR-9456)
MEF WT	Murine embryonic fibroblasts isolated from wildtype C57BL/6J mice and spontaneously immortalized	Generated by E. Ostermann (HPI, Hamburg)
iBMDM IFN-β-luc	Primary bone marrow macrophages were isolated from reporter mice and immortalized with a retrovirus expressing oncogenes	Kindly provided by M. Brinkmann (HZI, Braunschweig, Germany) [145]

p204-Myc SVEC4-10	SVEC4-10 cells stably transduced with p204-Myc expressing PMSCV-puro	This study
DDX3 $^{-/-}$ SVEC4-10	DDX3 knock-out generated using CRISPR/Cas9	This study
UBR5$^{-/-}$ SVEC4-10	UBR5 knock-out generated using CRISPR/Cas9	This study
ZBP1 $^{-/-}$ SVEC4-10	ZBP1 knock-out generated using CRISPR/Cas9	Kindly provided by W. J. Kaiser (University of Texas Health Science Center, San Antonio, USA) [151]

7.2 Viruses

Name	Description	Source
MCMV Smith "repaired"	MCMV Smith strain pSM3fr-MCK-2fl	[178]
MCMV-GFP	MCMV Smith strain, cloned as BAC, expressing GFP	[179]
MCMV/h3	Human cell-adapted MCMV-GFP	[39]
MCMV M117mut/h3	MCMV-GFP with introduced mutation in M117 gene	[41]
MCMV M45-HA	MCMV Smith pSM3fr-MCK-2fl with reinserted M45 full length ORF including a C-terminal HA tag	[83]
VSV-GFP	GFP-expressing vesicular stomatitis virus	[39]

7.3 Virus mutants generated in this work

Name	Description
MCMV Δ139-141	MCMV Smith strain with deleted m139-m141 by insertion of kanR
MCMV 139-V5-140-Flag-141-HA	MCMV Smith strain with introduced V5 epitope tag inserted on 5' end of m139, Flag tag on 5' end of m140 and HA tag on 3' end of m141
MCMV Δm139	MCMV Smith strain with introduced deletion of m139

MCMV m139-HA	MCMV Smith strain with insertion of HA-epitope tag on 3' end of m139
MCMV m139mut/h3	MCMV-GFP with introduced point mutation, deletion of Cytosine (ΔC) 297bp from the beginning of the m139 ORF
MCMV M117mut/h3+m139mut/h3	MCMV M117mut/h3 with introduced mutation (ΔC) into m139
MCMV HA-m139-STOP	MCMV Smith strain with inserted HA tag on 3' end of m139 and point mutation (STOP codon)
MCMV K7R[Δm139]	VACV gene HA-K7 cloned from pCMV6-HA-K7R vector into m139 ORF
MCMV K7[m139-STOPΔm02-06]	VACV gene HA-K7 cloned from pCMV6-HA-K7R vector into the nonessential m02-m06 region of MCMV (pSM3fr-MCK-2fl) by using the pReplacer system [37]

7.4 Bacteria

Name	Description	Growth temperature	Source
E.coli DH10B	F- mcrA Δ(mrr-hsdRMS-mcrBC) Φ80dlacZΔM15 ΔlacX74 endA1 recA1 deoR Δ(ara,leu)7697 araD139 galU GalK nupG rpsL λ-	37^0C	Life Technologies
E.coli GS1783	DH10B l cI857 Δ(cro-bioA)<>araC-PBADI-sceI	30^0C	[180]

7.5 Plasmids

Name	Description	Source
pcDNA3	Expression vector, ampR	Life Technologies
pEPkan-S	Template plasmid for *en passant* mutagenesis, contains I-Sce-aphA1 cassette, kanR	[180]
pSicoR-CRISPR-PuroR	Lentiviral expression vector, contains Cas9 gene, PuroR and site for cloning of gRNA	[181]
pMDG.2	Lentiviral second-generation packaging plasmid, ampR	[181]

pCMVR8.91	Lentiviral second-generation packaging plasmid, ampR	[181]
pMSCVpuro	Retroviral expression vector, used for retrovirus production for transduction of eukaryotic cells, ampR, puroR	Clontech Laboratories
pCMV-HA-K7R	K7R from Vaccinia virus cloned into pCMV-HA vetor, ampR	Kindly provided by M. Schroeder (Maynooth University, Maynooth, Ireland) [118]
pReplacer	Based on pBluescriptII KS+, plasmid for homologous recombination to insert genes in the m02-m06 region of MCMV, *ampR*	[37]
pGL3basic-IFNβ-Luc (IFNβ-Luc)	812 bp murine IFNβ promoter region	Kindly provided by M. Brinkmann (HZI, Braunschweig, Germany) [154]
pRL-Renilla	Express Renilla luciferase	Promega
pBS- TRS1-HA	Express human cytomegalovirus TRS1 with a C-terminal HA tag	Cloned R. Brost (HPI, Hamburg)
pcDNA3-IRS1-His	Express human cytomegalovirus IRS1 with a C-terminal 6X his tag	Kindly provided by A. Geballe (Fred Hutchinson Cancer Research Center, Seattle, USA)
pCDNA3-IKKε	Encodes mouse IKKε gene	Kindly provided by R. Lin (McGill University, Montreal, Canada)
pCMV6-ifi204	Ifi204 Mouse Tagged ORF Clone	Origene (BC010546)
pCDNA3-DDX3-HA	DDX3-HA expressing vector	Addgene (44975)

7.6 Plasmids generated for this work

Name	**Description**	**Cloning approach**
pCDNA3-m140-Flag3x-KAN	Shuttle vector contains MCMV m140 N-terminally Flag3X-tagged, kanR flanked by homology regions inserted into m140 cloned into pCDNA3	Generated in two steps: (1) m140-Flag3x amplified from MCMV BAC Smith by specific primers and inserted into pCDNA using BamHI and XbaI cutting sites; (2) kanR was amplified from pEPkan-S by specific primers and inserted by ligation using Bam HI cutting site into pCDNA-m140-Flag3X
pcDNA3-HA-m139	MCMV m139 with HA tag on N-terminus cloned into pcDNA3	m139 amplified from MCMV Smith and inserted into pCDNA3 using EcoRI and EcoRVcutting sites
pcDNA3-HA-m139mut/h3	Truncated protein m139mut/h3 with HA tag on N-terminus cloned into pCDNA3	m139 amplified from MCMV m139mut/h3 and inserted into pCDNA3 using EcoRI and EcoRV cutting sites
pMSCV-puro-p204-Myc	Murine protein p204 C-terminally Myc-tagged cloned into pMSCV-puro	p204 was amplified from pCMV6-ifi204 was inserted into pMSCV-puro by ligation using Eco RI cutting site
pCMV-HA-K7-KAN	VACV HA-K7 with inserted kanR flunked by homology regions cloned into pCMV-puro	kanR with homology regions was amplified from pEPkan-S and inserted by ligation to the EcoRI cutting side into pCMV-HA-K7
pReplacer-K7-Kan	VACV HA-K7 with inserted kanR flunked by homology regions cloned into pReplaser vector	HA-K7 amplified by specific primers from pCMV-HA-K7 and inserted by ligation using SalI and Mfe cutting sites
pCDNA-DDX3-Myc	Human DDX3 C-terminally Myc-tagged cloned into pCDNA vector	DDX3 was amplified from pCDNA3-DDX3-HA by specific primers and cloned by Gibson assembly cloning

		into pCDNA using XhoI and EcoRI cutting sites
pCDNA-HA-US22	HCMV US22 with N-terminal tag cloned into pcDNA3	US22 was amplified from TB40/E BAC and inserted by ligation into pCDNA vector using EcoRI and XhoI

7.7 Primers

Name	Sequence	Application
US22_del_FWD	CTAGCGATCGGAGCCGGTTTCCATGTTGTTGCTCGTCGATCCCGCCTGAGTAGGGATAACAGGGTAATCGATTT	To delete m139-141 from MCMV Smith strain by insertion of kanR
US22_del_REW	ATGGAGAGGCCGGTGACGGCGAACGCCATCTCCGCGTACAAGCGGGTGATGCCAGTGTTACAACCAATTAACC	
FWD_US22_deletion_kan	ATATTGAACGGGACGGAGGT	To sequence verify the insertion of kanR in the m139-m141 gene region
REW_US22_deletion_kan	GCCTCGCCATCACATAAA	
139_del_FWD	CATAATCTCGCGCTCGCTCTTCTCCTTGCCGCCGTCGAACATGTCCATGGTAGGGATAACAGGGTAATCGATTT	To delete m139 from MCMV Smith strain by insertion of kanR
139_del_REW	ATGTGGTCTCTCCGCGGCGCCCAGAGACGCGACCTGCGTTTCGATGGTCAGCCAGTGTTACAACCAATTAACC	
FWD_139_insert	CGACTTCAAGAGCTTCCA	To sequence verify m139 gene
REW_139_insert	CCGAACACCTGAAACGTC	
139_del_FWD_sequencing	TGCGGCACGGCTTTTATA	
139_del_REW_sequencing	AGGACTGGACGGATACCAA	
ECOR1_139_HA_tag_REV	TTAAGAATTCATGTACCCATACGATGTTCCAGATTACGCTTGGTCTCTCCGCGGCGCCCA	To clone HA-m139 into pcDNA3
M139_FWD	TATAGATATCCTAGCGATCGGAGCCGGTTT	
141_HA_FWD	GCCGCTGGTGGGGTGGGGGGGGTGATGGTGGGGGTGTGGCTAAGCGTAATCTGGAACATCGTATGGGTATAGGGATAACAGGGTAATCGATTT	To insert HA tag in m141 for generation of 139-V5-140-Flag-141-HA MCMV
141_HA_REW	GATCGTCCCCTTCTACCGCGCGCGGCCGGGTCCCTCGGAGACCTACCCATACGATGTTCCAGATTACGCTGCCAGTGTTACAACCAATTAACC	
139_V5_FWD	GTCGCGTCTCTGGGCGCCGCGGAGAGACCACGTAGAATCGAGACCGAGGAGAGGGTTAGGGATAGGCTTACCCATTAGGGATAACAGGGTAATCGATTT	To insert V5 tag in m139 for generation of 139-V5-140-Flag-141-HA MCMV
139_V5_REW	GCCAGACGGAGCAGACAGAGAGAGAGAAGGATGGGTAAGCCTATCCCTAACCCTCTCCTCGGTCTCGATTCTACGGCCAGTGTTACAACCAATTAACC	

M140_Flag3X_ shuttle plasm_FWD	ACCATTATCACCATCATCTCATCCGGCGAGATGGACTACAAGGACCACGACG	To amplify m140-Flag3X from shuttle plasmid to clone into BAC MCMV Smith for generation of 139-V5-140-Flag-141-HA MCMV
M140_Cterm_FL3X_shuttle_REV	TCTGCTCCGTCTGGCGCCGGCGCCGTCAACTCACGGTCTGCAGAGTCTGAGC	
140_BAMHI_FLAG	TTAAAAGCTTATGGACTACAAGGACCACGACGGTGACTACAAGGACCACGACATCGACTACAAGGACGACGACGACAAGGACAGCACACTGTGGGAGTC	To clone m140 from BAC MCMV Smith into shuttle vector pcDNA-m140-Flag3X
140_FWD	TATATCTAGATCACGGTCTGCAGAGTCTGA	
Flag3X-KAN-FWD	GGATCCATGGACTACAAGGACCACGACGGTGACTACAAGGACCACGACATCGACTATAGGGA TAA CAG GGTAATCGATTT	To amplify kanR with homology region for further insertion into shuttle plasmid pcDNA-m140-Flag3x-KAN
Falg3X-KAN-REV	TTAAGGATCCGCCAGTGTTACAACCAATTAACC	
HA_139_FWD_Smith	CGAAACGCAGGTCGCGTCTCTGGGCGCCGCGGAGAGACCAAGCGTAATCTGGAACATCGTATGGGTACATCCTTCTAGGGATAACAGGGTAATCGATTT	To insert HA tag for HA-m139 MCMV
HA_139_REV_Smith	CGCCGGCGCCAGACGGAGCAGACAGAGAGAGAGAAGGATGTACCCATACGATGTTCCAGATTACGCTTGGTCTCTCGCCAGTGTTACAACCAATTAACC	
139_HA_FWD_Smith	GCGCCCCCCCGCGAGCGGCTGACACAGCGCCGCTGGACTAAGCGTAATCTGGAACATCGTATGGGTAGCGATCGGATAGGGATAACAGGGTAATCGATTT	To insert HA tag for m139-HA MCMV
139_HA_REV_Smith	GGGATCGACGAGCAACAACATGGAAACCGGCTCCGATCGCTACCCATACGATGTTCCAGATTACGCTTAGTCCAGCGCCAGTGTTACAACCAATTAACC	
139_H3_trunc_FWD	GTCTGACCTGTTCATAGATCGCGCCGCGCTGGACGGGACCGGCGCTCTGACGCGGGCTCCGCCAGTGTTACAACCAATTAACC	To insert point mutation (ΔC 293 nucleotides from 3' end) into m139 for generation of m139mut/h3
139_H3_trunc_REV	GAGTCGCTCTCGCTGTCGCGGGAGCCCGCGTCAGAGCGCCGGTCCCGTCCAGCGCGGCGCTAGGGATAACAGGGTAATCGATTT	
ECoRv_HAm139_trunc_FwD_cor	TATAGATATCTCAGCGAGTAGAGTCGCTGCG	For cloning of HA-m139mut/h3 into pcDNA3
P204_CDNA_ECORI_FWD	TTAAGAATTCGTCGACTGGATCCG	To re-clone p204-Myc from pCMV6-IFI204 into pMSCV-puro
P204_CDNA_ECORI_MYC_REV	TATAGAATTCTTACAGATCCTCTTCTGAGATGAGTT	
p204_SEQ_FWD	GAATCACCAGAACATGAAG	To sequence verify p204
p204_SEQ_REV	TGTTCTCCACACACTAAC	

m139-HA_STOP_KAN_REV	CGACGAGTGGTGTTTGGCGTACGAGGATTGCATGGACCAGTAGTTCGGAGAATACGGCGGCGCCAGTGTTACAACCAATTAACC	To introduce STOP codon into m139 in the HA-m139 MCMV
m139-HA_STOP_KAN_FWD	GGAAGGCTCCTCTCGTCCACGCCGCCGTATTCTCCGAACTACTGGTCCATGCAATCCTCGTTAGGGATAACAGGGTAATCGATTT	
gRNA_p204_2_fwd	ACCGATTCTGGGGTTGTGATTTT	To generate gRNAs for p204 CRISPR/Cas9 knock-out
gRNA_p204_2_rev	AAACAAAATCACAACCCCAGAAT	
gRNA_p204_3_fwd	AACGAATTGACTTCCACTGAAGA	
gRNA_p204_3_rev	AAACTCTTCAGTGGAAGTCAATT	
gRNA_p204_4_fwd	AACGAACATGCTTCATGCTACAG	
gRNA_p204_4_rev	AAACCTGTAGCATGAAGCATGTT	
EF1A reverse colony primer	TCTAGGCACCGGGTCAATTGC	To sequence verify gRNA insertion into RP-418 Cas9-puro vector
IFNbeta_FWD_MB_qPCR	CTGGCTTCCATCATGAACAA	qPCR for IFN-β
IFNbeta_REV_MB_qPCR	AGAGGGCTGTGGTGGAGAA	
actin F	AGAGGGAAATCGTGCGTGAC	qPCR for β-Actin
actin R	CAATAGTGATGACCTGGCCGT	
DDX3_FWD_Gibson	CTAGCGTTTAAACGGGCCCTCTAGACTCGAGCCGCCACCATGGAACAA	To clone DDX3-Myc into pCDNA3 by Gibson assembly cloning
DDX3_REV_Myc_Gibson	ACTAGTCCAGTGTGGTGGAATTCTGCAGATTCACAGATCCTCTTCTGAGATGAGTTTTTGTTCGTTACCCCACCAGTCAACC	
gRNA_1_DDX3_FWD	ACCGTGGAGTTCTAGTAAAGATA	To generate gRNAs for DDX3 CRISPR/Cas9 knock-out
gRNA_1_DDX3_REV	AAACTATCTTTACTAGAACTCCA	
gRNA_2_DDX3_FWD	ACCGCTTCTCTGTTCCTTAAATG	
gRNA_2_DDX3_REV	AAACCATTTAAGGAACAGAGAAG	
gRNA_3_DDX3_FWD	ACCGACATTCCAGTCGAAGCAAC	
gRNA_3_DDX3_REV	AAACGTTGCTTCGACTGGAATGT	
ECORI_US22_HA_FWD	TTAAGAATTCATGTACCCATACGATGTTCCAGATTACGCTTCCCTACTCACCAAAGCCGC	To clone HA-US22 gene from TB40/E into pCDNA3
XhoI_US22_REV	TATACTCGAGTTAGGGACCCGGGTCTGGT	
gRNA1_EDD_FWD	ACCGCTTTTGTGTTTGAAGGTTA	To generate gRNAs for UBR5 (EDD) CRISPR/Cas9 knock-out
gRNA1_EDD_REV	AAACTAACCTTCAAACACAAAAG	
gRNA2_EDD_FWD	ACCGCTCCAGTACATTCAGAGGT	
gRNA2_EDD_REV	AAACACCTCTGAATGTACTGGAG	
gRNA3_EDD_FWD	ACCGGCTACTATTAAACAGTGTG	
gRNA3_EDD_REV	AAACCACACTGTTTAATAGTAGC	
gRNA4_EDD_FWD	ACCGATGGCAGAATTTGTAGGAT	
gRNA4_EDD_REV	AAACATCCTACAAATTCTGCCAT	
EcoRI_K7R_Kan_FWD	TTAAGAATTCAGATGGCGACTAAATTAGATTATGAGGATGCTGTTTTTTACTTTTAGGGATAACAGGGTAATCGATTT	To re-clone K7 from pCMV-HA-K7 into shuttle vector pCMV-HA-K7-KAN
EcoRI_Kan_REV	TATAGAATTCGCCAGTGTTACAACCAATTAACC	
K7Rinsm139FWD	CAGCCGAAAGGTGATGTACTCCCGCACGAGTGTGTACGTCGTGTCTCAATTCAATTTTTTTTCTAGA	To replace m139 by HA-K7-KAN on the

K7Rinsm139REV	GTTGACGGCGCCGGCGCCAGACGGAGCAGACAGAGAGAGAGAAGGATGTACCCATACGATGTTC	backbone of MCMV Smith
SAlIK7RpReplREv	TATAGTCGACTCAATTCAATTTTTTTT	To clone K7 into pReplacer
Mfe_K7R_pRepl	TTAACAATTGATGTACCCATACGATGTTCC	
mo2_BAC_seq_fwd	GTACCCGCAAGTCGATCT	To sequence verify insertion of pReplacer-HA-K7 into m139-STOP MCMV
m06_BAC_seq_rev	CCCCTCATTCTCTCACTCG	

7.8 Antibodies

7.8.1 Primary antibodies

Antigen	Clone	Species	Application (dilution)	Source
V5	R960-25	mouse	western blot (1:1000) immunofluorescence (1:500)	Invitrogen
Flag	polyclonal	rabbit	western blot (1:1000)	Sigma-Aldrich
Flag	M2	mouse	western blot (1:1000)	Sigma-Aldrich
HA	16B12	mouse	western blot (1:1000)	Covance
HA	3F10	rat	immunofluorescence (1:300)	Sigma-Aldrich
B-actin	AC-74	mouse	western blot (1:3000)	Sigma-Aldrich
MCMV IE1	Croma101	mouse	western blot (1:1000)	S. Jonjic, University of Rijeka, Croatia
MCMV IE3	serum	rabbit	western blot (1:1000)	Eva Borst, MHH
MCMV E1	serum	rabbit	immunofluorescence (1:500)	J. Kerry, Eastern Virginia Medical School, USA [144]
MCMV E1	Croma103	mouse	western blot (1:1000) immunofluorescence (1:500)	S. Jonjic, University of Rijeka, Croatia
MCMV M45	M45.01	mouse	western blot (1:1000)	S. Jonjic, University of Rijeka, Croatia
MCMV M57	M57.02	mouse	western blot (1:1000)	S. Jonjic, University of Rijeka, Croatia
LSD1	polyclonal	rabbit	western blot (1:500)	Cell Signalling
GAPDH	14C10	rabbit	western blot (1:1000)	Cell Signalling
p204	polyclonal	rabbit	western blot (1:500)	Abcam
Myc	4A6	mouse	western blot (1:100)	Millipore

			immunofluorescence (1:500)	
DDX3	C-4	mouse	western blot (1:500)	Santa Cruz Biotechnology
UBR5	B-11	mouse	western blot (1:1000)	Santa Cruz Biotechnology

7.8.2 Secondary antibodies

Antigen	Conjugate	Species	Application (dilution)	Source
Mouse Ig	HRP	goat	western blot (1:3000)	Dako Cytomation
Rabbit Ig	HRP	goat	western blot (1:3000)	Dako Cytomation
Rat Ig	Alexa 488	goat	immunofluorescence (1:1000)	Invitrogen
Mouse Ig	Alexa 488	goat	immunofluorescence (1:1000)	Invitrogen
Rabbit Ig	Alexa 488	goat	immunofluorescence (1:1000)	Invitrogen
Rat Ig	Alexa 633	goat	immunofluorescence (1:1000)	Invitrogen
Mouse Ig	Alexa 647	goat	immunofluorescence (1:1000)	Invitrogen
Mouse Ig	Alexa 555	goat	immunofluorescence (1:1000)	Invitrogen
Rabbit Ig	Alexa 555	goat	immunofluorescence (1:1000)	Invitrogen
Rat Ig	Alexa 555	goat	immunofluorescence (1:1000)	Invitrogen

7.8.3 Nuclear dyes

Name	Application (dilution)	Source
Hoechst 33342	immunoflurescence (1:1000)	Thermo Fisher Scientific
DRAQ5	immunoflurescence (1:1000)	Biostatus

7.9 Chemicals and reagents

7.9.1 Antibiotics

Name	Application	Concentration	Source
Ampicillin	selection of bacteria	100 µg/ml	Roth
Chloramphenicol	selection of bacteria	15 µg/ml	Roth
Kanamycin	selection of bacteria	100 µg/ml	Roth
Penicillin	cell culture media supplement	100 U/ml	Sigma-Aldrich

Streptomycin	cell culture media supplement	100 µg/ml	Sigma-Aldrich
Puromycin	selection of transduced cells	1 µg/ml	Sigma-Aldrich
L-(+)-Arabinose	Selection of bacteria	1% (w/v)	Sigma-Aldrich

7.9.2 Enzymes

Name	**Source**
Dream Taq Green DNA polymerase and buffer	Thermo Fischer Scientific
Fast Digest restriction enzymes and buffer	Thermo Fischer Scientific
PRECISOR DNA polymerase and buffer	BioCat
T4-DNA-ligase and buffer	Thermo Fischer Scientific
RevertAid H Minus Reverse Transcriptase	Thermo Fischer Scientific
SYBR™ Green PCR Master Mix	Thermo Fischer Scientific

7.9.3 Molecular mass standards

Name	**Source**
O'GeneRuler™ DNA Ladder Mix	Thermo Fisher Scientific
PageRuler™ Prestained Protein Ladder	Thermo Fisher Scientific

7.9.4 SILAC reagents

Name	**Source**
L-arginine	Sigma-Aldrich
L-arginine-$^{13}C_6$	Sigma-Aldrich
L-lysine	Sigma-Aldrich
L-lysine-$^{13}C_6$	Sigma-Aldrich
L-proline	Sigma-Aldrich
Stable L-glutamine	Sigma-Aldrich

7.9.5 Other reagents and chemicals

Name	**Source**
Anti-HA Affinity Matrix (anti-HA rat, clone 3F10)	Roche
Pierce™ ECL Western Blotting Substrate	Thermo Fisher Scientific
Lumigen ECL Ultra (TMA-6)	Beckman Coulter
Nitrocellulose membrane (0.2 µm)	GE Healthcare Life Science
Polybrene	Millipore

Polyethylenimine (PEI), branched	Sigma-Aldrich
PolyFect® Transfection reagent	Qiagen
Lipofectamine 2000 Transfection Reagent	Thermo Fisher Scientific
Protease inhibitor cocktail cOmplete™ mini, EDTA free	Roche
Whatman® gel blotting paper, Grade GB003	Sigma-Aldrich
Centrinone	Hycultec
KU-60019	Selleckchem
Cycloheximide	Sigma-Aldrich
Actinomycin D	Sigma-Aldrich
RNase inhibitor RiboLock	Thermo Fisher Scientific
Nycodenz	Progen
Protein A-agarose	Roche
Protein G-agarose	Roche

7.10 Kits

Name	Source
BCA Protein Assay Kit	Thermo Fisher Scientific
innuPREP DNA mini kit	Analytik Jena
innuPREP RNA Mini Kit	Analytik Jena
mi-Plasmid Miniprep Kit	Metabion
NucleoBond Gel and PCR Clean-up	Macherey-Nagel
NucleoBond Xtra Midi	Macherey-Nagel
Gibson Assembly® Ultra Kit	BioCat
TURBO DNA-free™ Kit	Thermo Fisher Scientific
NE-PER™ Nuclear and Cytoplasmic Extraction Reagents	Thermo Fisher Scientific
TURBO DNA-free Kit	Ambion
Luciferase Assay System	Promega
Dual-Luciferase® Reporter Assay System	Promega

Other commonly used chemicals were purchased from Roth, Merck or Sigma-Aldrich.

7.11 Media and buffers

7.11.1 Cell culture media and buffers

Name	Source
Dulbecco's Modified Eagle Medium (DMEM), high glucose	Sigma-Aldrich
Dulbecco's Phosphate Buffered Saline (PBS) (1x)	Sigma-Aldrich

Fetal calf serum (FCS)	PAN Biotech
Newborn calf serum (NCS)	PAN Biotech
OptiMEM-I	Thermo Fisher Scientific
penicillin/streptomycin (100 x)	Sigma-Aldrich
trypsin-EDTA (1x)	Sigma-Aldrich
Dulbecco's Modified Eagle Medium (DMEM) for SILAC	Thermo Fisher Scientific
Fetal bovine serum, dialyzed (dFBS)	Thermo Fisher Scientific

7.11.2 Cell culture media

Media	**Recipe**
DMEM 10 % NCS	DMEM + 10 % (v/v) NCS and 1 % (v/v) penicillin/streptomycin
DMEM 10 % FCS	DMEM + 10 % (v/v) FCS and 1 % (v/v) penicillin/streptomycin
DMEM SILAC light (R0K0)	DMEM for SILAC + 10 % (v/v) dFCS and 1 % (v/v) penicillin/streptomycin Supplements added: 84 mg/l L-arginine, 143 mg/l L-lysine, 200 mg/l L-proline, 584 mg/l stable L-glutamine Filtered using 0.22 µm sterile filter
DMEM SILAC heavy (R6K6)	DMEM for SILAC + 10 % (v/v) dFCS and 1 % (v/v) penicillin/streptomycin Supplements added: 84 mg/l L-arginine-$^{13}C_6$, 143 mg/l L-lysine-$^{13}C_6$, 200 mg/l L-proline, 584 mg/l stable L-glutamine Filtered using 0.22 µm sterile filter

7.11.3 Bacteria medium

Lysogeny broth (LB) medium (Lennox)	Roth
Lysogeny broth (LB) agar	LB medium with 15 g/l agar

7.11.4 Agarose gel electrophoresis

Buffer	Components	Application
50x TAE	2 M Tris 50 mM EDTA 5.7 % (v/v) acitic acid ddH2O	Diluted to 1x with ddH2O before using. Applied for preparing agarose gel and as running buffer

	pH 8.0	
10 x TBE	990 mM Tris 40 mM EDTA 990 mM borate ddH2O pH 8.0	Diluted to 0.5 x with ddH2O before using. Applied for preparing agarose gel and as running buffer

7.11.5 SDS polyacrylamide gel electrophoresis (SDS-PAGE)

Buffer	**Components**	**Application**
4x SDS sample loading buffer	150 mM Tris 2 mM EDTA 20 % (v/v) glycerol 4 % (v/v) SDS 10 % β-mercaptoethanol bromophenol blue ddH2O pH 6.8	Diluted to 1x with ddH2O before using. Applied for lysing cell samples and as loading buffer
10 x Laemmli running buffer	250 mM Tris 1.92 M glycine 1 % (w/v) SDS dd H2O	Diluted to 1x with ddH2O before using. Applied for Laemmli gel running buffer
10 x TBS-T	100 mM Tris 1,5 M NaCl 1 % (v/v) Tween dd H2O pH 7.5	Diluted to 1x with ddH2O before using. Used for antibody dilutions and washing of nitrocellulose membranes
Transfer buffer (semi-dry)	50 mM Tris 150 mM NaCl 0.04 % (v/v) SDS 20 % (v/v) methanol dd H2O	Used for semi-dry transfer

Transfer buffer (wet-blot)	25 mM Tris 192 mM Glycine 20 % methanol dd H2O	Used for wet transfer
10X Cathode buffer	1 M Tris Base 1 M Tricine 1 % SDS dd H2O	Diluted to 1x with ddH2O before using. Applied as top running buffer for tricine-SDS-PAGE
10X Anode Buffer	2 M Tris dd H2O pH 8.9	Diluted to 1x with ddH2O before using. Applied as lower running buffer for tricine-SDS-PAGE.
Tricine gel buffer	3M Tris base 0.3% SDS pH 8.5 dd H2O	Used for preparing tricine gels.
Coomassie Fixing Buffer	50 % Methanol 10 % Acetic acid 40 % ddH2O	For fixing SDS-PAGE gels for Coomassie staining
Coomassie Staining Buffer	Coomassie Fixing Buffer 0.1 % (v/v) Coomassie R-250	For staining SDS-PAGE gels for Coomassie staining
Coomassie Destaining Buffer	40 % Methanol 10 % Acetic acid 50 % ddH2O	For destaining SDS-PAGE gels for Coomassie staining

7.11.6 Buffers for immunoprecipitation

Buffer	**Components**	**Application**
NP-40 lysis buffer (sterile filtered for SILAC samples)	50 mM Tris-HCl 150 mM NaCl 1% (v/v) Nonidet P-40 pH 7.5	Used for lysing cell samples and as loading buffer

Minimal washing buffer (sterile filtered for SILAC samples)	50 mM Tris-HCl 150 mM NaCl	Used for washing the beads in immunoprecipitation
IP Washing Buffer 1	10 mM Tris-HCl 150 mM NaCl 150 mM NaCl 0.2 % Nonidet P-40 2 mM EDTA pH7.6	Used for washing the beads in immunoprecipitation
IP Washing Buffer 2	10 mM Tris-HCl 500 mM NaCl 0.2 % Nonidet P-40 2 mM EDTA pH7.6	Used for washing the beads in immunoprecipitation
IP Washing Buffer 3	10 mM Tris-HCl pH7.6	Used for washing the beads in immunoprecipitation

DNA preparation from bacteria (“Mini prep”)

Buffer	Components	Application
S1	50 mM Tris 10 mM EDTA 100 µg/ml RNAse A dd H2O pH 8.0	Used to resuspend bacteria pellet
S2	200 mM NaOH 1 % (v/v) SDS dd H2O	Used for bacteria lysis
S3	2.8 M calcium acetate pH 5.1	
Tris-HCl	10 mM Tris dd H2O pH 8.0	Used to dissolve DNA

8 Methods

8.1 Molecular biology methods

8.1.1 Preparation of *E.coli* DH10B electrocompetent bacteria

A single colony of *E.coli* DH10B was inoculated into 10 mL of pre-warmed LB medium. The bacteria culture was grown overnight at 37 °C with continuous shaking. 2ml of bacteria from the overnight culture was added to 200 ml of LB medium and was incubated at 37 °C with continuous shaking. OD600 was continually measured using a cell density meter Ultrospec 10 (Amersham Biosciences). Once OD600 reached 0.5–0.6, the bacteria culture was on placed ice and chilled for 20 minutes. Bacteria were further pelleted by centrifugation for 10 minutes at 4°C applying the speed of 5000 × *g*. The supernatant was discarded after the centrifugation and the pellet was resuspended in 100 ml of ice-cold sterile water and pelleted again. After a second washing step with water, the bacterial pellet was resuspended in 10ml of 10% ice-cold glycerol and pelleted again. Ultimately, the bacterial pellet was dissolved in 1ml of 10% ice-cold glycerol and immediately aliquoted. The obtained aliquots were stored at -80 °C.

8.1.2 Preparation of *E.coli* GS1783 electrocompetent bacteria

A single colony of *E.coli* GS1783 with the respective BAC clones was inoculated in 10 ml of pre-warmed LB broth with 15 µg/ml chloramphenicol (1:2500) in a bacterial shaker at 30°C overnight. The overnight culture was diluted at 1:40 ratio in LB broth containing 15 µg/ml chloramphenicol and was shaken at 30 °C. Once the OD600 reached 0.5–0.6, the culture was transferred into a water bath shaker at 42 °C for 15 minutes. Subsequently, the bacterial culture was chilled down on ice for 30 minutes. The bacteria were further pelleted by centrifugation for 10 minutes at 4 °C applying the speed of 5000×g. The supernatant was discarded after the centrifugation and the pellet was resuspended in 100 ml of ice-cold sterile water and pelleted again. After a second washing step with water, the bacterial pellet was resuspended in 10ml of 10% ice-cold glycerol and pelleted again. Following the washing steps, the pellet was dissolved in 1 ml of 10% ice-cold glycerol, immediately aliquoted and stored at -80 °C.

8.1.3 Transformation of bacteria

Electrocompetent bacteria was transformed by electroporation. 50 µl of frozen *E.coli* GS1783 electrocompetent bacteria was thawed on ice and mixed with 150 ng of PCR-amplified DNA fragment. For transformation of *E.coli* DH10B 10 ng of supercoiled plasmid or 4 µl of ligation product were used. After 5 minutes incubation on ice the mix was transferred into pre-chilled 2 mm electroporation cuvettes and pulsed using the Gene Pulser XCell (BIO-RAD) with the settings of 2500 V, 25 µF and 200 Ω. Immediately after electroporation, 1 ml of warm LB medium was added to the cuvettes, mixed with transformed bacteria and transferred into a microcentrifuge tube. Bactria were then incubated on a Thermomixer comfort 5355 (Eppendorf) for 1 hour at 30 ^{0}C for *E.coli* GS1783 or 37 ^{0}C for *E.coli* DH10B. Next, the bacteria were pelleted by centrifugation for 3 minutes applying the speed of 2000 × *g*. The bacteria were plated on LB agar with corresponding antibiotics and incubated overnight in a bacteria incubator (IPP400, Memmert).

8.1.4 Storage of bacteria

For long term storage of bacteria, 700 µl of an overnight culture was mixed with 300 µl of autoclaved 86% glycerol and frozen at -80 °C.

8.1.5 Preparation of BAC and plasmid DNA at the large scale ("midi prep")

For the preparation of large yields of high-copy vectors and BACs, a NucleoBond Xtra Midi kit (Macherey-Nagel) was used. Bacteria were inoculated in the 200 ml of LB broth supplemented with required antibiotics. BAC or plasmid DNA was isolated according to the manufacturer's protocol. The BAC DNA pellet was dissolved using 150 µl of Tris-HCl buffer (pH 8), while plasmid DNA was dissolved using 500 µl of Tris-HCl buffer.

8.1.6 Preparation of BAC and plasmid DNA at the smaller scale ("mini prep")

Single clone bacteria were inoculated in 5 ml of LB broth supplemented with required antibiotics. The cultures were incubated overnight at 30 °C for *E.coli* GS1783 and at 37 °C for *E.coli* DH10B. 2 ml from overnight culture was pelleted at 4 °C applying the speed of 16000 × g. The obtained bacteria pellet was resuspended with 300µl of ice-cold S1 buffer. 300µl of S2 buffer was added to the centrifuge tube with resuspended bacteria and inverted several times. Next, 300µl of ice-cold S3 buffer was added to the same tube and again inverted several times. Tubes were then centrifuged at 4 °C at the speed of 16000 × g. To precipitate DNA, the supernatant was transferred to the new centrifuge tube and supplemented with 0.8 volumes of isopropanol and immediately inverted 3 times. The precipitated DNA was centrifuged at 4 °C using the speed of 16000 × g. After the centrifugation the supernatant was discarded, and the pellet was washed with 500µl of 70% EtOH. After the additional centrifugation step at 4 °C using 16000 × g, the DNA pellet was dried at room temperature and dissolved in 50µl of 10mM Tris-HCl (pH 8). In order to facilitate the resuspension of the DNA pellet, the tubes were incubated at 37 °C with continuous shaking for 1 hour.

8.1.7 Polymerase chain reaction

Polymerase chain reaction (PCR) was performed using DreamTaq DNA Polymerase (Thermo Scientific) according to the manufacturer's protocol. For high-fidelity amplifications, which were further used for cloning, PRECISOR DNA Polymerase (BioCat) was used according to the manufacturer's instructions.

8.1.8 DNA restriction

DNA restriction was performed using FastDigest restriction enzymes (Thermo Scientific) according to the manufacturer's protocol. 1 µg of plasmid DNA was used for analytical plasmid restriction and 2 µg of plasmid DNA was used for cloning procedures. Plasmid DNA was digested at 37^0C for 20 minutes using the reaction set up according to the manufacturer's instructions. For analytical BAC restriction, 1-3 µg of BAC DNA was digested at 37°C for 1.5 hours.

8.1.9 Agarose gel electrophoresis

1% (w/v) TAE agarose gels were used for analysis of plasmid DNA and PCR products; 0.6% (w/v) agarose TBE gels were used for BAC DNA fragments. Gels contain ethidium bromide (EB, 0.5 µg/ml). The size of the bands was identified using O'GeneRuler. DNA bands were visualized under UV light using a UV-Transilluminator (ECX-F20.M, VILBER). The pictures of the gels were taken using a GelDoc XR+ (BIO-RAD) with the Image Lab Software.

8.1.10 DNA purification

PCR products or other DNA fragments run through the TAE agarose gel and cut out for further analysis. The DNA was purified using a NucleoSpin Gel and PCR clean up kit according to the manufacturer's instructions. The concentration and quality of the purified DNA was measured by a NanoDrop-1000 (Peqlab) photometer. DNA was stored at 4 °C prior further application.

8.1.11 DNA ligation

T4-DNA ligase was used for ligation of linearized vector and inserts. The reaction set up was prepared according to the manufacturer's instructions. The vector and insert were mixed at molecular ratio of 1:3 to 1:5. Ligation was performed in a Thermomixer (Eppendorf) at 22 °C for 2 hours.

8.1.12 Extraction of total RNA

Total RNA was isolated from 3-5 x 10^5 eukaryotic cells using the innuPREP RNA Mini Kit (Analytik Jena) according to the manufacturer's instructions. Total RNA was eluted using 44 µl of RNase-free water. The remaining DNA was removed by using TURBO-DNA-free kit following the manufacturer's instructions. RNA concentration (OD260) was measured using a NanoDrop-1000 (Peqlab) photometer. RNA was stored at – 80 °C.

8.1.13 Complementary DNA (cDNA) synthesis

1.5 µg of total RNA was reverse transcribed using RevertAid H Minus Reverse Transcriptase and oligo[dT]18 according to the manufacturer's instructions. The reverse transcriptase was inactivated by a final heating step for 10 minutes at 70 °C. The synthesized cDNA was stored at -20 °C.

8.1.14 *Quantitative* polymerase *chain reaction* (qPCR)

100 ng of cDNA was added to the SybrGreen real time PCR Mastermix (Life technologies) mixed with specific primers (10 µM each). Each cDNA was measured in triplicate. Quantitative polymerase chain reaction (qPCR) was performed in MicroAmp™ Fast Optical 96-Well Reaction Plate (Thermo Fisher Scientific) on an ABI PRISM 7900HT Fast Real-Time PCR System (Applied Biosystem). Transcripts were quantified using the ΔΔCt method and normalized to a housekeeping gene (Actin).

8.1.15 DNA sequencing

For sequencing of BAC or viral DNA the region of interest was amplified by PCR before using PRECISOR DNA Polymerase (BioCat). DNAs were sequenced by SEQLAB Sequence Laboratories, Göttingen GmbH. MCMV m139-STOP and m139-HA BACs were completely sequenced by the Next Generation Sequencing (NGS). The sequencing was performed by Daniela Indenbirken at NGS facility (HPI). The analysis of the data was done by Malik Alawi from the Bioinformatics Core at the University Medical Center Hamburg-Eppendorf, Germany.

8.1.16 *En passant* BAC muthagenesis

The modifications in the viral genome cloned into the bacterial artificial chromosome (BAC) were done using *en passant* mutagenesis using the protocol published by Tischer et al. [180]. To begin with, short linear DNA fragments with homologs of the viral genome needed to be generated. For this purpose, primers were designed for each mutagenesis and synthesized by Life Technologies. The kanamycin resistance gene and I-SceI-aphAI-cassette was amplified from the The pEP-Kan-S plasmid. The plasmid template was removed by DpnI digestion. PCR product was purified. *E. coli* GS1783 carrying related viral genome was transformed with 150 ng of PCR product. 10 colonies were picked 24 hours after plating the bacteria on agar dish and inoculated in LB medium to prepare mini prep DNA. BAC DNA was isolated and digested using HindIII, EcoRV or XbaI enzymes. Digested DNA was loaded into the gel and the BAC restriction pattern was analyzed. The clones with correct digestion pattern were then selected for the second recombination procedure. A single colony was inoculated into 2 ml LB medium containing chloramphenicol and cultured at 30 °C for 2-3 hours until medium was turning cloudy. 2 ml of LB medium containing 2% (w/v) L-arabinose was added and cultured for one more hour. The culture was then immediately transferred into the water bath for 15 minutes at 42 °C with continuous shaking to induce the expression of recombinase. Afterwards the culture was transferred into the 30 °C shaker. After 1 hour of incubation, the bacteria density was determined by OD600. The bacteria were diluted with LB medium according to the OD600: 1:1000 (OD600<0.5) or 1:10000 (OD600>0.5). 100 µl of diluted culture was plated on the agar plate containing chloramphenicol and 1% (w/v) L-arabinose. The resulting colonies were analyzed by BAC digestion. Positive clones were further analyzed by PCR amplification of the target region and sequenced. “Midi prep” DNA was isolated for selected positive clones. BAC DNA was then used the transfection of 10.1 fibroblasts.

8.1.17 Gibson assembly cloning

Gibson assembly was used to re-clone pcDNA-DDX3-Myc from pcDNA3-DDX3-HA. pcDNA3 plasmid was digested using XhoI and EcoRI. DNA fragment for insertion into pcDNA was PCR-amplified by specific primers to insert Myc tag and overlapping sequences with the pcDNA3. pcDNA3-DDX3-HA was used as a template. The DNA fragments purified through the gel ligated following the Gibson Assembly Ultra Master Mix A and Mix B according to the manufacturer’s instructions.

8.2 Cell biology and virology methods

8.2.1 Cell culture

All cells used in this study were incubated in a Hera Cell CO2 incubator (Heraeus) at 37 °C, 80 % relative humidity and 5 % CO2. Cells were grown on 145 mm tissue culture dishes or plates (96-well, 12-well, 6-well). All cell culture work was done using a Laminar flow hood (HeraSafe, Heraeus). All cells, except NIH/3T3 and SVEC4-10 cells, were cultured in complete Dulbecco's modified Eagle medium (DMEM) complemented with 10% fetal calf serum (FCS) and 100 IU Penicillin/100 µg Streptomycin at 37 °C and 5% CO_2. Instead of 10% FCS the cell culture media for NIH/3T3 contained 10% of newborn calf serum (NCS) or 5% FCS for SVEC4-10 cells. Cells were split each time they were reaching approximately 90% confluency. For splitting, cells were washed with PBS and 0.25% Trypsin-EDTA solution was applied to the monolayer. After neutralization with growth medium, the cells were transferred to the new cell culture dishes. The cell number was determined using an automated cell counter (TC10, BioRad). For that 10 µl of the cell suspension was loaded into the counting slides.

For freezing, the cell suspension was pelleted at 37^0C, 500 × *g* for 8 minutes. The obtained cell pellet was resuspended in freezing medium (FCS with 10% DMSO) and transferred into a cryotube. The cells were then immediately frozen at -80 °C. The cells were further transferred to liquid nitrogen for long-term storage.

The cells were thawed in a 37 °C water bath and immediately transferred to a 15 ml Falcon tube. Cells were then pelleted at 37 °C, 500g for 8 minutes. The cell pellet was resuspended in 10 ml growth medium and transferred to a 100 mm culture dish.

8.2.2 Stable isotope labeling by amino acids in cell culture (SILAC)

For SILAC, SVEC4-10 cells were cultivated in SILAC medium, supplemented with 10% dialyzed FCS in the presence of light arginine and lysine or heavy arginine and lysine (+ 6.0201 Da) for 8 passages.

8.2.3 Transfection of plasmid DNA

Plasmid DNA was transfected using polyethylenimine (PEI) or Lipofectamine 2000. Phoenix or HEK-293T cells were transfected using PIE. For transfection, 4 x 10^6 cells were seeded on 100 mm dishes. The next day 8 µg of vector DNA was diluted in 1 ml of serum-free DMEM medium. After mixing, 21 µl of PEI was added to the diluted DNA. The mixture was mixed by vortexing and incubated for 15 minutes at room temperature. The transfection mix was added to the cells drop by drop. 8 hours post transfection the medium was changed to a fresh one.

NIH/3T3 or HEK-293A cells were transfected by Lipofectamine 2000. 1 × 10^5 of NIH/3T3 or 3× 10^5 of HEK-293A cells were seeded on 12-well plates one day before transfection. The following day 1 µg of plasmid DNA was diluted in 50 µl of OptiMEM-I (Life Technologies). In parallel, 2 µl of Lipofectamine 2000 (Life Technologies) was diluted in 50 50 µl of OptiMEM-I. Diluted Lipofectamine was then added to diluted DNA and incubated for 5 minutes at room temperature. DNA-lipofectamine complex was added to cells. 8 hours post transfection the medium was changed to a fresh one.

8.2.4 Transfection of BAC DNA

BAC DNA was transfected in 10.1 fibroblasts using Polyfect transfection reagent (Qiagen). 1.5 x 10^5 cells seeded on 6-well plate one day before transfection. The following day 3 µg of BAC DNA was diluted in 100 µl of serum-free DMEM. 32 µl of Polyfect was added to diluted DNA and mixed. The DNA- Polyfect mixture was incubated for 20 minutes at room temperature. Afterwards 500 µl of DMEM + 10% FCS was added to the mixture and loaded to the cells. Reconstitution of infectious MCMV was monitored and documented by detection of cytopathic effects (CPE) using an inverted fluorescence microscope Axiovert 40 CFL (Zeiss).

8.2.5 Production of retrovirus and lentivirus

Retrovirus was produced from a pMSCV-puro vector transfected into Phoenix cells. Transfection was done in 100mm dishes following the method described above. The supernatant from the transfected cells was harvested 48 and 72 hours post transfection sterilized using a 0.45 µm filter and directly used for transduction of target cells.

Lentivirus was produced from HEK-293T cells. Transfection was done in 100mm dishes. 4 µg of pSicoR-CRISPR-PuroR was mixed with 3 µg of packaging plasmid pCMVdR8.91 and 1 µg of envelope plasmid pMD2.G in 1 ml of serum-free medium. The supernatant from the transfected cells was harvested 48 and 72 hours post transfection sterilized using a 0.45 µm filter and directly used for transduction of target cells.

8.2.6 Transduction of cells

1.5 × 10^5 SVEC-10 cells were seeded in a well of a 6-well plate. The following day, the cell culture medium was replaced with 3 ml of retroviral or lentiviral supernatant collected at 48 hours post transfection and supplemented with Polybrene (5 µg/ml). The infection was enhanced by centrifuging at 37 °C, 1000 × *g* for 30 min. 6 hours post infection the supernatant was removed, washed with PBS and replaced by a fresh cell culture medium. The next day the procedure was repeated using retroviral or lentiviral supernatant collected at 72 hours post transfection. The next day cells were trypsinized and transferred to 100mm cell culture dish and the following day 1.5 µg/ml Puromycine was applied and replaced every third day. Non-transduced cells were treated by puromycin and used as a control.

8.2.7 Generation of knockouts using CRISPR/Cas9 method

CRISPR/Cas9 system was used to knock out DDX3 and UBR5 genes in SVEC4-10 cells. The gRNAs that specifically target the selected genes of interest were designed using the online tool E-CRISP (http://www.e-crisp.org/E-CRISP/). Selected gRNAs were synthesized by Life Technologies and cloned into pSicoR-CRISPR-PuroR vector. The cloning procedure was adapted from the protocol published by van Diemen el al. [181]. The positive clones were sequence-verified, and plasmid DNA was prepared. Lentivirus was produced according to the method described above. The positive cells were selected using Puromycin. Single cell-clones were obtained by limiting dilutions in 96-well plates. The expression levels of the protein of interest were verified by Western blot using specific antibodies.

8.2.8 Infection of cells with MCMV

Cells were infected with MCMV using specific multiplicities of infection (MOI) based on the tissue culture infection dose 50 per milliliter ($TCID_{50}$/ml) of a virus stock. The amount of the virus stock used for an infection was calculated using following equation:

$$\frac{(number\ of\ cells)\ *\ MOI}{TCID_{50}/ml} = volume\ of\ virus\ stock\ in\ ml$$

The required volume of the virus stock was diluted in the growth medium and added to the cells. If needed, the centrifuge enhancement was applied at 37 °C using 1000 × *g* for 30 minutes.

8.2.9 Preparation of MCMV stocks

10 cell culture 150mm dishes with 2×10^6 10.1 cells each were infected at MOI of 0.025. 3 and 5 days after infection, the virus-containing supernatants were collected from the infected cells. Cell debris was removed by centrifugation at 4 °C using 6000 g for 15 minutes. The supernatant was transferred to the fresh tubes and centrifuged at 4 °C using 25800 × *g* for 3 hours. The supernatant was discarded, and the virus pellet was dissolved in 1 ml of growth medium at 4 °C overnight. The next day the virus pellet was resuspended, and the remaining cell debris was removed by centrifugation at 4 °C using 2000 × *g* for 10 minutes. The resuspended virus was loaded on top of Nycodenz gradient medium (18 ml) in an ultracentrifuge tube (Beckmann Coulter). The ultracentrifugation was performed at 4 °C using 50126 × *g* for 90 min using a L70 Ultracentrifuge (Beckmann Coulter). Then the obtained pellet was dissolved in 500 µl of growth medium at 4 °C overnight. The virus stock was aliquoted and stored at -80 °C.

8.2.10 Titration of MCMV stocks

The $TCID_{50}$/ml method was used to determine the virus concentration in CMV stocks or in supernatants collected from infected cells. 2000 10.1 cells were seeded in each well of a 96-well plate. The following day serial dilution of virus ranging from $1:10^1$ to $1:10^8$ (for virus-containing supernatants) or $1:10^3$ to $1:10^{10}$ (for virus stock) were prepared. Growth medium from each dilution was added to one entire row for two 96-well plates. One plate was directly placed in the incubator, while for the other plate the centrifuge enhancement was applied. After 6 days, the number of infected wells in each dilution was counted and the viral titer was determined using the Spearman-Kärber method [182].

Virus stocks for in vivo experiments and MCMV from organ homogenates were titrated using plaque assay. 4×10^4 M2-10 B4 cells were seeded in 48-well plates. The following day, virus dilutions ranged from 1:10^1 to 1:10^8 (organ homogenates) or 1:10^3 to 1:10^{10} (for virus stock) were prepared. Each virus stock titrated in quadruplicates; organ homogenates were titrated in duplicates. Each independent dilution was transferred to the corresponding wells in the cell culture plate. The plates were incubated for 3 hours in the cell culture incubator. Next, each well was covered with 400 µl of methylcellulose. Virus titers were calculated by plaque forming unit [183].

8.3 Protein biochemistry methods

8.3.1 Cell lysis for immuboblotting

For the standard virus kinetics experiments, cells from 6-well plates were washed with PBS and lysed in 100 µl of 2x Laemmli buffer. For protein lysates with determined concentration by BCA protein assay 4x Laemmli buffer was added to samples. Samples were then heated at 94°C for 10 min and either used directly or stored at – 20 °C.

8.3.2 Protein concentration measurement

Protein concentration was measured using BCA Protein assay kit (Thermo Fisher Scientific). Protein lysates were diluted in ratio 1:5 in PBS in duplicates in 96 well plate. BSA standard curve was prepared using the dilutions of BSA (2.0 mg/ml) in PBS. 100 µl of a 50:1 mix of the BCA solutions A and B were added to each sample and standards. After 20 minutes of incubation at 37 °C, absorbance at 562 nm was measured using FLUOstar Omega reader (BMG Labtech). The BSA standard curve was used to calculate the protein concentration.

8.3.3 SDS polyacrylamide gel electrophoresis (SDS-PAGE) and western blot

SDS-PAGE according to Laemmli was used for the separation of proteins with a molecular weight more than 100 kDa [184]. For Laemmli SDS-PAGE 4% stacking gels and 10% resolving gels were prepared according to the the Laemmli gel recipe. 7% resolving gels were prepared for separation of proteins with a large molecular weight (more than 150 kDa). Laemmli running buffer was used for running of Laemmli SDS-PAGE.

Tricine SDS-PAGE was used for the separation of proteins less than 100 kDa following the protocol published by Schagger [185]. For Tricine SDS-PAGE 10% resolving gels and 4%

stacking gels were prepared according to the tricine gel recipe. 15% resolving gels were prepared for separation of proteins with a small molecular weight (less than 30 kDa). The anode buffer as the lower electrode buffer and cathode buffer as the upper electrode buffer used for running of Tricine SDS-PAGE.

10 to 30 µg of protein lysate was loaded into the gel and run at 60 V using MiniPROTEAN Tetra Cell-System (BIO-RAD). Once samples entered the resolving gel, the voltage was increased to 80 V.

Once the proteins were separated in the SDS-PAGE, they were transferred on a nitrocellulose membrane (Hybond ECL, GE Healthcare) by semi-dry sandwich blotting. Transfer was done by applying 25 V for 60 minutes in a Transblot Semi-dry Transfer Cell (BioRad). Wet blotting was performed for a transfer of the proteins with the large molecular weight (more than 150 kDa) using a Mini Trans-Blot cell (BIO-RAD) with wet transfer buffer at 60 V for 80 minutes.

After transfer, the membranes were blocked using 5% (w/v) non-fat milk powder or BSA in TBS-T for 45 minutes. Primary antibodies were diluted in 5% milk powder or BSA TBS-T. Membranes with primary antibodies were incubated overnight at 4 °C. The following day the membranes were stepwise washed using TBS-T buffer. Secondary antibodies coupled with Horseradish peroxidase (HRP) were diluted in 5% milk powder or BSA TBS-T. The membranes were incubated with antibodies for 1 hour at room temperature. Afterwards the membranes were washed in TBS-T and incubated with Pierce™ ECL Western Blotting Substrate (Thermo Fisher Scientific) for 5 minutes in the dark. For the weak signals, blotting substrate containing 10% (v/v) of Lumigen ECL Ultra (TMA-6) (Beckman Coulter) was applied and imaged using X-ray films or Fusion Capture Advance FX7 16.15 (Peqlab) device.

8.3.4 Immunoprecipitation

For immunoprecipitation 1.8 x 10^6 cells were seeded in 6-well plates one day before infection. The following day the cells were infected, and 24 hours post infection, the cells were washed with PBS and lysed on ice for 30 minutes using NP-40 buffer. The cells were then scraped and transferred to microcentrifuge tubes and the cell debris was removed by spinning down at 16000 × *g* for 10 minutes at 4°C. The supernatant was transferred to the fresh tube. 1:10 of the protein lysate was immediately mixed with 100 µl of Laemmli sample buffer, boiled at 95 ^{0}C for 5 minutes and stored at -20 ^{0}C afterwards. The rest of the protein lysate was used for immunoprecipitation by adding Anti-HA Affinity Matrix from rat IgG1 (Roche). 50 µL of affinity matrix was added to each 1 ml of the lysate. The protein lysates with affinity matrix were incubated overnight at the rotating platform at 4 °C. The next day, the matrix was pelleted using 16000 × *g* at 4°C, the supernatant was discarded, and the matrix was washed six times. After each washing step the matrix was pelleted, and the supernatant was discarded. The matrix was washed three times with IP buffer 1, two times with IP buffer 2 and one time with IP buffer 3. After the last washing step, the supernatant was completely removed and 2x Laemmli sample buffer was added to the dry beads. The proteins were eluted by heating the sample to 95 ^{0}C for 5 minutes. Protein lysates and immunoprecipitation were separated by SDS-PAGE and analysed by Western blot.

8.3.5 Immunoprecipitation for mass spectrometry analysis

Heavy and light labeled SVEC4-10 cells were infected with MCMV m139-HA and MCMV WT at MOI 5 $TCID_{50}$/cell and lysed 24 hours post infection using sterile filtered NP-40 buffer. Protein concentration in the lysates was measured using BCA protein assay kit. 1 mg of each whole lysate was used for IP, the rest of the sample was kept as a lysate control. 25 µg PAA and 25 µl PGA were added to each sample for preclearing for 1 h at 4 °C using a rotating platform. Beads were pelleted by centrifugation and the supernatants were transferred to the new microcentrifuge tubes. 75 µl Anti-HA Affinity Matrix was added to each tube and incubated overnight 1 h at 4 °C using a rotating platform. The following day the beads were pelleted using 16000 × *g* at 4°C. The beads were washed six times using sterile-filtered minimal washing buffer. After the last washing step 50 µl of Laemmli sample buffer was added to each sample and proteins were eluted by by heating to 95 °C for 10 minutes. 10 µl of each of the lysate was used for immunoblotting, while 20 µl of each of the lysate was mixed as following: heavy labeled MCMV m139-HA with light labeled MCMV WT infected cells, light labeled MCMV m139-HA with heavy labeled MCMV WT infected cells. The mixed samples were loaded into the SDS page and proteins were stained using Coomassie staining.

8.3.6 Immunofluorescence

Cells were seeded on 8-well µ-slides (Ibidi) one day before transfection or infection. At the defined time points cells were fixed using 4% Paraformaldehyde for 15 minutes. Three washing steps with PBS for 10 minutes were used in between all the steps. The remaining aldehyde groups were blocked using 50mmol/L ammonium chloride. Afterwards, the cells were permeabilized with 0.3% triton X-100 for 15 minutes. Next, the cells were blocked using 0.2% gelatin for 20 minutes. Primary antibodies were diluted in 0.2% gelatin and applied to the cells and incubated for 1 hour. Next, the secondary antibodies diluted in 0.2% gelatin were applied to the cells for 30 minutes in the dark. Hoechst 33342 nuclear dye was applied simultaneously with secondary antibodies. DRAQ5 nuclear dye was diluted in PBS and applied to the cells for 5 minutes. Images were taken with confocal microscope Nikon A1.

8.3.7 Luciferase reporter assay

3×10^5 iBMDM IFN-β-luc reporter macrophages were seeded in 12-well plates one day before infection. The following day cells were infected at MOI 3. 3 hpi cells were washed with PBS and fresh growth medium was added. 8 hpi cells were lysed in 150 µl of Cell Culture lysis reagent (Promega), immediately scraped from the wells and transferred to the microcentrifuge tubes. Tubes were vortexed for 15 seconds and the lysates were spun down using 16000 × *g* for 15 seconds. The supernatant transferred to the new tubes and used for measurement of luminescence on a FLUOstar Omega reader (BMG Labtech) using Luciferase Substrate (Promega) according to the manufacturer’s protocol.

8.3.8 Dual luciferase assay

1.5×10^5 HEK-293A cells were seeded in 12-wells plates and the following transfected with 180 ng of pCDNA3-DDX3-HA, 180 ng of pCDNA3-IKKε, 300 ng of pGL3basic-IFNβ-Luc (IFNβ-Luc), 30 ng of pRL-Renilla using Lypofectamine and 500 ng of ORF expression plasmid or empty vector using Lipofectamine 2000 Transfection Reagent (Thermo Fisher Scientific). After 6 hours the medium was replaced by a fresh growth medium, and at 24 hours post transfection, cells were lysed in 150 µl of Passive lysis buffer scraped and cell lysates were immediately frozen at -80 ^{0}C. After thawing on ice the lysates were spun down using 16000 × *g* for 15 seconds and supernatant was kept for the measurement of luciferase activity. Luciferase activity was measured on a FLUOstar Omega reader (BMG Labtech) using a Dual Luciferase Reporter Assay (Promega) according to the manufacturer's protocol.

8.3.9 Cell fractionation assay

For cell fractionation assay, cell pellet from 2 x 10^6 10.1 cells were stepwise lysed to obtain cytoplasmic and nuclear fractions using NE-PER™ Nuclear and Cytoplasmic Extraction Reagents (Thermo Fisher Scientific) according to the manufacturer's instructions. Protein concentration was defined using BCA Protein assay kit. An equal amounts of nuclear and cytoplasmic fractions were loaded into the SDS page.

8.3.10 Coomassie Staining

Protein samples was run on SDS-PAGE gel. The gels were then fixed in Coomassie Fixing Buffer for 30 min at room temperature. Gels were then transferred to Coomassie Staining Buffer for 30 min at RT. Gels were then continually washed in Coomassie Destaining Buffer until protein bands were visible.

8.4 Liquid chromatography–mass spectrometry (LC-MS/MS)

LC-MS/MS and data analysis were performed by Dr. Christoph Krisp at the Institute of Clinical Chemistry and Laboratory Medicine (University Medical Center Hamburg-Eppendorf).

Protein bands stained with commassie blue were cut from the SDS-page. Each lane was then cut into 1 mm^3 cubes followed by destaining. Disulfide bonds of proteins in the gel matrix were reduced in the presence of 10 mM dithiotreitol (DTT, Fluka), alkylated in the presence of 20 mM iodoacetamide (IAA, Sigma) and digested with trypsin (1:50 protein:enzyme ratio, Promega) overnight. Generated peptides were eluted from the gel pieces and dried in a vacuum concentrator. Samples were resuspended in 0.1% formic acid (FA) and transferred into a full recovery autosampler vial (Waters). Chromatographic separation was achieved on a Dionex Ultimate 3000 UPLC system (Thermo Fisher Scientific) with a two-buffer system (buffer A: 0.1% FA in water, buffer B:

0.1% FA in Acetonitrile (ACN)). Attached to the UPLC was a C18 trapping column (Acclaim PepMap 100, 100 µm x 2 cm, 100 Å pore size, 5 µm particle size) for desalting and purification followed by a C18 analytical column (Acclaim PepMap 100, 75 µm x 50 cm, 100 Å pore size, 2 µm particle size). Peptides were separated using a 110 min gradient with increasing ACN concentration from 2% - 32% ACN. The eluting peptides were analyzed on a tribrid Orbitrap mass spectrometer (Fusion, Thermo Fisher Scientific) in data dependent acquisition (DDA) mode.

For DDA, the mass spectrometer was operated in Orbitrap – Iontrap mode at top speed for precursor selection for fragmentation. Therefore, observed precursors with charge stages +2 – +5 in a range from 400 – 1300 m/z in a MS1 survey scan ($2x10^5$ ions, 120,000 Resolution, 120 ms fill time) were analyzed by MS/MS (HCD at 30 normalized collision energy, $1x10^4$ ions, 60 ms fill time) within 3 seconds. A dynamic precursor exclusion of 20 s was used.

8.4.1 LC-MS/MS data analysis and processing

Acquired DDA LC-MS/MS data were searched against the mouse SwissProt protein data base downloaded from Uniprot (release August 2017, 16,909 protein entries), and the recombinant version of the murid herpes virus protein m139 using the Sequest algorithm integrated in the Proteome Discoverer software version 2.0. Mass tolerances for precursors were set to 10 ppm and 0.6 Da for fragments. Carbamidomethylation was set as a fixed modification for cysteine residues and $^{13}C_6$ Lysine, $^{13}C_6$ Arginine, the oxidation of methionine, pyro-glutamate formation at glutamine residues at the peptide N-terminus as well as acetylation of the protein N-terminus, methionine loss at the protein N-terminus and the Acetylation after methionine loss at the protein N-terminus were allowed as variable modifications. Only peptides with a high confidence (false discovery rate < 1% using a decoy data base approach) were accepted as identified.

Proteome Discoverer search results were imported into Skyline software version 4.2 allowing only high confidence peptides. Precursor traces (M, M+1, M+2) were extracted. Precursors with an idot product of > 0.9 in at least one sample were kept. For each peptide, the ration of heavy to light was calculated and the median peptide ratio per protein was estimated, which were then used for relative comparison.

8.5 In vivo experiments

Animal experiments were performed by Dr. E. Ostermann according to the recommendations and guidelines of the FELASA (Federation for Laboratory Animal Science Associations) and Society of Laboratory Animals (GV-SOLAS) and approved by the institutional review board and local authorities (Behörde für Gesundheit und Verbraucherschutz, Amt für Verbraucherschutz, Freie und Hansestadt Hamburg, reference number 017/2019). Six to eight-week-old BALB/c female mice (Janvier laboratories) were infected with 10^5 PFU MCMV per mouse using footpad injection. Organs were harvested on day 3 (popliteal lymph node) and day 14 (salivary glands) post infection. The weight of the organs was measured. Organs were placed into the tubes containing Lysing matrix D (MP Biomedicals) and homogenised using FastPrep-24 adapter (MP Biomedicals). Organ homogenates were titrated by plaque assay. Statistical significance was assessed using the Mann-Whitney test.

9 References

1. Ho, M., *The history of cytomegalovirus and its diseases.* Med Microbiol Immunol, 2008. **197**(2): p. 65-73.
2. Adland, E., et al., *Ongoing burden of disease and mortality from HIV/CMV coinfection in Africa in the antiretroviral therapy era.* Front Microbiol, 2015. **6**: p. 1016.
3. Crough, T. and R. Khanna, *Immunobiology of human cytomegalovirus: from bench to bedside.* Clin Microbiol Rev, 2009. **22**(1): p. 76-98, Table of Contents.
4. Sia, I.G. and R. Patel, *New Strategies for Prevention and Therapy of Cytomegalovirus Infection and Disease in Solid-Organ Transplant Recipients.* Clinical Microbiology Reviews, 2000. **13**(1): p. 83-121.
5. Wills, M.R., et al., *The immunology of human cytomegalovirus latency: could latent infection be cleared by novel immunotherapeutic strategies?* Cell Mol Immunol, 2015. **12**(2): p. 128-38.
6. Manicklal, S., et al., *The "Silent" Global Burden of Congenital Cytomegalovirus.* Clinical Microbiology Reviews, 2013. **26**(1): p. 86-102.
7. Hodowanec, A.C., et al., *Treatment and Prevention of CMV Disease in Transplant Recipients: Current Knowledge and Future Perspectives.* J Clin Pharmacol, 2018.
8. El Helou, G. and R.R. Razonable, *Letermovir for the prevention of cytomegalovirus infection and disease in transplant recipients: an evidence-based review.* Infect Drug Resist, 2019. **12**: p. 1481-1491.
9. Davidson A.J., H.M., Dolan A., Dardan D.J., Gatherer D., Hayward G.S., ed. *Comparative genomics of primate cytomegaloviruses*. Cytomegaloviruses. From molecular pathogenesis to intervention, ed. R. M.J. Vol. I. 2013, Caiser Academic Press
10. Rawlinson, W.D., H.E. Farrell, and B.G. Barrell, *Analysis of the complete DNA sequence of murine cytomegalovirus.* Journal of Virology, 1996. **70**(12): p. 8833-8849.
11. Murphy, E., et al., *Reevaluation of human cytomegalovirus coding potential.* Proc Natl Acad Sci U S A, 2003. **100**(23): p. 13585-90.
12. Terhune, S.S., J. Schroer, and T. Shenk, *RNAs are packaged into human cytomegalovirus virions in proportion to their intracellular concentration.* J Virol, 2004. **78**(19): p. 10390-8.
13. Varnum, S.M., et al., *Identification of proteins in human cytomegalovirus (HCMV) particles: the HCMV proteome.* J Virol, 2004. **78**(20): p. 10960-6.
14. Kattenhorn, L.M., et al., *Identification of proteins associated with murine cytomegalovirus virions.* J Virol, 2004. **78**(20): p. 11187-97.
15. Kinzler, E.R. and T. Compton, *Characterization of human cytomegalovirus glycoprotein-induced cell-cell fusion.* J Virol, 2005. **79**(12): p. 7827-37.
16. Wu, Y., et al., *Human cytomegalovirus glycoprotein complex gH/gL/gO uses PDGFR-α as a key for entry.* PLOS Pathogens, 2017. **13**(4): p. e1006281.
17. Martinez-Martin, N., et al., *An Unbiased Screen for Human Cytomegalovirus Identifies Neuropilin-2 as a Central Viral Receptor.* Cell, 2018. **174**(5): p. 1158-1171 e19.
18. Nguyen, C.C. and J.P. Kamil, *Pathogen at the Gates: Human Cytomegalovirus Entry and Cell Tropism.* Viruses, 2018. **10**(12).
19. Kalejta, R.F., *Tegument proteins of human cytomegalovirus.* Microbiol Mol Biol Rev, 2008. **72**(2): p. 249-65, table of contents.

20. Tang, Q. and G.G. Maul, *Mouse cytomegalovirus immediate-early protein 1 binds with host cell repressors to relieve suppressive effects on viral transcription and replication during lytic infection.* J Virol, 2003. **77**(2): p. 1357-67.
21. Kalejta, R.F., *Functions of human cytomegalovirus tegument proteins prior to immediate early gene expression.* Curr Top Microbiol Immunol, 2008. **325**: p. 101-15.
22. Scherer, M., E.M. Schilling, and T. Stamminger, *The Human CMV IE1 Protein: An Offender of PML Nuclear Bodies.* Adv Anat Embryol Cell Biol, 2017. **223**: p. 77-94.
23. Dunn, W., et al., *Functional profiling of a human cytomegalovirus genome.* Proc Natl Acad Sci U S A, 2003. **100**(24): p. 14223-8.
24. Meier., M.F.S.a.J.L., ed. *Human Herpesviruses: Biology, Therapy, and Immunoprophylaxis.*, ed. C.-F.G. Arvin A, Mocarski E. Vol. Basic virology and viral gene effects on host cell functions: betaherpesviruses. Immediate–early viral gene regulation and function. 2007, Cambridge University Press.
25. Sinclair, J., *Human cytomegalovirus: Latency and reactivation in the myeloid lineage.* J Clin Virol, 2008. **41**(3): p. 180-5.
26. Pari, G.S., *Nuts and bolts of human cytomegalovirus lytic DNA replication.* Curr Top Microbiol Immunol, 2008. **325**: p. 153-66.
27. David G. Anders, J.A.K., and Gregory S. Pari, ed. *Human Herpesviruses: Biology, Therapy, and Immunoprophylaxis.*, ed. C.-F.G. Arvin A, Mocarski E. Vol. Basic virology and viral gene effects on host cell functions: betaherpesviruses. DNA synthesis and late viral gene expression. 2007, Cambridge University Press.
28. Marschall, M., et al., *The human cytomegalovirus nuclear egress complex unites multiple functions: Recruitment of effectors, nuclear envelope rearrangement, and docking to nuclear capsids.* Rev Med Virol, 2017. **27**(4).
29. Moorman, N.J., et al., *A targeted spatial-temporal proteomics approach implicates multiple cellular trafficking pathways in human cytomegalovirus virion maturation.* Mol Cell Proteomics, 2010. **9**(5): p. 851-60.
30. Jean Beltran, P.M. and I.M. Cristea, *The life cycle and pathogenesis of human cytomegalovirus infection: lessons from proteomics.* Expert Rev Proteomics, 2014. **11**(6): p. 697-711.
31. Tandon, R. and E.S. Mocarski, *Viral and host control of cytomegalovirus maturation.* Trends Microbiol, 2012. **20**(8): p. 392-401.
32. Murray, L.A., X. Sheng, and I.M. Cristea, *Orchestration of protein acetylation as a toggle for cellular defense and virus replication.* Nature Communications, 2018. **9**(1): p. 4967.
33. Demogines, A., et al., *Dual host-virus arms races shape an essential housekeeping protein.* PLoS Biol, 2013. **11**(5): p. e1001571.
34. Perot, K., C.M. Walker, and R.R. Spaete, *Primary chimpanzee skin fibroblast cells are fully permissive for human cytomegalovirus replication.* J Gen Virol, 1992. **73 (Pt 12)**: p. 3281-4.
35. Smith, C.B., L.S. Wei, and M. Griffiths, *Mouse cytomegalovirus is infectious for rats and alters lymphocyte subsets and spleen cell proliferation.* Arch Virol, 1986. **90**(3-4): p. 313-23.
36. Tang, Q. and G.G. Maul, *Mouse cytomegalovirus crosses the species barrier with help from a few human cytomegalovirus proteins.* J Virol, 2006. **80**(15): p. 7510-21.
37. Jurak, I. and W. Brune, *Induction of apoptosis limits cytomegalovirus cross-species infection.* EMBO J, 2006. **25**(11): p. 2634-42.
38. Parrish, C.R., et al., *Cross-species virus transmission and the emergence of new epidemic diseases.* Microbiol Mol Biol Rev, 2008. **72**(3): p. 457-70.

39. Ostermann, E., et al., *Stepwise adaptation of murine cytomegalovirus to cells of a foreign host for identification of host range determinants.* Med Microbiol Immunol, 2015. **204**(3): p. 461-9.
40. Schumacher, U., et al., *Mutations in the M112/M113-coding region facilitate murine cytomegalovirus replication in human cells.* J Virol, 2010. **84**(16): p. 7994-8006.
41. Ostermann, E., et al., *Activation of E2F-dependent transcription by the mouse cytomegalovirus M117 protein affects the viral host range.* PLoS Pathog, 2018. **14**(12): p. e1007481.
42. Sinzger, C. and G. Jahn, *Human cytomegalovirus cell tropism and pathogenesis.* Intervirology, 1996. **39**(5-6): p. 302-19.
43. Smith, M.S., et al., *Human cytomegalovirus induces monocyte differentiation and migration as a strategy for dissemination and persistence.* J Virol, 2004. **78**(9): p. 4444-53.
44. Sinzger, C., M. Digel, and G. Jahn, *Cytomegalovirus cell tropism.* Curr Top Microbiol Immunol, 2008. **325**: p. 63-83.
45. Smith, M.S., et al., *Human Cytomegalovirus Induces Monocyte Differentiation and Migration as a Strategy for Dissemination and Persistence.* Journal of Virology, 2004. **78**(9): p. 4444-4453.
46. Aird, W.C., *Phenotypic heterogeneity of the endothelium: I. Structure, function, and mechanisms.* Circ Res, 2007. **100**(2): p. 158-73.
47. Conway, E.M. and P. Carmeliet, *The diversity of endothelial cells: a challenge for therapeutic angiogenesis.* Genome Biol, 2004. **5**(2): p. 207.
48. Michiels, C., *Endothelial cell functions.* J Cell Physiol, 2003. **196**(3): p. 430-43.
49. Aird, W.C., *Endothelial cell heterogeneity.* Cold Spring Harb Perspect Med, 2012. **2**(1): p. a006429.
50. Pober, J.S. and W.C. Sessa, *Evolving functions of endothelial cells in inflammation.* Nat Rev Immunol, 2007. **7**(10): p. 803-15.
51. Seckert, C.K., et al., *Liver sinusoidal endothelial cells are a site of murine cytomegalovirus latency and reactivation.* J Virol, 2009. **83**(17): p. 8869-84.
52. Bentz, G.L., et al., *Human cytomegalovirus (HCMV) infection of endothelial cells promotes naive monocyte extravasation and transfer of productive virus to enhance hematogenous dissemination of HCMV.* J Virol, 2006. **80**(23): p. 11539-55.
53. Valantine, H.A., *The role of viruses in cardiac allograft vasculopathy.* Am J Transplant, 2004. **4**(2): p. 169-77.
54. Rahbar, A. and C. Soderberg-Naucler, *Human cytomegalovirus infection of endothelial cells triggers platelet adhesion and aggregation.* J Virol, 2005. **79**(4): p. 2211-20.
55. Bentz, G.L. and A.D. Yurochko, *Human CMV infection of endothelial cells induces an angiogenic response through viral binding to EGF receptor and beta1 and beta3 integrins.* Proc Natl Acad Sci U S A, 2008. **105**(14): p. 5531-6.
56. Okabe, Y. and R. Medzhitov, *Tissue biology perspective on macrophages.* Nat Immunol, 2016. **17**(1): p. 9-17.
57. Geissmann, F., et al., *Development of monocytes, macrophages, and dendritic cells.* Science, 2010. **327**(5966): p. 656-61.
58. Shi, C. and E.G. Pamer, *Monocyte recruitment during infection and inflammation.* Nat Rev Immunol, 2011. **11**(11): p. 762-74.
59. Mosser, D.M. and J.P. Edwards, *Exploring the full spectrum of macrophage activation.* Nat Rev Immunol, 2008. **8**(12): p. 958-69.
60. Stevenson, E.V., et al., *HCMV reprogramming of infected monocyte survival and differentiation: a Goldilocks phenomenon.* Viruses, 2014. **6**(2): p. 782-807.

61. Stoddart, C.A., et al., *Peripheral blood mononuclear phagocytes mediate dissemination of murine cytomegalovirus.* J Virol, 1994. **68**(10): p. 6243-53.
62. Benedict, C.A., et al., *Specific remodeling of splenic architecture by cytomegalovirus.* PLoS Pathog, 2006. **2**(3): p. e16.
63. Hanson, L.K., et al., *Replication of murine cytomegalovirus in differentiated macrophages as a determinant of viral pathogenesis.* J Virol, 1999. **73**(7): p. 5970-80.
64. Crane, M.J., K.L. Hokeness-Antonelli, and T.P. Salazar-Mather, *Regulation of inflammatory monocyte/macrophage recruitment from the bone marrow during murine cytomegalovirus infection: role for type I interferons in localized induction of CCR2 ligands.* J Immunol, 2009. **183**(4): p. 2810-7.
65. Mocarski, E.S., ed. *Human Herpesviruses: Biology, Therapy, and Immunoprophylaxis.*, ed. C.-F.G. Arvin A, Mocarski E. Vol. Betaherpes viral genes and their functions. 2007, Cambridge University Press.
66. Menard, C., et al., *Role of murine cytomegalovirus US22 gene family members in replication in macrophages.* J Virol, 2003. **77**(10): p. 5557-70.
67. Karabekian, Z., et al., *Complex Formation among Murine Cytomegalovirus US22 Proteins Encoded by Genes M139, M140, and M141.* Journal of Virology, 2005. **79**(6): p. 3525-3535.
68. Bowie, A.G. and L. Unterholzner, *Viral evasion and subversion of pattern-recognition receptor signalling.* Nat Rev Immunol, 2008. **8**(12): p. 911-22.
69. Turner, M.D., et al., *Cytokines and chemokines: At the crossroads of cell signalling and inflammatory disease.* Biochim Biophys Acta, 2014. **1843**(11): p. 2563-2582.
70. Melchjorsen, J., *Learning from the messengers: innate sensing of viruses and cytokine regulation of immunity - clues for treatments and vaccines.* Viruses, 2013. **5**(2): p. 470-527.
71. Mesev, E.V., R.A. LeDesma, and A. Ploss, *Decoding type I and III interferon signalling during viral infection.* Nat Microbiol, 2019. **4**(6): p. 914-924.
72. Ma, Z., G. Ni, and B. Damania, *Innate Sensing of DNA Virus Genomes.* Annu Rev Virol, 2018. **5**(1): p. 341-362.
73. Pandey, S., T. Kawai, and S. Akira, *Microbial sensing by Toll-like receptors and intracellular nucleic acid sensors.* Cold Spring Harb Perspect Biol, 2014. **7**(1): p. a016246.
74. Yan, N. and Z.J. Chen, *Intrinsic antiviral immunity.* Nat Immunol, 2012. **13**(3): p. 214-22.
75. Gringhuis, S.I., et al., *HIV-1 blocks the signaling adaptor MAVS to evade antiviral host defense after sensing of abortive HIV-1 RNA by the host helicase DDX3.*
76. Soulat, D., et al., *The DEAD-box helicase DDX3X is a critical component of the TANK-binding kinase 1-dependent innate immune response.* EMBO J, 2008. **27**(15): p. 2135-46.
77. Motwani, M., S. Pesiridis, and K.A. Fitzgerald, *DNA sensing by the cGAS-STING pathway in health and disease.* Nat Rev Genet, 2019.
78. Stempel, M., B. Chan, and M.M. Brinkmann, *Coevolution pays off: Herpesviruses have the license to escape the DNA sensing pathway.* Med Microbiol Immunol, 2019. **208**(3-4): p. 495-512.
79. Marques, M., A.R. Ferreira, and D. Ribeiro, *The Interplay between Human Cytomegalovirus and Pathogen Recognition Receptor Signaling.* Viruses, 2018. **10**(10).
80. Schneider, W.M., M.D. Chevillotte, and C.M. Rice, *Interferon-stimulated genes: a complex web of host defenses.* Annual review of immunology, 2014. **32**: p. 513-545.

81. Fleming, S.B., *Viral Inhibition of the IFN-Induced JAK/STAT Signalling Pathway: Development of Live Attenuated Vaccines by Mutation of Viral-Encoded IFN-Antagonists.* Vaccines, 2016. **4**(3): p. 23.
82. Le, V.T., et al., *Mouse cytomegalovirus inhibits beta interferon (IFN-beta) gene expression and controls activation pathways of the IFN-beta enhanceosome.* J Gen Virol, 2008. **89**(Pt 5): p. 1131-41.
83. Krause, E., et al., *Murine cytomegalovirus virion-associated protein M45 mediates rapid NF-kappaB activation after infection.* J Virol, 2014. **88**(17): p. 9963-75.
84. Marshall, E.E. and A.P. Geballe, *Multifaceted evasion of the interferon response by cytomegalovirus.* J Interferon Cytokine Res, 2009. **29**(9): p. 609-19.
85. Magalhães, A.C., et al., *Peroxisomes are platforms for cytomegalovirus' evasion from the cellular immune response.*
86. Kim, J.E., et al., *Human Cytomegalovirus IE2 86 kDa Protein Induces STING Degradation and Inhibits cGAMP-Mediated IFN-beta Induction.* Front Microbiol, 2017. **8**: p. 1854.
87. Liu, Q., et al., *Modulation of Innate Immune Signaling Pathways by Herpesviruses.* Viruses, 2019. **11**(6).
88. Stempel, M., et al., *The herpesviral antagonist m152 reveals differential activation of STING-dependent IRF and NF-kappaB signaling and STING's dual role during MCMV infection.* EMBO J, 2019. **38**(5).
89. Li, T., J. Chen, and I.M. Cristea, *Human cytomegalovirus tegument protein pUL83 inhibits IFI16-mediated DNA sensing for immune evasion.* Cell Host Microbe, 2013. **14**(5): p. 591-9.
90. Goodwin, C.M., J.H. Ciesla, and J. Munger, *Who's Driving? Human Cytomegalovirus, Interferon, and NFkappaB Signaling.* Viruses, 2018. **10**(9).
91. Mathers, C., et al., *The Human Cytomegalovirus U<sub>L</sub>26 Protein Antagonizes NF-κB Activation.* Journal of Virology, 2014. **88**(24): p. 14289-14300.
92. Miller, D.M., et al., *Human cytomegalovirus inhibits major histocompatibility complex class II expression by disruption of the Jak/Stat pathway.* The Journal of experimental medicine, 1998. **187**(5): p. 675-683.
93. Zimmermann, A., et al., *A cytomegaloviral protein reveals a dual role for STAT2 in IFN-{gamma} signaling and antiviral responses.* J Exp Med, 2005. **201**(10): p. 1543-53.
94. Kim, Y.J., et al., *Consecutive Inhibition of ISG15 Expression and ISGylation by Cytomegalovirus Regulators.* PLOS Pathogens, 2016. **12**(8): p. e1005850.
95. Cassady, K.A., *Human cytomegalovirus TRS1 and IRS1 gene products block the double-stranded-RNA-activated host protein shutoff response induced by herpes simplex virus type 1 infection.* J Virol, 2005. **79**(14): p. 8707-15.
96. Budt, M., et al., *Specific Inhibition of the PKR-Mediated Antiviral Response by the Murine Cytomegalovirus Proteins m142 and m143.* Journal of Virology, 2009. **83**(3): p. 1260-1270.
97. Cridland, J.A., et al., *The mammalian PYHIN gene family: phylogeny, evolution and expression.* BMC Evol Biol, 2012. **12**: p. 140.
98. Zhao, H., et al., *The roles of interferon-inducible p200 family members IFI16 and p204 in innate immune responses, cell differentiation and proliferation.* Genes Dis, 2015. **2**(1): p. 46-56.
99. Ding, B. and P. Lengyel, *p204 protein is a novel modulator of ras activity.* J Biol Chem, 2008. **283**(9): p. 5831-48.

100. Luan, Y., P. Lengyel, and C.J. Liu, *p204, a p200 family protein, as a multifunctional regulator of cell proliferation and differentiation.* Cytokine Growth Factor Rev, 2008. **19**(5-6): p. 357-69.
101. Liu, C., et al., *MyoD-dependent induction during myoblast differentiation of p204, a protein also inducible by interferon.* Mol Cell Biol, 2000. **20**(18): p. 7024-36.
102. Hertel, L., et al., *The retinoblastoma protein is an essential mediator that links the interferon-inducible 204 gene to cell-cycle regulation.* Oncogene, 2000. **19**(32): p. 3598-608.
103. Semenova, N., et al., *Multiple cytosolic DNA sensors bind plasmid DNA after transfection.* Nucleic Acids Res, 2019.
104. Unterholzner, L., et al., *IFI16 is an innate immune sensor for intracellular DNA.* Nat Immunol, 2010. **11**(11): p. 997-1004.
105. Schattgen, S.A. and K.A. Fitzgerald, *The PYHIN protein family as mediators of host defenses.* Immunol Rev, 2011. **243**(1): p. 109-18.
106. Rolle, S., et al., *The interferon-inducible 204 gene is transcriptionally activated by mouse cytomegalovirus and is required for its replication.* Virology, 2001. **286**(2): p. 249-55.
107. Khadivjam, B., et al., *The ATP-Dependent RNA Helicase DDX3X Modulates Herpes Simplex Virus 1 Gene Expression.* J Virol, 2017. **91**(8).
108. McKinney, C., D. Yu, and I. Mohr, *A new role for the cellular PABP repressor Paip2 as an innate restriction factor capable of limiting productive cytomegalovirus replication.* Genes Dev, 2013. **27**(16): p. 1809-20.
109. Szappanos, D., et al., *The RNA helicase DDX3X is an essential mediator of innate antimicrobial immunity.* PLoS Pathog, 2018. **14**(11): p. e1007397.
110. Samir, P., et al., *DDX3X acts as a live-or-die checkpoint in stressed cells by regulating NLRP3 inflammasome.*
111. Bourgeois, C.F., F. Mortreux, and D. Auboeuf, *The multiple functions of RNA helicases as drivers and regulators of gene expression.* Nat Rev Mol Cell Biol, 2016. **17**(7): p. 426-38.
112. Ariumi, Y., *Multiple functions of DDX3 RNA helicase in gene regulation, tumorigenesis, and viral infection.* Frontiers in Genetics, 2014. **5**(423).
113. Ditton, H.J., et al., *The AZFa gene DBY (DDX3Y) is widely transcribed but the protein is limited to the male germ cells by translation control.* Hum Mol Genet, 2004. **13**(19): p. 2333-41.
114. Chen, C.Y., et al., *Targeted inactivation of murine Ddx3x: essential roles of Ddx3x in placentation and embryogenesis.* Hum Mol Genet, 2016. **25**(14): p. 2905-2922.
115. Soto-Rifo, R. and T. Ohlmann, *The role of the DEAD-box RNA helicase DDX3 in mRNA metabolism.* Wiley Interdiscip Rev RNA, 2013. **4**(4): p. 369-85.
116. Decker, C.J. and R. Parker, *P-bodies and stress granules: possible roles in the control of translation and mRNA degradation.* Cold Spring Harb Perspect Biol, 2012. **4**(9): p. a012286.
117. Gu, L., et al., *DDX3 directly regulates TRAF3 ubiquitination and acts as a scaffold to co-ordinate assembly of signalling complexes downstream from MAVS.* Biochem J, 2017. **474**(4): p. 571-587.
118. Schroder, M., M. Baran, and A.G. Bowie, *Viral targeting of DEAD box protein 3 reveals its role in TBK1/IKKepsilon-mediated IRF activation.* EMBO J, 2008. **27**(15): p. 2147-57.
119. Ariumi, Y., et al., *Hepatitis C Virus Hijacks P-Body and Stress Granule Components around Lipid Droplets.* Journal of Virology, 2011. **85**(14): p. 6882-6892.

120. Park, E.S., et al., *Co-degradation of interferon signaling factor DDX3 by PB1-F2 as a basis for high virulence of 1918 pandemic influenza.* EMBO J, 2019. **38**(10).
121. Loureiro, M.E., et al., *DDX3 suppresses type I interferons and favors viral replication during Arenavirus infection.* PLoS Pathog, 2018. **14**(7): p. e1007125.
122. Yedavalli, V.S., et al., *Requirement of DDX3 DEAD box RNA helicase for HIV-1 Rev-RRE export function.* Cell, 2004. **119**(3): p. 381-92.
123. Soto-Rifo, R., et al., *DEAD-box protein DDX3 associates with eIF4F to promote translation of selected mRNAs.* EMBO J, 2012. **31**(18): p. 3745-56.
124. Thulasi Raman, S.N., et al., *DDX3 Interacts with Influenza A Virus NS1 and NP Proteins and Exerts Antiviral Function through Regulation of Stress Granule Formation.* J Virol, 2016. **90**(7): p. 3661-75.
125. Wang, H., S. Kim, and W.S. Ryu, *DDX3 DEAD-Box RNA helicase inhibits hepatitis B virus reverse transcription by incorporation into nucleocapsids.* J Virol, 2009. **83**(11): p. 5815-24.
126. DeFilippis, V.R., et al., *Human cytomegalovirus induces the interferon response via the DNA sensor ZBP1.* J Virol, 2010. **84**(1): p. 585-98.
127. Cavignac, Y., et al., *The Cellular Proteins Grb2 and DDX3 Are Increased upon Human Cytomegalovirus Infection and Act in a Proviral Fashion.* PLoS One, 2015. **10**(6): p. e0131614.
128. Valiente-Echeverria, F., M.A. Hermoso, and R. Soto-Rifo, *RNA helicase DDX3: at the crossroad of viral replication and antiviral immunity.* Rev Med Virol, 2015. **25**(5): p. 286-99.
129. Luo, H., *Interplay between the virus and the ubiquitin-proteasome system: molecular mechanism of viral pathogenesis.* Curr Opin Virol, 2016. **17**: p. 1-10.
130. Shearer, R.F., et al., *Functional Roles of the E3 Ubiquitin Ligase UBR5 in Cancer.* Mol Cancer Res, 2015. **13**(12): p. 1523-32.
131. Xie, Z., et al., *Significance of the E3 ubiquitin protein UBR5 as an oncogene and a prognostic biomarker in colorectal cancer.* Oncotarget, 2017. **8**(64): p. 108079-108092.
132. Flack, J.E., et al., *Wnt-Dependent Inactivation of the Groucho/TLE Co-repressor by the HECT E3 Ubiquitin Ligase Hyd/UBR5.* Mol Cell, 2017. **67**(2): p. 181-193 e5.
133. Saunders, D.N., et al., *Edd, the Murine Hyperplastic Disc Gene, Is Essential for Yolk Sac Vascularization and Chorioallantoic Fusion.* Molecular and Cellular Biology, 2004. **24**(16): p. 7225-7234.
134. Rutz, S., et al., *Deubiquitinase DUBA is a post-translational brake on interleukin-17 production in T cells.* Nature, 2015. **518**(7539): p. 417-21.
135. Henderson, M.J., et al., *EDD mediates DNA damage-induced activation of CHK2.* J Biol Chem, 2006. **281**(52): p. 39990-40000.
136. Gudjonsson, T., et al., *TRIP12 and UBR5 suppress spreading of chromatin ubiquitylation at damaged chromosomes.* Cell, 2012. **150**(4): p. 697-709.
137. Zhang, T., et al., *UBR5-mediated ubiquitination of ATMIN is required for ionizing radiation-induced ATM signaling and function.* Proc Natl Acad Sci U S A, 2014. **111**(33): p. 12091-6.
138. Cipolla, L., et al., *UBR5 interacts with the replication fork and protects DNA replication from DNA polymerase eta toxicity.* Nucleic Acids Res, 2019.
139. Tomaic, V., et al., *Regulation of the human papillomavirus type 18 E6/E6AP ubiquitin ligase complex by the HECT domain-containing protein EDD.* J Virol, 2011. **85**(7): p. 3120-7.
140. Yoshida, M., et al., *Poly(A) binding protein (PABP) homeostasis is mediated by the stability of its inhibitor, Paip2.* EMBO J, 2006. **25**(9): p. 1934-44.

141. Ebeling, A., et al., *Molecular cloning and physical mapping of murine cytomegalovirus DNA.* J Virol, 1983. **47**(3): p. 421-33.
142. Hanson, L.K., et al., *Transcriptional analysis of the murine cytomegalovirus HindIII-I region: identification of a novel immediate-early gene region.* Virology, 1999. **260**(1): p. 156-64.
143. Hanson, L.K., et al., *Products of US22 Genes M140 and M141 Confer Efficient Replication of Murine Cytomegalovirus in Macrophages and Spleen.* Journal of Virology, 2001. **75**(14): p. 6292-6302.
144. Ciocco-Schmitt, G.M., et al., *Identification and characterization of novel murine cytomegalovirus M112-113 (e1) gene products.* Virology, 2002. **294**(1): p. 199-208.
145. Lienenklaus, S., et al., *Novel reporter mouse reveals constitutive and inflammatory expression of IFN-beta in vivo.* J Immunol, 2009. **183**(5): p. 3229-36.
146. Weisblum, Y., et al., *APOBEC3A Is Upregulated by Human Cytomegalovirus (HCMV) in the Maternal-Fetal Interface, Acting as an Innate Anti-HCMV Effector.* J Virol, 2017. **91**(23).
147. Owsianka, A.M. and A.H. Patel, *Hepatitis C virus core protein interacts with a human DEAD box protein DDX3.* Virology, 1999. **257**(2): p. 330-40.
148. Ko, C., et al., *DDX3 DEAD-Box RNA Helicase Is a Host Factor That Restricts Hepatitis B Virus Replication at the Transcriptional Level.* Journal of Virology, 2014. **88**(23): p. 13689-13698.
149. Ling, S. and W.C. Lin, *EDD inhibits ATM-mediated phosphorylation of p53.* J Biol Chem, 2011. **286**(17): p. 14972-82.
150. Cojocaru, M., et al., *Transcription factor IIS cooperates with the E3 ligase UBR5 to ubiquitinate the CDK9 subunit of the positive transcription elongation factor B.* J Biol Chem, 2011. **286**(7): p. 5012-22.
151. Guo, H., et al., *Species-independent contribution of ZBP1/DAI/DLM-1-triggered necroptosis in host defense against HSV1.*
152. Farrell, H.E., et al., *Lymph Node Macrophages Restrict Murine Cytomegalovirus Dissemination.* Journal of Virology, 2015. **89**(14): p. 7147-7158.
153. Fliss, P.M., et al., *Viral mediated redirection of NEMO/IKKgamma to autophagosomes curtails the inflammatory cascade.* PLoS Pathog, 2012. **8**(2): p. e1002517.
154. Chan, B., et al., *The murine cytomegalovirus M35 protein antagonizes type I IFN induction downstream of pattern recognition receptors by targeting NF-κB mediated transcription.* PLOS Pathogens, 2017. **13**(5): p. e1006382.
155. Wang, H. and W.-S. Ryu, *Hepatitis B virus polymerase blocks pattern recognition receptor signaling via interaction with DDX3: implications for immune evasion.* PLoS pathogens, 2010. **6**(7): p. e1000986-e1000986.
156. Brune, W. and C.E. Andoniou, *Die Another Day: Inhibition of Cell Death Pathways by Cytomegalovirus.* Viruses, 2017. **9**(9).
157. Ku, Y.-C., et al., *DDX3 Participates in Translational Control of Inflammation Induced by Infections and Injuries.* Molecular and cellular biology, 2018. **39**(1): p. e00285-18.
158. Baldanti, F., et al., *Human cytomegalovirus UL131A, UL130 and UL128 genes are highly conserved among field isolates.* Arch Virol, 2006. **151**(6): p. 1225-33.
159. Bughio, F., et al., *Human Cytomegalovirus UL135 and UL136 Genes Are Required for Postentry Tropism in Endothelial Cells.* 2015. **89**(13): p. 6536-6550.

160. Bronzini, M., et al., *The US16 Gene of Human Cytomegalovirus Is Required for Efficient Viral Infection of Endothelial and Epithelial Cells.* 2012. **86**(12): p. 6875-6888.
161. Brune, W., et al., *A Ribonucleotide Reductase Homolog of Cytomegalovirus and Endothelial Cell Tropism.* 2001. **291**(5502): p. 303-305.
162. Mack, C., et al., *Inhibition of proinflammatory and innate immune signaling pathways by a cytomegalovirus RIP1-interacting protein.* Proc Natl Acad Sci U S A, 2008. **105**(8): p. 3094-9.
163. Everett, R.D., G. Sourvinos, and A. Orr, *Recruitment of herpes simplex virus type 1 transcriptional regulatory protein ICP4 into foci juxtaposed to ND10 in live, infected cells.* J Virol, 2003. **77**(6): p. 3680-9.
164. Lenarcic, E.M., B.J. Ziehr, and N.J. Moorman, *An unbiased proteomics approach to identify human cytomegalovirus RNA-associated proteins.* Virology, 2015. **481**: p. 13-23.
165. Lai, M.-C., Y.-H.W. Lee, and W.-Y. Tarn, *The DEAD-box RNA helicase DDX3 associates with export messenger ribonucleoproteins as well as tip-associated protein and participates in translational control.* Molecular biology of the cell, 2008. **19**(9): p. 3847-3858.
166. Shih, J.W., et al., *Critical roles of RNA helicase DDX3 and its interactions with eIF4E/PABP1 in stress granule assembly and stress response.* Biochem J, 2012. **441**(1): p. 119-29.
167. Beckham, C.J. and R. Parker, *P bodies, stress granules, and viral life cycles.* Cell Host Microbe, 2008. **3**(4): p. 206-12.
168. Ziehr, B., H.A. Vincent, and N.J. Moorman, *Human Cytomegalovirus pTRS1 and pIRS1 Antagonize Protein Kinase R To Facilitate Virus Replication.* Journal of virology, 2016. **90**(8): p. 3839-3848.
169. Bierle, C.J., K.M. Semmens, and A.P. Geballe, *Double-stranded RNA binding by the human cytomegalovirus PKR antagonist TRS1.* Virology, 2013. **442**(1): p. 28-37.
170. Thulasi Raman, S.N., et al., *DDX3 Interacts with Influenza A Virus NS1 and NP Proteins and Exerts Antiviral Function through Regulation of Stress Granule Formation.* 2016. **90**(7): p. 3661-3675.
171. Mori, J., et al., *Human Herpesvirus-6 U14 Induces Cell-Cycle Arrest in G2/M Phase by Associating with a Cellular Protein, EDD.* PLoS One, 2015. **10**(9): p. e0137420.
172. Hossain, D., et al., *HIV-1 Vpr hijacks EDD-DYRK2-DDB1(DCAF1) to disrupt centrosome homeostasis.* J Biol Chem, 2018. **293**(24): p. 9448-9460.
173. Li, C.G., et al., *PPARgamma Interaction with UBR5/ATMIN Promotes DNA Repair to Maintain Endothelial Homeostasis.* Cell Rep, 2019. **26**(5): p. 1333-1343 e7.
174. E, X., et al., *An E2F1-mediated DNA damage response contributes to the replication of human cytomegalovirus.* PLoS Pathog, 2011. **7**(5): p. e1001342.
175. Nguyen, C.N., et al., *Regulation of p21 expression for anti-apoptotic activity of DDX3 against sanguinarine-induced cell death on intrinsic pathway.* Phytomedicine, 2019. **65**: p. 153096.
176. Swift, S., et al., *Rapid production of retroviruses for efficient gene delivery to mammalian cells using 293T cell-based systems.* Curr Protoc Immunol, 2001. **Chapter 10**: p. Unit 10 17C.
177. Harvey, D.M. and A.J. Levine, *p53 alteration is a common event in the spontaneous immortalization of primary BALB/c murine embryo fibroblasts.* Genes Dev, 1991. **5**(12B): p. 2375-85.

178. Jordan, S., et al., *Virus progeny of murine cytomegalovirus bacterial artificial chromosome pSM3fr show reduced growth in salivary Glands due to a fixed mutation of MCK-2.* J Virol, 2011. **85**(19): p. 10346-53.
179. Angulo, A., P. Ghazal, and M. Messerle, *The Major Immediate-Early Gene ie3 of Mouse Cytomegalovirus Is Essential for Viral Growth.* Journal of Virology, 2000. **74**(23): p. 11129-11136.
180. Tischer, B.K., G.A. Smith, and N. Osterrieder, *En passant mutagenesis: a two step markerless red recombination system.* Methods Mol Biol, 2010. **634**: p. 421-30.
181. van Diemen, F.R., et al., *CRISPR/Cas9-Mediated Genome Editing of Herpesviruses Limits Productive and Latent Infections.* PLoS Pathog, 2016. **12**(6): p. e1005701.
182. Ramakrishnan, M.A., *Determination of 50% endpoint titer using a simple formula.* World journal of virology, 2016. **5**(2): p. 85-86.
183. Zurbach, K.A., T. Moghbeli, and C.M. Snyder, *Resolving the titer of murine cytomegalovirus by plaque assay using the M2-10B4 cell line and a low viscosity overlay.* Virology journal, 2014. **11**: p. 71-71.
184. Laemmli, U.K., *Cleavage of Structural Proteins during the Assembly of the Head of Bacteriophage T4.* Nature, 1970. **227**(5259): p. 680-685.
185. Schagger, H., *Tricine-SDS-PAGE.* Nat Protoc, 2006. **1**(1): p. 16-22.

10 Appendix

10.1 Curriculum vitae

Lebenslauf entfällt aus datenschutzrechtlichen Gründen.

10.2 List of abbreviations

ActD	Actinomycin D
AIDS	Acquired immunodeficiency syndrome
AIM2	Absent in melanoma 2
AP	affinity purification
APCs	Antigen-presenting cells
ASC	Apoptosis-associated speck-like
ATM	Ataxia-telangiectasia-mutated
CCR2	CC-chemokine receptor 2
CD	cluster of differentiation
Cdan1	Codanin-1
cGAS	Cyclic GMP–AMP synthase
CHK2	Checkpoint kinase 2 kinase
CHX	Cycloheximide
CMV	Cytomegalovirus
CRISPR	Clustered Regularly Interspaced Short Palindromic Repeats
CRM1	Chromosomal Maintenance 1
DAI	DNA-dependent activator
DCs	Dendritic cells
DD	Death domain
DDX3	DEAD box helicase 3
ds	double stranded
DUB	Deubiquitinase
E	Early
EDD	E3 identified by Differential Display
EGFR	Epidermal growth factor receptor
eIF	Eukaryotic initiation factor
ER	Endoplasmic reticulum
FP	footpad
gB	Glycoprotein B
GFP	Green fluorescent protein
Gmip	GEM-interacting protein
HA	Hemagglutinin
HCMV	Human cytomegalovirus
HCV	Hepatitis C virus
HECT	Homologous to E6-AP C-terminus
HIV	Human immunodeficiency virus
Hpi	hours post infection
HPV	Human papilloma virus
HSV-1	Herpes simplex virus 1
ICAM-1	Intercellular adhesion molecule 1
IE	Immediate-early
IFI16	Gamma-interferon-inducible protein 16
IFIT1	Interferon-induced protein with tetratricopeptide repeats 1
IFIX	Interferon-inducible protein X
IFN	Interferon
IFNAR	IFN receptor
IFNGR	IFN gamma receptor
IFNLR	IFN lambda receptor 1

IKK	IκB kinase
IL	Interleukin
IRF	Interferon regulatory factor
IRS1	Internal repeat short
ISG	Interferon-stimulated gene
ISGF3	Interferon-stimulated gene factor 3
JAK	Janus kinase
L	Late
LCMV	Lymphocytic choriomeningitis virus
LPS	Lipopolysaccharides
LTβR	Lymphotoxin β receptor
MAPK	Mitogen-activated protein kinase
MAVS	Mitochondrial antiviral-signaling
MCMV	Murine cytomegalovirus
MDPs	Macrophage and dendritic cell precursors
MIEP	Major immediate early promoter
MNDA	Myeloid cell nuclear differentiation antigen
MNDAL	Myeloid cell nuclear differentiation antigen-like
MOI	multiplicity of infection
Mprip	Myosin phosphatase Rho-interacting protein
mRNA	messenger RNA
MS	mass spectrometry
MYD88	Myeloid differentiation primary response 88
NEMO	NF-κB essential modulator
NES	nuclear export signal
NF-κb	Nuclear factor 'kappa-light-chain-enhancer' of activated B-cells
NK	Natural killer
NLR	Nod-like receptor
NLRP3	Nucleotide-binding domain, leucine rich repeat containing receptor family Pyrin domain containing 3
p204	Phosphoprotein 204
PABP	poly(A)-binding protein
Paip2	PABP-interacting protein 2
PAMP	Pathogen-associated molecular pattern
PCR	polymerase chain reaction
PDGFRα	Platelet-derived growth factor receptor alpha
PI3K	Phosphatidylinositol 3-kinase
PKR	Protein kinase R
PLN	Popliteal lymph nodes
PLN	Popliteal lymph nodes
PML	Promyelocytic leukemia
PPARγ	peroxisome proliferator activated receptor γ
pRb	Retinoblastoma protein
PRR	Pathogen recognition receptor
PYD	Pyrin domain
RCMV	Rat CMV
RIG-I	Retinoic acid-inducible gene I
RLR	Retinoic acid-inducible gene I like receptor
RNP	Ribonucleoprotein
RORγt	Related orphan receptor gamma t

SG	Stress granule
SILAC	stable isotope labelling amino acids in cell culture
Sp1	Specificity protein 1
STAT	Signal transducer and activator of transcription
STING	Stimulator of interferon genes
TBK1	TANK-binding kinase 1
TCID$_{50}$	tissue culture infectious dose 50 %
Th	T helper
TLR	Toll-like receptor
TNF-a	Tumor necrosis factor-a
TRAF	TNF receptor associated factor
TRS1	Terminal repeat short
Ub	Ubiquitin
UBA	Ubiquitin activation
UBR	Ubiquitin Recognin Box
UBR5	Ubiquitin protein ligase E3 component n-recognin 5
vAC	Viral assembly complex
VACV	Vaccinia virus
VCAM-1	Vascular cell adhesion protein 1
VSV	Vesicular stomatitis virus
VSV	Vesicular stomatitis virus
WT	wildtype
ZBP1	Z-DNA-binding protein 1

10.3 List of the hazardous substances

Substance	GHS symbol	Hazard statements	Precautionary statements
2-mercaptoethanol	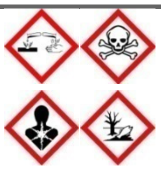	H301 + H331-H310-H315-H317-H318-H373-H410	P261-P280-P301 + P310 + P330-P302 + P352 + P310-P305 + P351 + P338 + P310-P403 + P233
Acetic acid	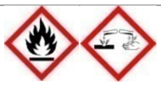	H226-H314	P280-P305 + P351 + P338-P310
Acrylamide	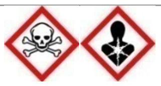	H301-H312 + H332-H315-H317-H319-H340-H350-H361f-H372	P201-P280-P301 + P310-P305 + P351 + P338-P308 + P313
Ammonium bicarbonate	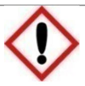	H302	P301 + P312 + P330
Ammonium persulfate	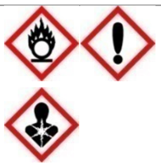	H272-H302-H315-H317-H319-H334-H335	P220-P261-P280-P305 + P351 + P338-P342 + P311
Ampicillin	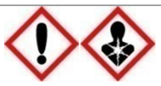	H315-H317-H319-H334-H335	P261-P280-P305 + P351 + P338-P342 + P311
Bis-acrylamide	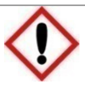	H302 + H332	
Boric acid	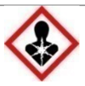	H360FD	P201-P308 + P313
Chloramphenicol	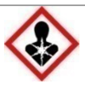	H350	P201-P308 + P313
Cycloheximide	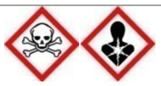	H302-H330-H341	P260-P281-P284-P310
EDTA	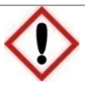	H319	P305 + P351 + P338
Ethanol	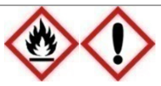	H225-H319	P210-P280-P305 + P351 + P338-P337 + P313-P403 + P235
Ethidium bromide	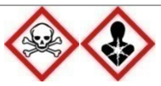	H302-H330-H341	P260-P281-P284-P310
Hydrochloric acid	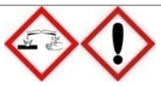	H290-H314-H335	P261-P280-P305 + P351 + P338-P310
Isopropanol	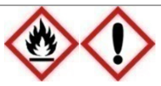	H225-H319-H336	P210-P261-P305 + P351 + P338
Kanamycin	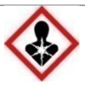	H360	P201-P308 + P313
Liquid nitrogen	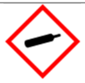	H281	P202-P271 + P403-P282

Methanol	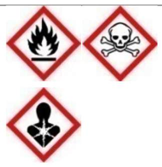	H225-H301 + H311 + H331-H370	P210-P260-P280-P301 + P310-P311
NP-40	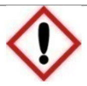	H319+H315	P264+P280
Penicillin	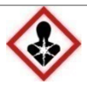	H317-H334	P261-P280-P342 + P311
Protein A-agarose	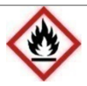	H226	
Protein G-agarose	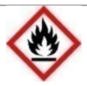	H226	
Puromycin	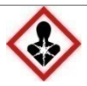	H373	
Sodium dodecyl sulfate	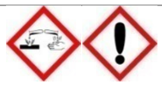	H315-H318-H335	P280-P304 + P340 + P312-P305 + P351 + P338 + P310
Sodium hydroxide	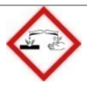	H290-H314	P280-P305 + P351 + P338-P310
Streptomycin	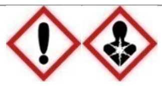	H302-H361	P281
TEMED	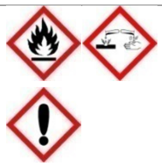	H225-H302-H314-H332	P210-P280-P305 + P351 + P338-P310
Triton X-100	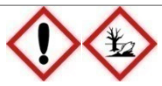	H302-H319-H411	P273-P280-P301 + P312 + P330-P337 + P313-P391-P501

10.4 Acknowledgments

I would like to thank my supervisor Prof. Dr. Wolfram Brune for giving me the opportunity to do a doctoral thesis in his lab and providing me with a challenging and interesting project. I highly appreciate his ongoing support and supervision during my PhD. I also would like to thank my second supervisor Prof. Dr. Melanie Brinkmann for her helpful advice and stimulating discussions during my PhD.

I would like to pay my special regards to Prof. Dr. Adam Grundhoff for reviewing my thesis, as well as Dr. Charlotte Uetrecht and Prof. Dr. Elke Oetjen for providing their expertise as members of my thesis defense committee.

I would like to thank Prof. Dr. Hartmut Schlüter and Dr. Christoph Krisp for performing mass spectrometry experiments, Dr. Eleonore Ostermann for performing in vivo experiments, and Malik Alawi for the analysis of next generation sequencing data. Here I also want to acknowledge Dr. William J. Kaiser, Dr. Martina Schroeder and Dr. Adam Geballe for providing me with useful materials.

I would like to express my gratefulness to Dr. Giada Frascaroli and Dr. Timothy Soh for critical reading of this manuscript, and to Kerstin Pawletko and Glen Meads for proofreading.

I would like to thank to Dr. Jiajia Tang and Dr. Eleonore Ostermann for teaching me laboratory techniques, and Dr. Giada Frascaroli for her bright scientific suggestions.

I am tremendously thankful to my current and former colleagues at the department of Virus Host Interactions. This work would not have been possible without their input. I want to specially thank Kerstin and Elena for their great help in the laboratory. Enrico, Renke, Yingqi, Martina, Tianyu, Luis, Umit, Theo, Tim, Victoria, Felix, Gabi, Leila, Antonio, Nathalie, Michaela, Florian, Xuan, Anna, it was a great pleasure to work with you.

I wish to express my deepest gratitude to my parents for their love and constant support. I have to send special thanks to my beloved sister Yuliia for her help and encouragement. Finally, I would like to thank my boyfriend Jean-Pierre for being by my side and enriching my life with joy.

10.5 Declaration upon oath

I hereby declare that this doctoral dissertation is my own work and that I have not used any sources other than those listed.

Hamburg, December 2019

Olha Puhach